Heuristics for Lagrangian Relaxation Formulations for the Unit Commitment Problem

A Dissertation Presented for the

Doctor of Philosophy

Degree

The University of Tennessee, Knoxville

Stephen Opeyemi Fatokun

August 2023

© by Stephen Opeyemi Fatokun, 2023
All Rights Reserved.

Dedicated to My Parents

Acknowledgments

I would like to express my greatest appreciation to my advisor, Dr. Kevin Tomsovic for his support, time, dedication, and most importantly for believing in me. I can look at science and engineering in a whole different way and will continue on this path because of his investment in me.

I would also like to acknowledge my committee members, Dr. Fangxing (Fran) Li, Dr. James Ostrowski, and Dr. Michael Starke for their eagerness to serve on my committee and most importantly for investing time to make my dissertation a quality one. Their contributions added a lot of improvements and dimensions to my work and for that I am grateful. I would also like to acknowledge the staff at the Bredesen Center for their support throughout my journey as a graduate student. I cannot forget to mention all the friends I made along the way for their contribution to my success.

My deepest appreciation goes to CURENT and the Engineering Research Center Program of the National Science Foundation and the Department of Energy under NSF Award Number EEC-1041877 for the unique funding opportunity. I am certainly grateful for the friendly atmosphere, state-of-the-art labs, talented students, and faculty members at CURENT.

Finally, I would like to express my appreciation to my family for their unwavering love, support, and patience. They all made it possible for me to complete this work.

Abstract

The expansion of distributed energy resources (DER), demand response (DR), and virtual bidding in many power systems and energy markets are creating new challenges for unit commitment (UC) and economic dispatch (ED) techniques. Instead of a small number of traditionally large generators, the power system resource mix is moving to one with a high percentage of a large number of small units. These can increase the number of similar or identical units, leading to chattering (switching back and forth among committed units between iterations). This research investigates alternative and scalable ways of increasing the high penetration of these resources.

First, the mathematical formulations for UC and ED models are reviewed. Then a new heuristic is proposed that takes advantage of the incremental nature of Lagrangian relaxation (LR). The heuristic linearizes and distributes the network transmission losses to appropriately penalize line flow and mitigate losses.

Second, a mixed integer programming (MIP) is used as a benchmark for the proposed LR formulation. The impact of similar and identical units on the solution quality and simulation run time of UC and ED was investigated using the proposed formulation.

Third, a system flexibility study is done using DR and a load demand pattern with a high penetration of renewables, creating a high daily ramp rate requirement. This work investigates the impact of available DR on spikes in locational marginal pricing (LMP).

Fourth, two studies are done on improving LR computational efficiency. The first proposes a heuristic that focuses on trade-offs between solution quality and simulation run time. The heuristic iterates over lambda and energy marginal price while the convergence issue is handled using Augmented LR (ALR). The second study proposes a heuristic that penalizes transmission lines with binding line limits. The proposed method can reduce

power flow in the transmission lines of interest, and considerably reduce the simulation time in optimization problems with a high number of transmission constraints.

Finally, the effect of a large number of similar and identical units on simulation run time is considered. The proposed formulation scales linearly with the increase in system size.

Table of Contents

1 Introduction **1**

1.1 Background 1

1.1.1 Renewable Based Distributed Energy Resources 1

1.1.2 Virtual Power Plants 2

1.1.3 Demand Response 4

1.1.4 Grid Flexibility 6

1.1.5 Unit Commitment and Economic Dispatch 10

1.2 Motivation 11

1.3 Dissertation Outline 12

1.4 Contributions 13

2 Literature Review **15**

2.1 Unit Commitment and Economic Dispatch 15

2.1.1 Unit Commitment 15

2.1.2 Security Constrained Economic Dispatch 16

2.2 Unit Commitment Formulations 17

2.3 Unit Commitment and Identical Units 19

2.4 Unit Commitment and Simulation Time 19

2.5 Unit Commitment and Transmission Flow Constraints 20

2.6 Unit Commitment and Distributed Algorithms 22

2.7 Unit Commitment and Flexibility Requirements 28

2.8 Unit Commitment and Industry Practices 29

3 Unit Commitment Formulation for Scalable Scheduling **32**

3.1 Model and Formulation of Unit Commitment and Economic Dispatch 32

3.1.1 Over-Generation Resulting from Similar and Identical Units 33

3.2 Non-Convex Optimization 33

3.2.1 Lagrangian Multiplier and the Dual Variable 35

3.2.2 Lagrangian Relaxation 35

3.2.3 Unit Commitment with Line Losses 38

3.3 Heuristic Formulation for Line-Losses 38

3.3.1 Formulation and Code Implementation 41

3.3.2 Modified PJM 5 Bus System 41

3.3.3 Test Result for the Base Case and Heuristic Formulation 44

3.3.4 Discussion of Simulation Results 48

3.3.5 Impact of 24-hour Horizon at 5-minute intervals 55

3.4 Discussion 57

4 LR Algorithm and Implementation **60**

4.1 Formulate a Benchmark for Solution Quality using MIP 60

4.1.1 Case 1 61

4.1.2 Case 2 65

4.2 Implementation of Network Constraints, System Reserve and LMP 65

4.3 LR and Scalabilty 75

4.3.1 Modified RTS-GMLC 73 Bus System 75

4.3.2 Benchmark for Simulation Time using MIP 77

4.3.3 Test Result for Case 1 77

4.3.4 Test Result for Case 2 81

4.3.5 Test Result for Case 3 83

4.3.6 Scalability Considering System Size 83

4.3.7 Discussion 86

4.4 Scalability for DA UC with Different Time Intervals 90

4.5 Conclusions 93

5 Computational efficiency using LR Formulations **96**
5.1 WECC 240 Bus System . . . 97
5.2 System Flexibility Requirement with DR . . . 100
5.2.1 Impact of Load Peak on Market Price and LMP . . . 101
5.2.2 Case Study of System Flexibility and LMP Spikes using DR . . . 101
5.2.3 Discussion . . . 102
5.3 Price Iteration Techniques using Augmented LR . . . 105
5.3.1 Augmented LR and Coupling Constraints . . . 105
5.3.2 Test Results using WECC 240 Bus System . . . 108
5.3.3 Discussion . . . 116
5.4 Effect of Transmission Limit on Optimization . . . 116
5.4.1 Incremental Optimization . . . 117
5.4.2 Effect of Line Flow Penalty on Transmission Limit . . . 117
5.4.3 Discussion . . . 124
5.5 Large System Integration of Similar and Identical DER Units . . . 126
5.5.1 Effect of a Large Volume of Similar and Identical Units on Simulation Run Time . . . 126
5.5.2 Discussion . . . 127
5.6 Conclusions . . . 127

6 Conclusion and Future Work **130**
6.1 Conclusion . . . 130
6.2 Future Work . . . 132

Bibliography **133**

Appendices **145**
A Data Information for WECC . . . 146
B Load Peak and Spike in LMPs . . . 149
C LR Formulations and Matlab Code . . . 152
C.1 Data Process . . . 152

C.2 Code Implementation 152
C.3 ED Implementation 154

Vita **155**

List of Tables

3.1 Generator parameters 43
3.2 Network parameters 45
3.3 System bus load for a 12-hour period 45
3.4 Generator and load data at Hour zero (Hour-0) 46
3.5 Hourly Generation Cost Difference for ED and OPF solutions 53
3.6 Hourly Generation Cost Difference and P loss Difference 54
3.7 Total Cost and Losses 54
3.8 Effect of the conservative weighting factor on generation cost and losses . . . 56
3.9 Original and reduced weighting factors considered 56
3.10 Scalability test for hourly vs 5-minute time periods and 288 time periods . . 58

4.1 Comparing UC and ED results for LR with Heuristic and Egret Case 1 . . . 62
4.2 Periodic cost of production for Case 1 64
4.3 Total cost of production for Case 1 64
4.4 Comparing UC and ED results for LR with Heuristic and Egret Case 2 . . . 66
4.5 Total cost of production for Case 2 67
4.6 RTS-79 Generation Mix 76
4.7 Production cost for Case 1 78
4.8 Cost Benchmark w.r.t Egret for Case 1 78
4.9 Production cost for Case 2 82
4.10 Cost Benchmark w.r.t Egret for Case 2 84
4.11 Production cost for Case 3 84
4.12 Cost Benchmark w.r.t Egret for Case 3 85

4.13 Cost w.r.t Egret for 1-hour and 5-minute intervals 94

5.1 Summary of results 115

List of Figures

1.1 Wind and solar energy trends . . . 3
1.2 Global Solar and Wind Capacity [63] . . . 3
1.3 Visibility of behind-the-meter resources to ISO/RTO [80] . . . 5
1.4 NYISO reliability program and historical enrollment data [36] . . . 7
1.5 PJM Economic DR Capability in Energy Market in MW (3/1/2006-4/2/2021) [61] . . . 7
1.6 Correlation between installed capacity of Pumped Hydro and Nuclear [24] . . . 8
1.7 Electrical energy storage capacity by technology type in the U.S. (2019) [93] 9

2.1 Major energy sources in the U.S. 1950-2020 [28] . . . 24
2.2 Percentage time allocation for Asynchronous and Synchronous Algorithms [78] 26
2.3 Actual aggregate Computation and Communication time for Asynchronous and Synchronous Algorithms [78] . . . 27
2.4 Run Time vs Number of Periods for LR and MIP [86] . . . 30

3.1 Power market bids and actual market price . . . 34
3.2 Lagrangian Relaxation Optimization Approach . . . 42
3.3 Modified PJM 5-bus system . . . 43
3.4 Comparing the base case system with the heuristic case for a 12-hour time horizon . . . 47
3.5 Losses are calculated by solving OPF using MATPOWER . . . 49
3.6 Additional power output obtained from solving OPF using MATPOWER . . . 50
3.7 Real and reactive losses obtained from solving OPF using MATPOWER . . . 51
3.8 A Day-Ahead UC and ED with 5-minute interval and 288 time periods . . . 58

4.1 Plots of UC and ED results for LR with Heuristic and Egret for Case 1 . . . 63
4.2 Plots of UC and ED results for LR with Heuristic and Egret for Case 2 . . . 67
4.3 Modified PJM 5 bus system with 4 main units and 2 reserve units 69
4.4 Iterative Optimization Approach 70
4.5 Network constraint UC considering reserves and LMP 71
4.6 Network constraint UC considering reserves and LMP with heuristic 72
4.7 Modified PJM 5 bus LMP result considering line limit and reserve (3D) . . . 73
4.8 Modified PJM 5 bus LMP result considering line limit and reserve (2D) . . . 74
4.9 Solution benchmark for Case 1 79
4.10 Hourly cost difference between Heu-iter and Egret for Case 1 80
4.11 Hourly cost difference between Heu-iter and Egret for Case 2 84
4.12 Hourly cost difference between Heu-iter and Egret for Case 3 85
4.13 Linear increase in total load size and number of units 87
4.14 Increase in the total cost of production with increase in problem size 87
4.15 Plot of simulation run time for all 3 formulations and all 3 cases 88
4.16 Total number of units committed per period 89
4.17 Simulation run time for increasing load and number of units 91
4.18 Simulation run time considering 1-hour, 30-minute, 15-minute, and 5-minute time intervals 92

5.1 Fuel cost function for gas fired plants 99
5.2 Modified demand and the effect on hourly marginal energy cost 103
5.3 LMP spikes and available DR 104
5.4 Effect of increasing % DR 106
5.5 Base case flowchart 109
5.6 Heuristic for committing least number of units 109
5.7 Heuristic for committing optimum number of units by iterating over λ 110
5.8 Number of units committed for case 1, case 2, and case 3 111
5.9 Hourly marginal energy price for case 1, case 2, and case 3 113
5.10 Plot of the hourly cost of generation for case 1, case 2, and case 3 114

5.11 Base case with no line penalty . . . 119
5.12 Heuristic case with targeted line penalties . . . 121
5.13 Line flow as a function of penalty . . . 122
5.14 Total costs differences Using the base case as reference . . . 123
5.15 Flowchart for transmission penalty algorithm . . . 125
5.16 Simulation run time for increasing volume of DER . . . 128

A.1 WECC annual peak hourly demand . . . 147
A.2 WECC hourly load for August 10, 2004 . . . 147
A.3 Modified WECC load using CAISO RES data from July 2, 2022 . . . 148
B.1 Daily peaks and RA capacity for August and September 2022 [3] . . . 150
B.2 Average daily prices across markets Aug-Sep 2022 [3] . . . 150
B.3 Electricity prices variation at the SP15 and NP15 hubs. . . . 151
C.1 Code flowchart . . . 153

Nomenclature

i	Index of buses, or, index of generators.
j	Index of load buses.
k	Index of transmission lines.
t	Index of time periods.
NG	Total number of generators.
NK	Total number of transmission lines.
NT	Total time period.
T	Total time period.
C_i	Cost of generation from unit P_i (\$).
D_{it}	Demand at bus i and period t.
$P_i^{\max}$	Maximum generation capacity for unit i.
$P_i^{\min}$	Minimum generation capacity for unit i.
P_{it}	Generator power output for unit i at period t (MW).
P_{load}^t	Total demand at time period t.
RD_i	Ramp-down rate of unit i.
RU_i	Ramp-up rate of unit i.

$R_i^{\min}$ Minimum capacity of spinning reserve for unit i.

R_i^{shut} Available shut-down capacity for unit i.

R_i^{start} Available start-up capacity for unit i.

R_{it} Committed reserve capacity from unit i at period t.

S_i Startup cost/shutdown cost ($).

q_{it} Capacity cost of committed reserve for unit i at time period t ($).

u_{it} 1 if unit i is committed at time period t and 0 if not.

J^* Optimum primal solution.

U_{it} 1 if unit i is committed at time period t and 0 if not.

α Scaling factor for updating λ.

ϵ relative duality gap.

λ^t Market price at time t.

$\mathcal{L}$ Lagrangian function.

a_i Constant part of the cost function for unit i.

b_i Linear part of the cost function for unit i.

c_i Quadratic part of the cost function for unit i.

q^* Optimum dual value.

DF_i Delivery factor at bus i.

LF_i Loss factor at bus i.

L_{flow}^t Estimated line loss as a function of the injected power.

P_i Injected power at bus i.

P_{Loss} Total (network) system losses (MWh).

R_k Line resistance for line k.

$\boldsymbol{P_{inj}}$ The vector of the net injected power at each bus.

$\boldsymbol{W}$ Weighting factor as a function of the individual line resistance.

$\frac{\partial(P_{Loss})}{\partial P_i}$ Incremental transmission loss as a function of power injection at bus i.

$F_k^{\max}$ Maximum transmission capacity limit for line k.

GSF_{ki} Generation shift factor from unit i to line k.

ACPF AC power flow.

DCPF DC power flow.

DER Distributed energy resources.

DR Demand response.

ED Economic dispatch.

LR Lagrangian relaxation.

MIP Mixed integer programming.

OPF Optimal power flow.

UC Unit commitment.

Chapter 1

Introduction

This work is motivated by the impact of a high penetration of Distributed Energy Resources (DER) on the North American (NA) grid, and how this affects the existing unit scheduling techniques in the electrical power markets. The integration of a large number of non-conventional energy resources such as DER, virtual trading, and Demand Response (DR) implies that many more units will be scheduled for the grid. This would lead to a very large increase in the number of similar or identical units, which makes solving Unit Commitment (UC) problems even more difficult. New scalable and efficient UC algorithms will be required to handle the increasing number of resources and issues with similar and identical units respectively. This research focuses on formulating scalable and efficient optimization techniques, and frameworks that can handle the ever-increasing distributed grid resources with quality solutions within acceptable solution time for the markets.

1.1 Background

1.1.1 Renewable Based Distributed Energy Resources

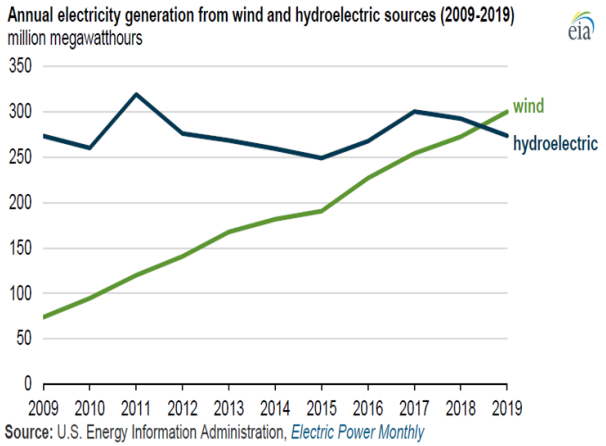
Several countries, including Germany, Denmark, Japan, and the USA, have led innovations in renewable-based DER. These countries see a potential for lowering the overall cost of energy and becoming energy independent [10]. As the awareness of the benefits of renewable energy resources increases, so does the number of interested countries. Renewable-based

DER are also of interest because they can help decrease CO_2 emissions, decrease resistive transmission losses and improve system reliability [1]. Today, many renewable-based DER have reached a level of maturity, with solar and wind prices competitive with conventional technologies, such as coal. From a U.S. Energy Information Administration (EIA) report of Feb 2020, the overall energy generated from wind surpassed that of hydro in the year 2019 as shown in Figure 1.1a [27]. Similarly, the predicted 'duck curve' in the CAISO market due to solar resources has begun to manifest itself, requiring an average of 13GW upward ramping in the 3 hours preceding sunset as shown in Figure 1.1b [25]. In 2021, the solar PV global capacity and wind power global capacity reached 942 and 845 gigawatts respectively, as shown in Figures 1.2a and 1.2b [63].

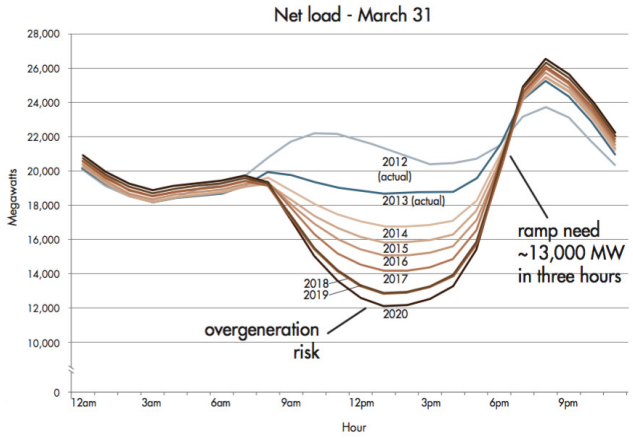
Considering the current trend of renewable energy capacity increase, deliberate steps have to be taken to ensure a secure and reliable integration of renewable-based DER into the power grid. It is worth noting that the benefits associated with renewable-based DER are not without drawbacks. The intermittent nature of the two fastest-growing renewable energy resources has introduced various operational challenges. Engineers and researchers have proposed numerous new control approaches to maintain grid frequency and voltage performance [1, 10, 12, 66]. A passive addition of DER and distributed generators (DG) to the grid creates security and reliability issues. The installation of renewable-based DER on the transmission side of the grid can create problems with over-generation and reduce system reliability. On the medium voltage (MV) level of the grid, DER integration could be limited by the size of the transformers and the lack of visibility to the Distribution System Operators (DSO). While at the low voltage (LV) level, a passive integration of a large amount of DER could create issues with power quality, voltage, system stability, and protection. In all cases, there will be a need for grid expansion at the high volt (HV), MV, and LV levels of the grid [30].

1.1.2 Virtual Power Plants

The concept of a virtual power plant (VPP) is the aggregation of distributed generators (including renewable energy resources), flexible or controllable loads, and energy storage systems (ESS) in order to monitor and control them as a single power plant. The aggregated

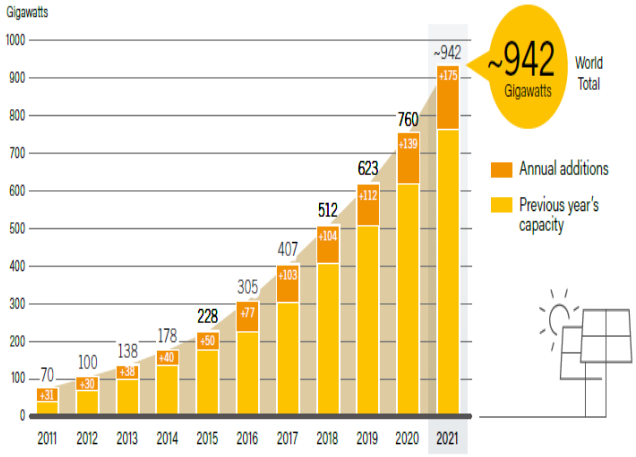


(a) Wind Surpasses Hydro [27]

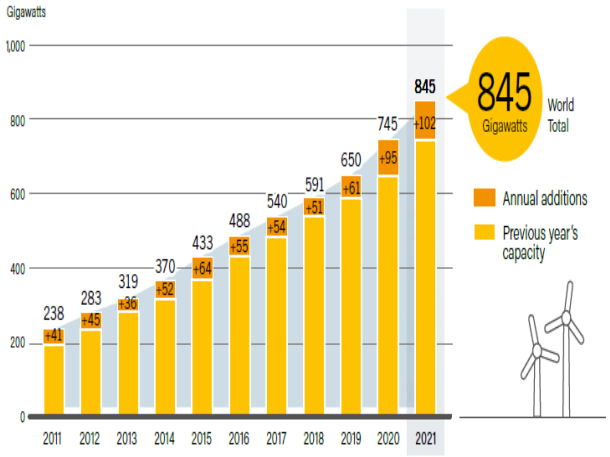


(b) 13GW ramping in 3hrs CAISO [25]

Figure 1.1: Wind and solar energy trends



(a) Global Solar Capacity



(b) Global Wind Capacity

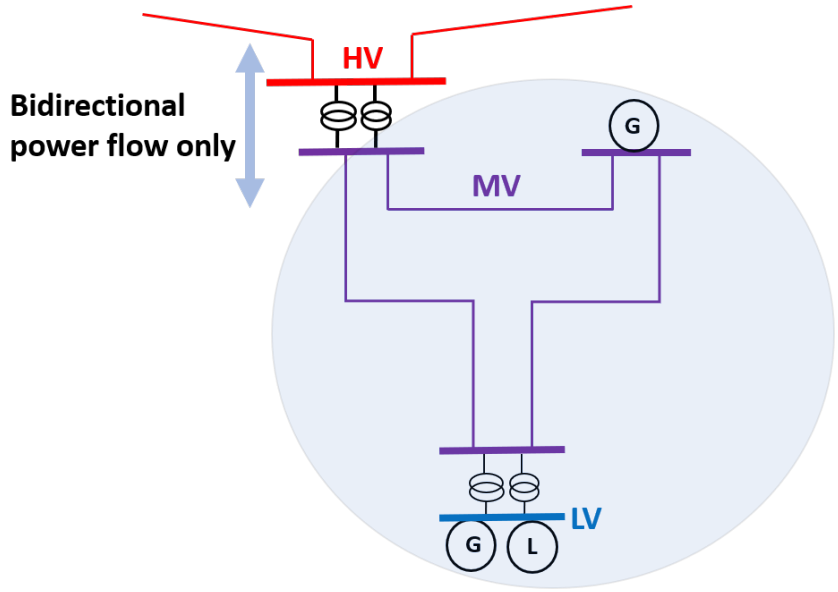
Figure 1.2: Global Solar and Wind Capacity [63]

resources could be distributed across a load center or as part of a microgrid. A central control unit known as the energy management system (EMS) coordinates the resources in the VPP and communicates with the ISO or RTO to provide an acceptable level of visibility on the power grid [19, 80].

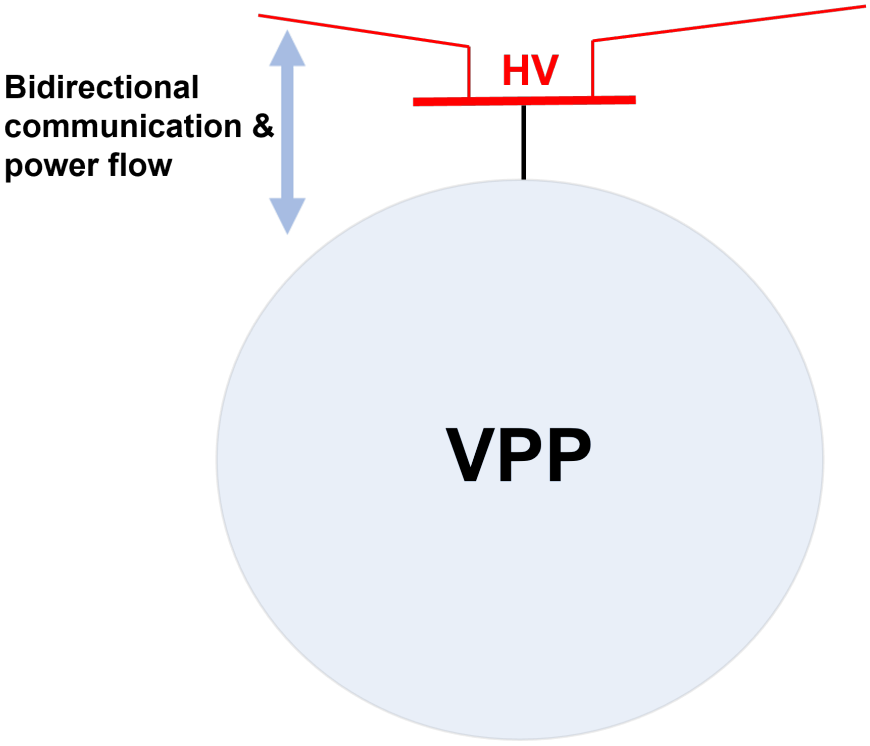
VPPs have been proposed as an active pathway for grid integration of DER. A VPP can reduce variability and uncertainties on the power grid, driving down the reserve capacity needed for grid security and reliability. Today, many countries no longer struggle with a low supply of renewable energy resources, instead, they have to deal with over-generation and negative electric market prices. Figure 1.3a shows a typical system with different voltage levels (LV, MV, HV), while Figure 1.3b shows a typical VPP with bidirectional communication. In addition to the uncertainties in the load forecast, TSO/ISO has to deal with additional uncertainties in the energy generation at the LV, MV, and HV levels of the power system network. Even if additional renewable power injection is not permitted at the LV level, behind the meter installation of DER by consumers can make load suddenly disappear or appear on the grid. To make the best use of the resources and technologies available to us today, a VPP can help coordinate resources like controllable and interruptible loads with demand response for mitigating the effect of sudden step load changes [20].

1.1.3 Demand Response

Demand response (DR) is the change in customer's energy usage in response to either varying electricity price or incentive payments in order to lower the usage of electricity in times of high demand or to help with system stability. As part of DER, DR can act as a controllable or interruptible load for grid stability. From [2], customers can respond to DR by reducing their electricity usage when the price is high, shifting peak operations to off-peak periods, or use onsite generators to meet the required load. DR programs can be categorized into two main types, incentive-based programs (IBP) and price-based programs (PBP). For example, the NYISO DR programs are designed for either reliability or economic purposes. The reliability programs are Emergency Demand Response Program (EDRP) and Installed Capacity-Special Case Resource (ICAP/SCR) program. They are implemented either by reducing load or applying qualified generators as resources to shave load peaks during system



(a) DER not visible to ISO/RTO



(b) DER visible to ISO/RTO

Figure 1.3: Visibility of behind-the-meter resources to ISO/RTO [80]

emergencies. The economic DR programs are the Day-Ahead Demand Response Program (DADRP) for the Energy market and the Demand-Side Ancillary Services Program (DSASP) for the Ancillary Service market. The economic programs encourage more flexible load to bid into the market, offer participants the opportunity to curtail their load, and drive down energy prices [36]. Figure 1.4 shows the historical enrollment of the NYISO DR programs.

Limitations and Challenges of Demand Response

As mentioned above, even though DR has a number of benefits, it is not without drawbacks and has been only slowly adopted by customers. For example, it can be seen from Figure 1.5 that enrolling and retaining customers in the PJM DR program has been challenging. Research has not been able to understand and categorize customers' behavior in a way that would directly translate into increasing and sustaining customers' participation. Some known limitations to customers' participation include technology cost and financing, opportunity cost and potential savings, and response fatigue [44]. More important to this research is the difficulty of existing UC and ED optimization techniques to handle a high influx of small grid resources such as DR and virtual trading. An influx of grid resources as these will increase the number of optimization variables required for solving the UC and ED. In addition, it is difficult to know if customers will respond and what percent of the available capacity. The latter adds a unique type of uncertainty to the optimization problem.

1.1.4 Grid Flexibility

Traditionally, the electric power system was designed to track in real-time, the known changes and uncertainty in load by adjusting the generation. The typical base-load generators like nuclear and coal are not nimble enough to track the variation in load. Faster responding units, such as natural gas and hydro, provided much of the tracking. Pumped hydro plays a big role in grid flexibility where available as can be seen from the correlation of nuclear and pumped hydro installation Figure 1.6 [24]. In 2019 hydropower accounted for about 93% of utility-scale storage power in GW and 99% of electrical energy storage in GWh [93]. Figure 1.7 compares different electrical energy storage resources by technology type in the

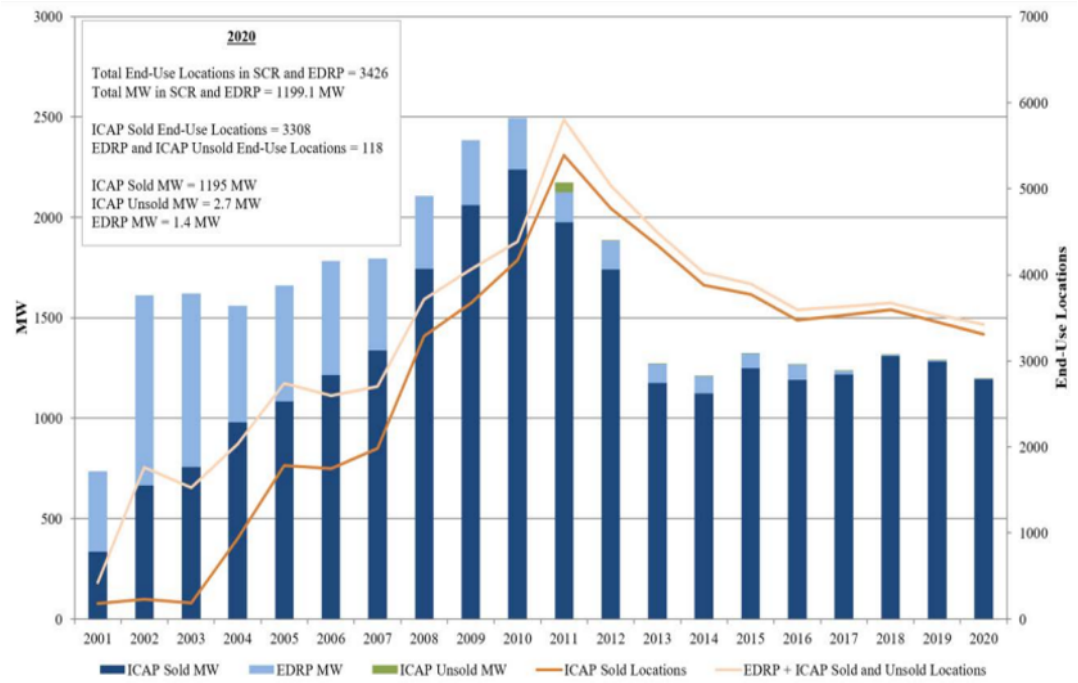


Figure 1.4: NYISO reliability program and historical enrollment data [36]

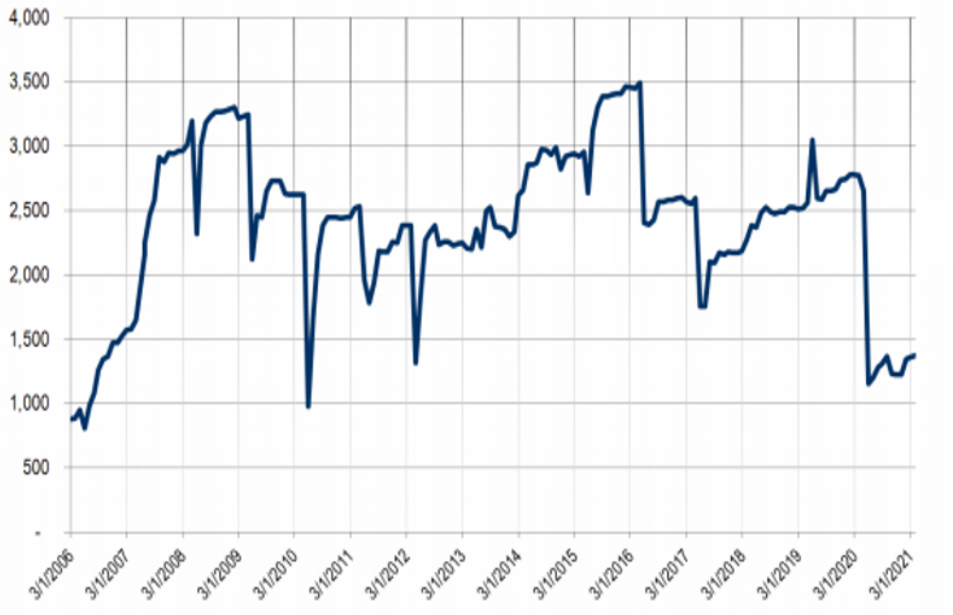


Figure 1.5: PJM Economic DR Capability in Energy Market in MW (3/1/2006-4/2/2021) [61]

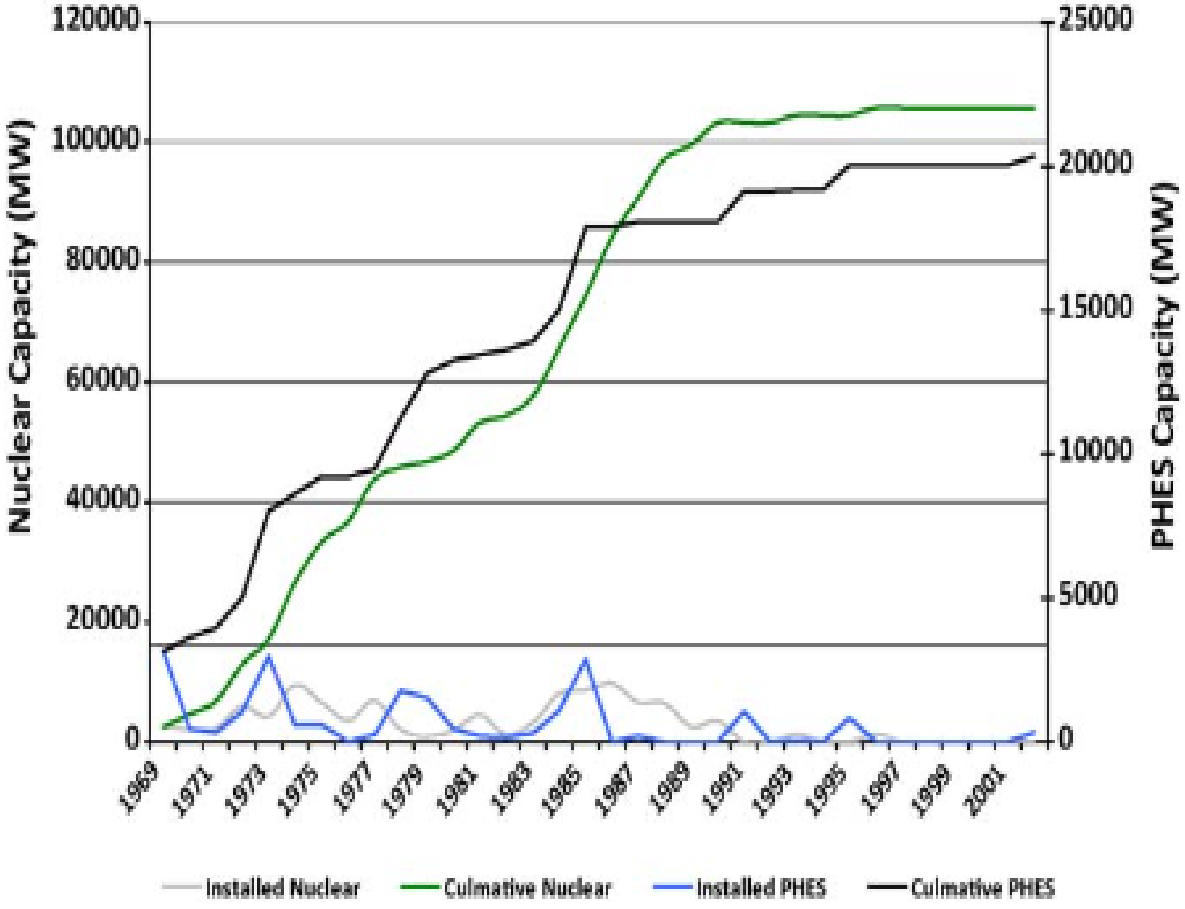


Figure 1.6: Correlation between installed capacity of Pumped Hydro and Nuclear [24]

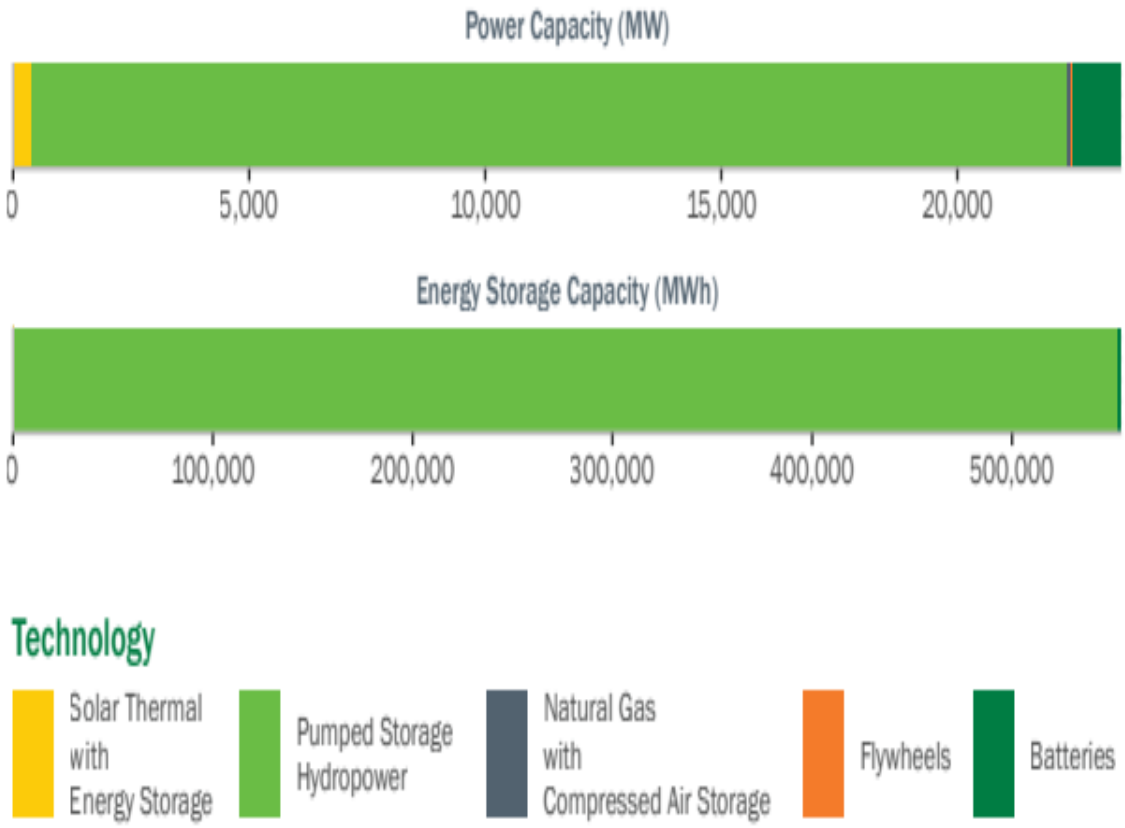


Figure 1.7: Electrical energy storage capacity by technology type in the U.S. (2019) [93]

year 2019.

With the influx of renewable-based DER and wind surpassing hydro as the most-used renewable energy in 2019 (see Figure 1.1a above) [27], power system engineers are now re-thinking grid flexibility. Generation alone might not be the best way to track variation in load, since renewable energy sources are now adding an additional layer of uncertainty and in some cases, increasing the required ramp-rate capacity for the system. The power system grid flexibility is now being considered as not just the ability for power generation to match load at all times but a case where the system can respond rapidly to large variations in both demand and generation. The requirement for grid flexibility depends on evolving new market structures, system operation, grid software and hardware, and legislation [35]. For example, the legislation around the reduction in CO_2 emission would need a great deal of change in the traditional flexibility requirement.

1.1.5 Unit Commitment and Economic Dispatch

Unlike most commodities and products, electricity cannot be stored economically for future use and requires a physically connected link at all times for its transportation [94]. For the above-mentioned reasons, electricity markets do not just determine the required capacity but also schedule which generators provide power and the amount of generation needed from each unit per time. The complexity of keeping generation as close as possible to demand requires committing the right units and dispatching the right amount of electricity at all times. Most ISOs and RTOs schedule their power system resources across multiple time horizons. The day-ahead (DA) unit commitment (UC) aims for the most economic resource combination while considering limits and possible uncertainties. In the DA time horizon, less flexible resources like the base-load units are committed earlier to provide sufficient time for them to respond. The hour-ahead (HA) scheduling takes care of excesses or deficiencies in the committed units. This is implemented by rescheduling units that are flexible enough within the HA time frame or committing additional units that are fast enough to start up in that time frame [55]. With the increase of non-dispatchable units in the power grid, the 15-minute and 5-minute time horizon for UC and economic dispatch (ED) is becoming popular in many electricity markets. Midcontinent Independent System Operator (MISO) is

now able to dispatch and make payment at the 5-minute horizon [72]. Finally, the real-time (RT) scheduling responds to variations occurring during the actual dispatch time.

The state-of-the-art UC and ED software uses a mixed-integer programming (MIP) technique. MIP guarantees a global optimum solution especially when the number of variables (units) is small. As the percentage of DER increases in the power grid, the number of dispatchable and non-dispatchable resources increases, making the solution run-time larger than acceptable [98]. In recent times, power system researchers have intensified efforts to find scalable optimization techniques. Much of the focus has been on scaling up the MIP technique by decentralizing large power system networks, using tie-lines or virtual tie-lines as links between areas [41].

1.2 Motivation

The future of the electrical power grid is trending towards one with a high penetration of DER. Some drivers of the changing landscape are state and regional clean energy targets, environmental activism, better technologies, and changing marketplace (smaller customers are interested in grid participation). Also, since electric power consumers are now more informed about the benefits of clean energy to the environment, they are becoming more interested in the source of the energy they consume. The current increase in DER, especially with many small resources will further exacerbate the existing difficulties in power systems scheduling. These challenges include an increasing number of similar units, high volume of transmission constraints, increasing uncertainty in unit capacities (intermittent resources), lack of resource visibility to ISOs and RTOs, poor power quality, over-generation of power, over-committing of reserves, low system inertial, voltage issues, and a host of other stability problems. Dealing with the effect of high penetration of DER will definitely require a significant amount of grid flexibility. This dissertation will investigate methods of achieving quick and efficient ways of allocating resources to reduce the effect of uncertainty, similar and identical units, and transmission constraints on the power system stability using scalable optimization techniques.

As power system resources shift away from the typical large but few units to the distributed unit types, scalability becomes an issue when solving UC and ED problems. The volume of transmission constraints can quickly increase which would in turn increase the number of iterations for clearing out all violations in the UC and ED solution [15]. An important tool for solving the optimization problem is MIP. MIP guarantees an optimum solution but does not scale well. MIP is in the class of non-deterministic polynomial-time complete (NP-complete) problems. This means that MIP problems cannot be solved in a quick deterministic algorithm time frame. Although NP-complete problems are solvable for some large problems, the running time for such problems quickly becomes unacceptably slow for large systems [98]. To mitigate this challenge, research has focused on re-formulating MIP into sub-problems. Partitioning a larger problem into multiple sub-problems will end up creating more shared variables as each sub-problem needs to coordinate and share information with other sub-problems for optimality. Lagrangian relaxation (LR) technique on the other hand is intuitive and scales well with increasing variables and, hence, is a good candidate for solving UC and ED problems of the future grid.

Although several researchers have used the LR in a hybrid format and have also focused on methods of updating lambda, solving the problem of similar generators while iterating over price (lambda) remains an important challenge. In addition, improving UC and ED solutions as the system size and resources grow without adversely impacting the simulation run time remains a problem. This trade-off between UC and ED solution quality and simulation run time remains a challenge. In this dissertation, we formulate, design, and investigate LR techniques that allow a high penetration of Distributed Energy Resources (DER) that can maintain an acceptable simulation run time.

1.3 Dissertation Outline

The chapters of the dissertation are as follows:

Chapter 2 briefly reviews literature that is relevant to UC and ED.

Chapter 3 formulates a UC model that estimates the line losses from the transmission network data. The model uses a heuristic that includes the estimated line losses and electrical distance of generation centers from load centers to differentiate between similar and identical generators. The proposed formulation can distinguish between similar and identical units when they are the marginal units, using their electrical distances from the load center. The solution quality can also be improved when compared to the classical LR formulation.

Chapter 4 benchmarks the formulation from Chapter 3 using Egret. First, the solution quality was investigated via a modified PJM 5 bus system. The system scalability is then investigated using the RTS-GMLC 73 bus system. The RTS-GMLC 73 bus system is modified to include identical units and then benchmarked with Egret.

Chapter 5 studies the computational efficiency of different LR formulations. First, the WECC 240 bus system data was formatted and a base UC model was designed. Then the impact of DR on system flexibility, peak load, market price, and LMP is considered. Third, the computational efficiency of the proposed formulation is considered using ALR. Fourth, a line flow penalty for transmission limit is proposed and implemented. The penalty is aimed at speeding up simulation run time and reducing the number of iterations in solving SCUC. Finally, the effect of a large volume of similar and identical units on the proposed formulation is considered.

1.4 Contributions

This work proposes a new model with a heuristic that takes advantage of estimated line losses for UC and ED. The estimated line losses act as additional cost penalties that distinguish between similar and identical units when they are not co-located. When compared to using the actual line loss calculation, the proposed algorithm is much faster. Units are also selected in a way that improves the OPF solution when compared with a lossless UC formulation. Numerical solutions show that the proposed algorithm compares well to the MIP solution

in small and large systems and scales linearly as the number of optimization intervals and system size increases.

A new algorithm that takes advantage of the incremental nature of LR is proposed. The algorithm incorporates further iteration over λ and offers a good trade-off between solution quality and scalability for large optimization problems.

A new line flow penalty is proposed to reduce the number of iterations and simulation run time. The line flow penalty is an extension of the line loss estimate and is localized at transmission lines with binding limits. Apart from the improvement in solution time, it is easy to select a penalty value for the system as there are little or no effects on solution quality for a wide range of penalty values.

Chapter 2

Literature Review

2.1 Unit Commitment and Economic Dispatch

The goal of performing UC and ED is to operate the system at the lowest cost possible at all times by committing the appropriate units and dispatching the proper amount of resources from each unit [89] while maintaining system security. In recent times, the committed units also have to track more significant uncertainties in the load, while concepts, such as DR can help dispatch load for frequency regulation. The effect of high penetration of DER on the power grid cannot be fully understood without fully understanding the additional layer of complexity this integration adds to UC and ED processes.

2.1.1 Unit Commitment

A generalized UC formulation was proposed by Baldick [6] for both hydro and thermal units. The objective function and system constraints are as follows [6, 55]

$$\min_{p_{it},u_{it},R_{it}} \{\sum_{t=1}^{NT}\sum_{i=1}^{NG}[C_i(P_{it},u_{it}) + S_i(u_{it}) + q_{it}R_{it}]\} \tag{2.1}$$

$$\sum_{i=1}^{NG} P_{it} = \sum_{j=1}^{ND} D_{jt} \qquad \forall t \tag{2.2}$$

$$P_i^{\min} u_{it} \leq P_{it} \leq P_i^{\max} u_{it} \qquad \forall i,\, \forall t \tag{2.3}$$

$$P_{it} + R_{it} \leq P_i^{\max} \qquad \forall i, \forall t \tag{2.4}$$

$$0 \leq R_{it} \leq u_{it}(RU_{i\tau}) \qquad \forall i, \forall t \tag{2.5}$$

$$\sum_{i=1}^{NG} R_{it} \geq R_t^{\min} \qquad \forall t \tag{2.6}$$

$$P_{it} - P_{i,t-1} \leq RU_i u_{i,t-1} + R_i^{\text{start}}(u_{it} - u_{i,t-1}) \qquad \forall i, \forall t \tag{2.7}$$

$$P_{it} - P_{i,t-1} \geq -RD_i u_{it} - R_i^{\text{shut}}(u_{i,t-1} - u_{it}) \qquad \forall i, \forall t \tag{2.8}$$

$$R_i^{\text{start}} = \max RU_i, P_i^{\min} \qquad \forall i \tag{2.9}$$

$$R_i^{\text{shut}} = \max RD_i, P_i^{\min} \qquad \forall i \tag{2.10}$$

$$\sum_{i=1}^{NG} GSF_{ki} P_{it} - \sum_{j=1}^{ND} GSF_{kj} D_{jt} \leq F_k^{\max} \qquad \forall k, \forall t \tag{2.11}$$

Equation (2.1) seeks to minimize the overall cost of generation by selecting the right combination of units. C is the cost of generation of unit P_i excluding the start-up/shut-down cost and reserve cost. P is the power output while i and t represent the unit and the time respectively. S is the unit start-up cost, R is the committed reserve, u indicates if a unit is committed or not ($u = 0/1$) and q is the capacity cost of the reserve. Constraint (2.2) guarantees that the demand is met at all times while (2.3) and (2.4) caps the unit's lower and upper limits and available reserve, respectively. Constraint (2.5) puts a cap on the maximum spinning reserve capacity while (2.6) indicates the minimum allowable reserve at a particular time. Constraints (2.7) and (2.8) reflect the ramp-up and ramp-down capabilities of each unit respectively. Constraints (2.9) and (2.10) ensure that the start-up reserve and shut-down reserve do not violate the minimum operational level of the unit ($P_i^{\min}$). Transmission limits are ensured by (2.11) using a DC load flow. The Generation Shift Factor (GSF) reflects a DC load flow approximation. Security constraints are considered implicit in the flow constraints.

2.1.2 Security Constrained Economic Dispatch

While UC determines which units and resources get committed, security constrained ED (SCED) optimally dispatches the committed resources to minimize the cost of operation,

considering the reliability and operational limits. Hence, the SCED formulations would not require constraints parameters like u_{it} and S_i which help decide what units or resources are committed. A formulation of SCED is as follows [6, 23, 55].

$$\min_{p_{it},R_{it}} \{\sum_{t=1}^{NT}\sum_{i=1}^{NG}[C_i(P_{it}) + q_{it}R_{it}]\} \tag{2.12}$$

$$\sum_{i=1}^{NG} P_{it} = \sum_{j=1}^{ND} D_{jt} \qquad \forall t \tag{2.13}$$

$$P_i^{\min} \leq P_{it} \leq P_i^{\max} \qquad \forall i,\, \forall t \tag{2.14}$$

$$P_{it} + R_{it} \leq P_i^{\max} \qquad \forall i,\, \forall t \tag{2.15}$$

$$0 \leq R_{it} \leq RU_{i\tau} \qquad \forall i,\, \forall t \tag{2.16}$$

$$\sum_{i=1}^{NG} R_{it} \geq R_t^{\min} \qquad \forall t \tag{2.17}$$

$$-RD_i\Delta t \leq P_{it} - P_{i,t-1} \leq RU_i\Delta t \qquad \forall i,\, \forall t \tag{2.18}$$

$$\sum_{i=1}^{NG} GSF_{ki}P_{it} - \sum_{j=1}^{ND} GSF_{kj}D_{jt} \leq F_k^{\max} \qquad \forall k,\, \forall t \tag{2.19}$$

The objective function in equation (2.12) is to minimize the overall cost of operation by determining the outputs of the already committed units. Constraint (2.13) balances the demand and supply, while constraints (2.14) and (2.15) cap the unit output and the spinning reserve respectively. Constraint (2.16) limits the reserve of a unit and (2.17) fixes the minimum required reserve by the system at time t. Constraint (2.18) limits the ramping rates of each unit and the transmission line flows are limited by constraint (2.19). Note ED must be solved as a part of the UC, although for computational efficiency it may be approximated.

2.2 Unit Commitment Formulations

Saravanan et al. [82] grouped UC formulations into three techniques, namely; conventional, non-conventional, and hybrid problem formulations. Exhaustive enumeration, branch

and bound, dynamic programming (DP), simulated annealing (SA), Mixed Integer Linear Programming (MILP), Lagrangian Relaxation (LR), Benders Decomposition, and Tabu search are some of the classified methods under conventional techniques. Land and Doig [50] proposed the branch and bound method for optimizing problems where some or all the variables are only allowed to exist as discrete values. Like the branch and bound method, the exhaustive enumeration method also deals with discrete variables. It is the easiest method to implement and it enumerates all possible combinations of the discrete variables, guaranteeing global minimum at the expense of computational time and resources [82]. The basic DP is similar to the exhaustive enumeration method in that it checks through all possible states at every interval. This method drops off infeasible states but still has to deal with a large number of feasible states. A large amount of memory, as well as computational time and resources, are required for obtaining a global optimum and hence, DP is generally not appropriate for solving large problems [81, 85]. The MIP technique is an improvement of the integer programming technique that allows for non-integer functions in the optimization problem. MIP improvements have led to the ability to solve large problems with a good level of accuracy. This is however possible at the expense of computational time and resources, [81]. The Benders Decomposition method solves the optimization problem in two stages. A master problem commits the units, which forms the second step sub-problems for ED. A shortcoming of the Benders Decomposition method is the difficulty in solving the master problem [81, 59]. The LR method is unique for its ability to relax and separate each unit from the coupling constraints that make solving UC problems difficult [13]. Unlike most optimization techniques, LR is intuitive, making it possible to track the progress of the solution at all times. The dual problem makes it possible to break the problem into smaller parts and units are committed by iteration over price. A major challenge for the fundamental LR technique is that there exists a duality gap (the difference between the optimal solution and the dual problem-solution). A second problem arises if there are many similar units in the system. Multiple solutions could have about the same cost (flat bottom) and many combinations of units give the same result. This could also lead to chattering from similar units that get committed or de-committed together when they are the marginal units [81, 82].

2.3 Unit Commitment and Identical Units

The impact of similar and identical units on the solution quality and simulation time has continued to garner the attention of researchers. Qiaozhu et al. [76] studied the impact of identical units on LR based methods. The duality gap and solution oscillations increase considerably, leading to poor solutions and extended simulation time. They applied ALR and a surrogate subgradient to the problem while solving subproblems in a successive manner. They observed considerable improvements in the solution quality when compared to the classical LR method. Nikolaidis et al. [64] approached the identical units issue in UC, using a double decomposition method. They considered a situation where the simulation time is prioritized over solution quality. The proposed approach greatly improved the simulation time.

When UC problems are solved with MIP, symmetries are observed within the solutions [17, 47, 54, 60, 68]. Symmetries in optimization problems occur when multiple combinations of units with the same objective (or almost equal objective depending on the MIP gap tolerance) are observed. The addition of identical units into the UC problems makes it even harder to solve. Schrock in [83] considered the effect of identical and nearly identical generators on UC solution and simulation time, using symmetry-exploiting techniques. The research concluded that the symmetry-exploiting techniques can be used as a backup for standard models especially when time is of the essence. Knueven et al. in [45] reformulated the MILP by aggregating units with identical properties. They reported that the redundancy associated with symmetry solutions is greatly reduced, thereby reducing the associated computational difficulty.

2.4 Unit Commitment and Simulation Time

The simulation time for SCUC continues to be a challenge for ISOs as the number of small units continues to grow in the power system. Researchers have continued to focus on ways of reducing the simulation run time with minimal or no impact on solution quality. This need

is part of the reason for the introduction of the Grid Optimization (GO) Competition by the Advanced Research Projects Agency-Energy (ARPA-E) (https://gocompetition.energy.gov).

Ostrowski et al. proposed tight MILP formulations that can considerably improve simulation time. They introduced new constraints which are incorporated into the operating region of the generators [67]. Several researchers have also focused on aggregating generators to reduce the number of decision variables. Langrene et al. considered the effect of the increasing number of constraints with the increasing number of units. They proposed a dynamic way of implementing the constraints in the aggregated units. The problem size can be considerably reduced. A clustered UC approach was proposed by Poncelet et al. for system and resource planning [74]. Based on the difficulty of solving UC problems for time periods beyond one week, they grouped units based on the technology type and year of investment. The proposed model has a large impact on the simulation time and does have the potential for integration into current power system models. The research by Palmintier et al. [69] focuses on reducing the computational time by aggregating similar (not identical) units. The idea here is to replace binary variables with integer variables with the ability to commit each unit independently. By reducing the overall decision variables, they reported that the proposed model can speed up the simulation time with solution errors of up to 1.8%. Meus et al. in [62] considered the benefits of clustering similar or identical units. They highlighted the possible solution errors that can occur from aggregating nonidentical units. Finally, they combined a clustered UC with a traditional UC which can reduce computational time while guaranteeing an acceptable solution.

2.5 Unit Commitment and Transmission Flow Constraints

Solving non-convex optimization problems can be difficult even for a relatively small system. A type of constraint that could make the already difficult non-convex problem even much harder is transmission flow constraints. Hence, a lot of research efforts have gone into reducing the impact of this constraint on UC solution quality and simulation time. In order

to ensure the feasibility of SCED, Ma et al. in [59] proposed a Benders decomposition UC approach. The master problem solves a relaxed UC problem (no transmission constraints) using ALR while subproblems are solved by adjusting the output of the committed units. In a different study [58], they integrated voltage constraints into the transmission constraint problem. Here, the subproblem is further broken into two subproblems for active and reactive power flows respectively. They reported that the iterative process can minimize the generation production cost. Zhao and Yamashiro in [102] proposed a successive de-commitment UC technique while tracking transmission losses and flow limits. The method outperformed the dynamic programming method (DP) which was widely used during the early days of power system deregulation. An integrated SCUC approach was proposed by Cong et al. where transmission line and natural gas transmission constraints are considered [22]. A decomposition method was used, creating different subproblems for electrical transmission lines and gas transmission. This is an iterative process where the constraint data is updated for new transmission violations and this is reintroduced into the master problem. Lotfjou et al. also did a study that considers the economic benefits of integrating DC transmission lines into the SCUC problem [57]. A master problem solves the UC problem while the subproblems take care of the hourly transmission constraints. They reported an improvement from the simplified DC method but noted that replacing AC lines with DC lines can negatively impact solution convergence. A transmission switching approach was introduced into the SCUC by Khodaei and Shahidehpour to mitigate transmission violation and improve solution quality [43]. Like most of the previous studies, they used a decomposition method where the subproblem takes care of the transmission constraints and violations. If the subproblem is unable to mitigate all violations, the required changes are included in the master problem for the next iteration. Pandzic et al. in [70] proposed a 3 binary variable approach (which includes the power generation, start-up, and shut-down cost) instead of the commonly used single binary variables. They reported that the improvement in the proposed method is a result of the depth of the cut. A cut that leads to a small duality gap reduces the solution search space and hence, improves the computational performance. Lee et al. in [51] proposed a multi-stage robust UC with transmission constraints. Using the cutting plan and column generation methods, they

reported a great reduction in solution time. Rabbuni and Guru in [77] considered improving the computational time for UC with transmission constraints by solving the problem via a piecewise linear cost function instead of a quadratic cost function. They observed that the improvement in computational time comes at a cost in the solution quality. Dvorkin et al. [26] investigated a transmission-constrained UC, using stochastic optimization for initial solutions and switching to interval optimization depending on system conditions. The hybrid optimization method is computationally intensive but outperforms the classical stochastic UC method. Papavasiliou et al. studied a transmission-constrained UC using parallel computing [71]. The uncertainty in the system is considered using LR for stochastic UC. The simulation run time is validated using well-studied UC scenarios. Li et al. [53] studied the effect of transmission constraints on UC using a combined heat and power (CHP) model. They highlighted the difficulty associated with wind energy integration in a CHP model. For a well-managed system, They showed some possible benefits of wind integration using the proposed model. The studies in [33, 56] considered the effect of UC with transmission constraints in AC models. A data-driven UC approach was proposed by Pineda et al. [73]. Using historical data, transmission lines that are unlikely to reach or exceed their flow limits are identified and are removed from the model. They reported a considerable improvement in simulation with minimal or no impact on solution quality. Chen et al. [15] proposed an incremental approach to increasing the number of transmission constraints in the SCUC DA problem. Identified transmission lines with binding transmission limits are added to the optimization problem in batches and the iteration process continues until no more violations are found.

2.6 Unit Commitment and Distributed Algorithms

To achieve global optimums instead of local solutions, UC and ED algorithms are usually modeled as centralized algorithms. The concept of centralized optimization algorithms is however being disrupted by the steady growth of DER and reductions of thermal units like coal in the energy mix. To replace the capacity of a decommissioned coal plant reliably, several DER units will be required. The replacement of capacity is needed because the

increase in annual energy consumption is slowing and in some years negative. Figure 2.1 shows the trend in annual U.S. energy consumption [28]. With energy consumption staying relatively flat and a high level of DER penetration, the number of variables and constraints required to solve a typical UC and ED problem will be beyond the capability of most centralized MIP formulations.

MIP is a state-of-the-art optimization technique but does not scale well with the increase in the number of discrete variables and constraints. In order to deal with the effect of the steady increase in DER on the electric power grid, many researchers are focused on distributed optimization algorithms. Kargarian and Fu [40] proposed a hierarchical model of systems of systems (SoS) for SCUC. While considering an active distribution grid (ADG) that can be independently controlled by a distribution company (DISCO). They also accounted for the transmission grid that is controlled by the ISO. To avoid the bottleneck associated with MIP for problems of this nature, they decoupled the SCUC problem into an SoS and introduced a decentralized decision-making solution to model the interaction between the SoS. The studies only account for the integration of dispatchable DGs like diesel generators and gas turbines. Further studies incorporating non-dispatchable DGs, such as wind and solar are needed for a robust and generalized conclusion. Feizollahi et al. [32] worked on improving scalability and computational speed by focusing on a large-scale decentralized optimization model. Their formulation improves on the alternating direction method of multiplier (ADMM) by applying heuristics. In a self-commitment setting, generation companies' sensitive information, as well as market participants' cost data are protected since only phase angle data from boundary buses are exchanged. In general, their work favors a decentralized system of a large number of small regions over a few large regions. It should be noted that their work was based on an hourly time horizon which does not capture the true cost of uncertainties.

In Kargarian et al. [42], the proposed optimization technique focused on reducing the decision variables at all times. Sub-problems are connected by tie-lines, using auxiliary variables instead of the actual variable that couples the zones. The proposed method also takes advantage of LR for inter-regional calculations and MIP method for local calculations of each sub-problems. Similar to previous decentralized optimization techniques, their

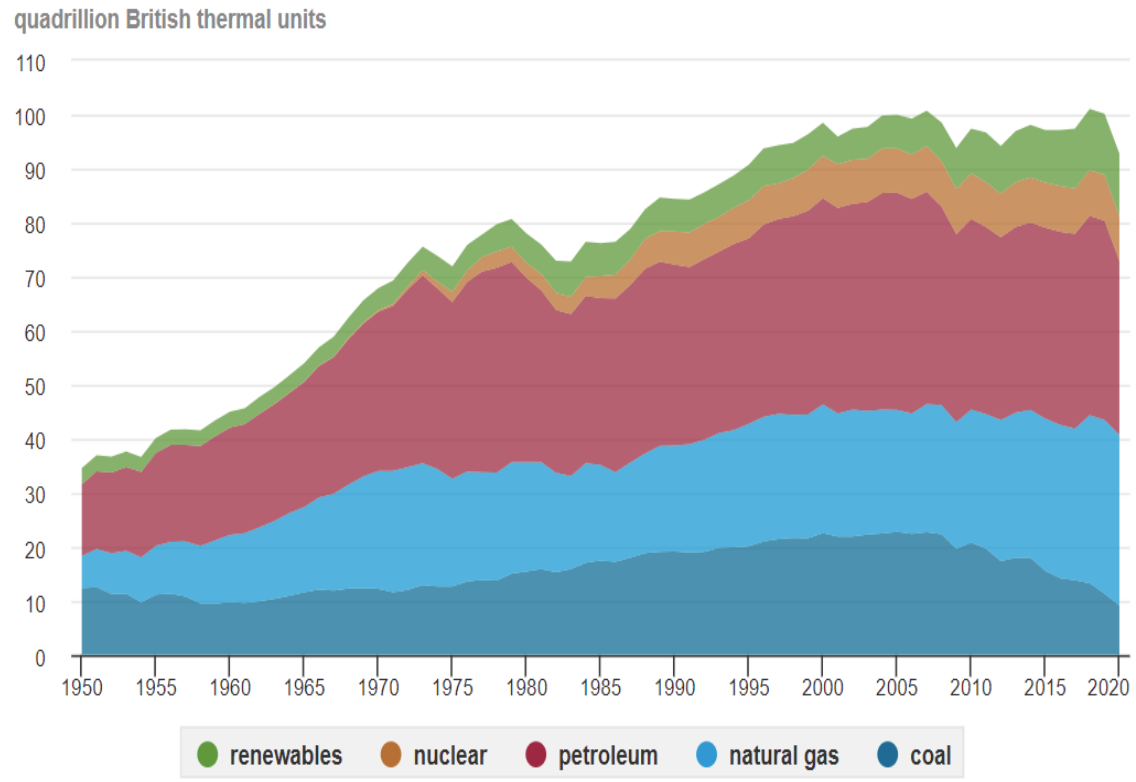
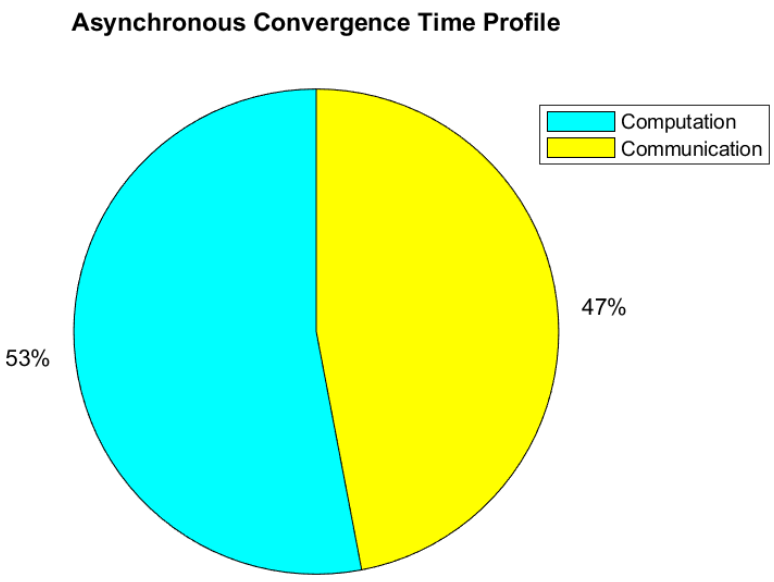


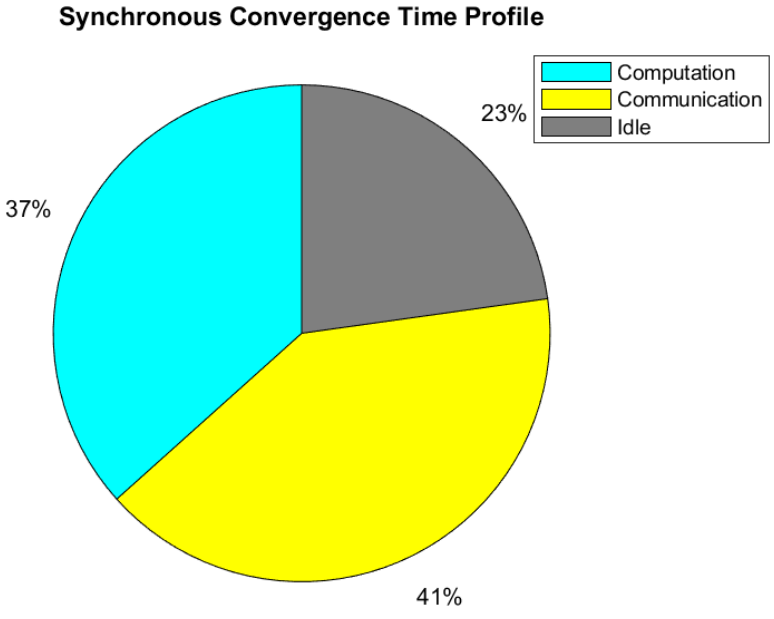
Figure 2.1: Major energy sources in the U.S. 1950-2020 [28]

algorithm is synchronous. This means that all shared decision variables can only be updated when all sub-problems are completely solved. Although this is an improvement from the centralized optimization method, the acceleration in generation scheduling time is limited by the slowest sub-problem solving time. The asynchronous decentralized optimization techniques is considered a solution to the above mentioned challenge. Bragin and Luh in [11] addressed the unacceptable optimization CPU time by introducing asynchronism into the existing decentralized optimization formulations. The decentralized sub-problems are calculated individually but shared variables are updated at predefined time intervals. Heuristics like shrinking step sizes as the optimization computation progresses helps avoid chattering around the optimum solution. Because the alternate direction method of multipliers (ADMM) is only appropriate for convex problems and cannot be easily applied to MILP, the surrogate Lagrangian relaxation (SLR) method is introduced. They reported that the proposed method is robust and has a fast convergence rate. A further study will be needed with the system transmission constraints included to better understand the scalability of the proposed method. Ramanan et al. [78] proposed an asynchronous decentralized optimization algorithm that extends on some recent results of ADMM formulations. An IEEE 118 bus system was zoned into 10 sub-regions and a comparison of synchronous and asynchronous algorithms was made. Figure 2.2 shows the percentage of resources allocated to computation, inter-regional communication, and system idle time while Figure 2.3 shows the actual computation and communication time.

Wang et al. [97] proposed a decentralized network constrained UC (NCUC) where the power flow data across the tie-lines are coupling variables instead of the typical bus voltage angles. They reported an improved convergence when compared to the bus voltage angle method of coupling. To guarantee convergence of the non-convex problem, several heuristics were applied to the ADMM based algorithm. The algorithm was then changed from synchronous to asynchronous for further studies. They found that the asynchronous algorithm helps with the computation time but does not necessarily guarantee convergence. Apart from changing decentralized UC algorithms from synchronous to asynchronous, researchers also proposed cases where generation companies can react to signals from the

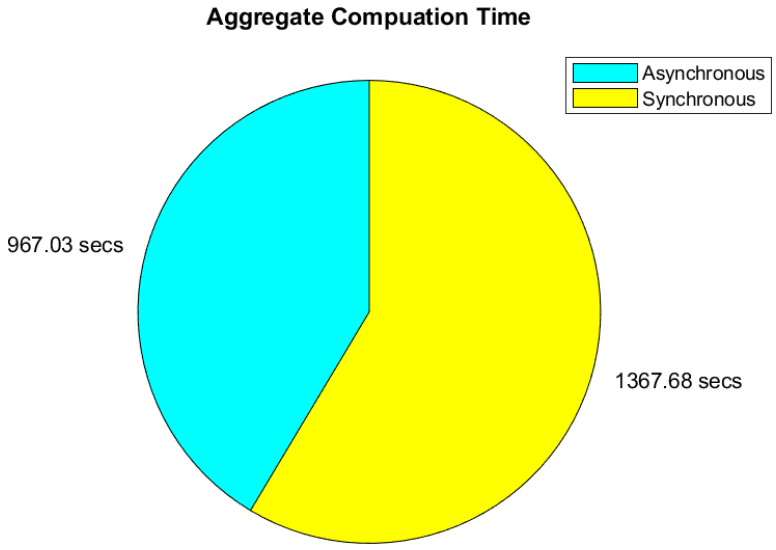


(a)

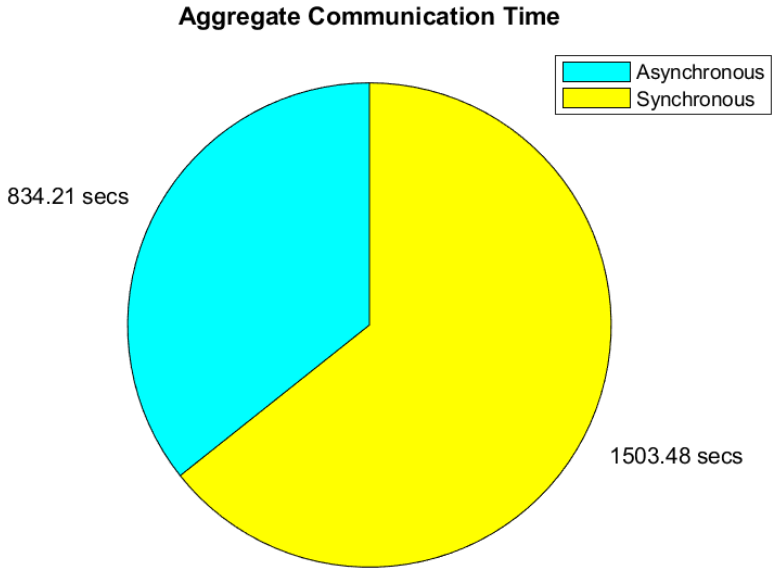


(b)

Figure 2.2: Percentage time allocation for Asynchronous and Synchronous Algorithms [78]



(a)



(b)

Figure 2.3: Actual aggregate Computation and Communication time for Asynchronous and Synchronous Algorithms [78]

ISO/RTO by self-commit their resources. This idea was well studied at the peak of the electrical power market deregulation movement [32].

2.7 Unit Commitment and Flexibility Requirements

As the percentage capacity of DER continues to increase in the power grid, many UC studies have focused on the new flexibility requirements of the grid. The research performed by Shuai et al. [84] centers on mitigating negative environmental effects while improving the economics and the reliability of the power grid by taking into account the effect of unit flexibility requirements and environmental constraints. The environmental constraints here are ecological regulations for hydro units and emission limits for high CO_2 emitting units. A formal definition of system flexibility was proposed by Tongxin et al. [91]. System flexibility was classified into four major factors namely: system response time, additional cost thresholds, available system control action, and maximum allowed system deviation. A bi-level mathematical formulation of security constraint unit commitment (SCUC) with gas transmission flexibility was investigated by Badakhshan et al. [5]. The uncertainty in gas supply was modeled using fuzzy logic while the nonlinearity in gas transmission was addressed via a genetic algorithm. Numerical results indicate an improvement in the cost of scheduling and mitigation to the non-feasible solutions that may arise if gas transmission limitations are not considered.

Gonzalez et al. [34] also investigated the power systems' flexibility benefits that can be derived by considering a network constraint Combined Heat and Power (CHP) UC of a 24-hours time horizon. The studies in [95] proposed a model that ties the flexibility of DR resources with a high level of wind integration. The work utilizes a two-stage stochastic UC formulation that considers a day-ahead and an intra-day time horizon that offset the effect of variation of wind resource, taking advantage of DR. It was concluded that associated cost to response time is the most valuable indicator for flexible DR scheduling. Zhang et al. in [101] investigated a unified UC formulation framework for continuous evaluation of a flexible and sustainable power system. Their work focused on creating a backbone on which simulations can be performed in the planning of the future power system. A fast linear programming

(LP) model was formulated to incorporate the complexities that arise from the integration of a large share of DER and multiple time scales. They concluded that the proposed model is more suitable for flexibility studies when compared with binary unit commitment (BUC) and MILP. An improved Clustered Unit Commitment (CUC) model was proposed by Germán et al. [65], for proper classification of power system flexibility requirements. By taking advantage of unit constraints, such as ramp-rate limits and startup/shutdown, they were able to show a more precise representation of the hidden flexibility of CUC. Jain et al. [37] investigated a framework of seasonal SCUC to better understand the power system flexibility capacity that is required for a high level integration of DER. They considered thermal units, such as nuclear plants, and expensive resources, e.g., Energy Storage Systems (ESS). It was concluded that a day-ahead SCUC does not give an accurate account of the necessary curtailments, as well as flexibility requirements for system stability. At a low level of DER integration, it is economical to improve the operational flexibility of existing resources while investing in flexible energy storage resources will help with a high level of DER penetration.

2.8 Unit Commitment and Industry Practices

In 2002, PJM actively worked on switching from the LR to MIP optimization technique. Although the LR technique was sufficient for solving the size of the problem at that time, PJM engineers had to consider that market deregulation was going to more than double the current size as well as raise new concerns of market fairness with the UC solution. Research has shown that when compared to LR, MIP guarantees global optimality, improved capability for modeling complex constraints, and is more user-friendly [86]. Developers, however, found that as the size of the problem increases, the required memory size and run time increases exponentially with MIP while LR increases linearly as seen in Figure 2.4. This complexity makes solving the PJM Reliability Analysis problem, which normally spans a 3-7 day horizon, difficult. To solve this problem for a 7-day horizon, the first 2 days were modeled with a 1-hour time period, the next two days are modeled as a 2-hour time period while the last 3 days are modeled as a 4-hour time period. This reduces the size of the problem while sacrificing some accuracy in the solution.

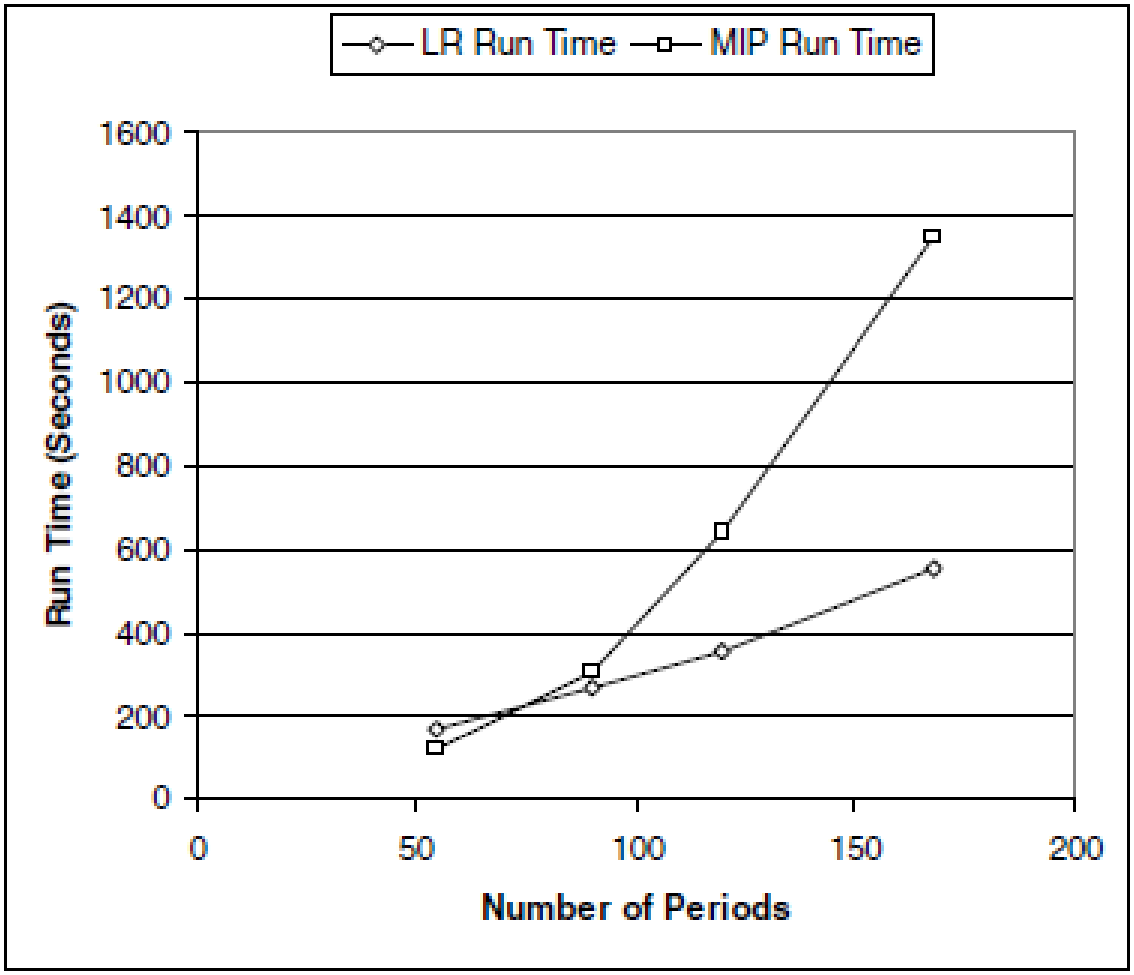


Figure 2.4: Run Time vs Number of Periods for LR and MIP [86]

In recent times, MISO has reported that even a Day-Ahead problem could be difficult to solve as the size and complexity of the power market continues to grow. The increase in virtual trading volume combined with transmission constraints can greatly increase the density of the matrix of the MIP optimization model [15]. A dense system in this case refers to a matrix with a large number of non-zeros in the constraint matrix of the optimization model. At the time of this study in late 2016, MISO only observed a few cases of undesirable performance, which can be improved by increasing the acceptable solution time. The frequency of this occurrence is expected to increase with the rise in the volume of virtual trading and development in the electric power market. All of the above has led to an ongoing interest in this area of research.

The maximum allowed time for solving a day-ahead problem in the MISO market is 4 hours. A typical day in the MISO electric market includes solving the day-ahead SCUC problem, verifying the result for uncommitted units or units dispatched at losses, and then, fixing issues by repeating the initial steps or manually adjusting input data if they run out of the allotted 4 hours time limit. Market participants match the clearing price with their expected profits and may dispute the market solution, hence, the need for solution verification. The above challenges underline the importance of solving the SCUC problem incrementally. Incremental problem solving is an edge the LR has over MIP. One of MISO's approaches to solving this problem was collaborating with IBM to integrate incremental heuristics into their commercial solver. The solver is designed to solve optimization problems using LR on transmission constraints and it is called IBM_LR.

Chapter 3

Unit Commitment Formulation for Scalable Scheduling

In this chapter, we propose a deterministic unit commitment (UC) and economic dispatch (ED) model that takes advantage of the incremental and intuitive nature of Lagrangian Relaxation (LR) to differentiate between similar units, reduce over-generation, and minimize the duality gap that is associated with non-convex optimization problems.

3.1 Model and Formulation of Unit Commitment and Economic Dispatch

As indicated in Section 2.8, the fundamental MIP algorithm approach can determine the best combination of units during the UC process. For a large system with many units, there are usually multiple optimal combinations resulting in multiple optimal solutions. The selected optimal solution might be arbitrary, leaving out some units that could have been profitable at the market price. Such units are termed "out-of-money" for that schedule [15]. Market participants who are owners of "out-of-money" resources often dispute such market solutions. In some cases, units are out-of-money for system security reasons while some other cases are associated with bad solutions. ISOs and researchers in this field are therefore

interested in optimization algorithms that reduce the solution verification time and avoid unnecessary solution disputes.

While the LR algorithm solves optimization problems incrementally, the fundamental MIP algorithm does not necessarily solve optimization problems by prioritizing the cheaper units. Figure 3.1 shows an ideal bidding market where only bids that are equal to or below the market price are accepted (bids in the lower left corner). In the MISO market, for example, engineers are considering using the LR technique because units are not committed in an incremental manner under the MIP technique.

3.1.1 Over-Generation Resulting from Similar and Identical Units

A common issue associated with the LR optimization technique is the problem of over-generation. When units with similar characteristics are present within a power system and they are the marginal units at that point in time, then, chattering (switching back and forth among committed units between iterations) and over-generation can occur. A second reason for over-generation is the high penetration and injection of renewable energy resources in the power grid at times of low demand can lead to curtailment [100]. In this chapter, the focus is only on the over-generation problems that are related to similar units. To take full advantage of the incremental nature of the LR technique without increasing the simulation run time, we formulate some heuristics that penalizes line losses to mitigate the over-generation problem by differentiating between similar units.

3.2 Non-Convex Optimization

The optimum solutions of convex and bounded optimization problems are always guaranteed. In reality, most optimization problems are non-convex in nature and the optimum solutions are not guaranteed. The cost functions of non-convex optimization problems are usually non-continuous and more complex in nature. In addition to the cost function, some of the variables are constrained to be binary (1 or 0) and/or integers.

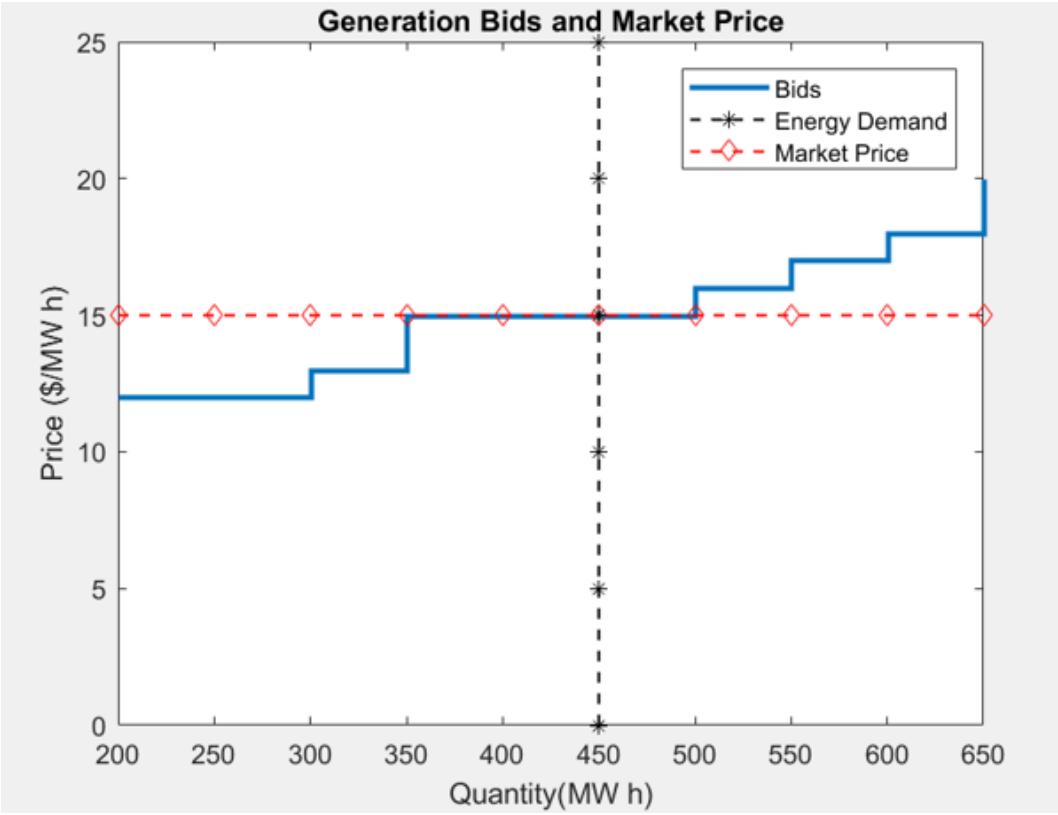


Figure 3.1: Power market bids and actual market price

3.2.1 Lagrangian Multiplier and the Dual Variable

When solving convex optimization problems with the Lagrange method, the Lagrange multiplier and the primal can be obtained directly by eliminating the problem variables. The problems can also be solved with optimum solution guaranteed by directly solving for the Lagrange multiplier. In this case, the Lagrange multiplier is termed a dual variable, and solving UC problems by using the dual variable is termed Lagrange Relaxation [99].

When LR is applied to non-convex problems, the primal and the dual value are not equal and the difference is termed a duality gap. The degree of accuracy can be measured by the duality gap. The duality gap is the ratio of the difference between the primal (J^*) and dual value (q^*) to the dual value [21], and it is expressed as

$$\epsilon = \frac{J^* - q^*}{q^*} \tag{3.1}$$

The closer to zero a duality gap is, the closer the solution to the optimum. For this reason, most LR research has focused on ways of reducing the duality gap without increasing the computational time and burden. The typical approach to this problem is by improving or searching for a superior method of updating the value of lambda during the iteration process [88]. In this work, the duality gap and generation production cost are reduced by penalizing an approximation of the line losses. Using the generation shift factor (GSF), the distributed effect of the line-flow arising from the power injection from each bus is approximated and applied to penalize the power injection at that bus.

3.2.2 Lagrangian Relaxation

From subsection 2.1.1 of page 15, the Lagrangian for the UC formulation can be re-written as

$$\mathcal{L}(P, U, \lambda) = \sum_{t=1}^{T} \sum_{i=1}^{NG} (a_i + b_i P_i + c_i P_i^2) U_{it} + \sum_{t=1}^{T} \lambda^t \left(P_{\text{load}}^t - \sum_{i=1}^{NG} P_i U_{it} \right) \tag{3.2}$$

the coupling constraint ($P^t_{\text{load}} - \sum_{i=1}^{NG} P_i U_{it}$) in the second term of the Lagrangian equation makes the problem more difficult to solve. To simplify the problem using LR, the coupling constraint is relaxed [99]. The dual value can be expressed as

$$q^*(\lambda) = \max_{\lambda^t} q(\lambda) \tag{3.3}$$

this is the maximization of the Lagrangian function with respect to λ and the relationship between the primal and the dual is expressed as

$$q(\lambda) = \min_{P_i^t, U_i^t} \mathcal{L}(P, U, \lambda) \tag{3.4}$$

since the dual variable (λ) cannot be expressed explicitly, a good initial value is chosen and fixed for minimizing $\mathcal{L}(P, U, \lambda)$ in equation 3.4 with respect to P_i^t and U_i^t. Using the new values of P_i^t and U_i^t, the value of λ^t is updated and equation 3.3 is then maximized with respect to λ^t. The process is repeated until the relative duality gap (ϵ) from equation 3.1 reaches an acceptable tolerance. If the Lagrangian function is differentiable, λ^t can be updated by the gradient method and can be expressed as

$$\lambda^{k+1} = \lambda^k + \left[\frac{\partial}{\partial \lambda} q(\lambda)\right] \alpha \tag{3.5}$$

where λ^k is the λ at iteration k, and the partial derivative of equation 3.2 with respect to λ gives

$$\frac{\partial}{\partial \lambda} q(\lambda) = \sum_{t=1}^{T} \left(P^t_{\text{load}} - \sum_{i=1}^{NG} P_i U_{it} \right) \tag{3.6}$$

To enhance convergence, the value of α is dependent on the sign of the gradient (equation 3.6). Hence, the step size in one direction is greater than the step size in the other direction and it is mathematically expressed as

$$\alpha = m \quad \text{for} \quad \frac{\partial}{\partial \lambda} q(\lambda) > 0 \tag{3.7}$$

$$\alpha = n \quad \text{for} \quad \frac{\partial}{\partial \lambda} q(\lambda) < 0 \tag{3.8}$$

where $m > n$. Assuming that the value of λ^t is fixed, then equation 3.2 can be rewritten as

$$\mathcal{L}(P, U, \lambda^t) = \sum_{t=1}^{T} \sum_{i=1}^{NG} (a_i + b_i P_i + c_i P_i^2) U_{it} + \sum_{t=1}^{T} \lambda^t P_{\text{load}}^t - \sum_{t=1}^{T} \sum_{i=1}^{NG} \lambda^t P_i U_{it} \tag{3.9}$$

where the term $\lambda^t P_{\text{load}}^t$ is a constant and can be eliminated. The resulting equation is

$$\mathcal{L}(P, U, \lambda^t) = \sum_{i=1}^{NG} \left[\sum_{t=1}^{T} \left\{ (a_i + b_i P_i + c_i P_i^2) U_{it} - \lambda^t P_i U_{it} \right\} \right] \tag{3.10}$$

it can be seen from equation 3.10 that each generator unit i can be separated as

$$\mathcal{L}(P, U, \lambda^t) = \sum_{t=1}^{T} \left\{ (a_i + b_i P_i + c_i P_i^2) U_{it} - \lambda^t P_i U_{it} \right\} \tag{3.11}$$

and can be minimized independently as

$$\min \mathcal{L}(P, U, \lambda^t) = \min \sum_{t=1}^{T} \left\{ (a_i + b_i P_i + c_i P_i^2) U_{it} - \lambda^t P_i U_{it} \right\} \tag{3.12}$$

since a unit is online when $U_{it} = 1$ and offline when $U_{it} = 0$. The solution of equation 3.11 can only be less than 0 when $U_{it} = 1$ and the combination of P_i and λ^t gives a negative value as expressed below

$$\left\{ (a_i + b_i P_i + c_i P_i^2) U_{it} - \lambda^t P_i U_{it} \right\} < 0 \tag{3.13}$$

The generation output value (P_i) is updated as shown below

$$P_i = [\frac{(\lambda - b_i)}{2c_i}] \tag{3.14}$$

while the value of λ is updated as seen in equations 3.5 to 3.8.

3.2.3 Unit Commitment with Line Losses

Most simplified UC and ED problems are generally formulated without the network limits and losses. In reality, network limits and losses need to be accounted for, especially during or after solving the ED problem [14, 38, 48]. The energy balance equations (2.2 and 2.13) in Section 2.1 hold for lossless systems. A system with losses accounted for can be mathematically represented as

$$\sum_{i=1}^{NG} P_i = P_{\text{load}} + P_{\text{Loss}} \tag{3.15}$$

The marginal loss price is a function of the delivery factor (DF) [52] and can be expressed as

$$DF_i = 1 - LF_i = 1 - \frac{\partial(P_{\text{Loss}})}{\partial P_i} \tag{3.16}$$

where

DF_i = delivery factor at bus i;

LF_i = loss factor at bus i;

P_{Loss} = total system loss;

P_i = injected power at bus i;

$\frac{\partial(P_{\text{Loss}})}{\partial P_i}$ = incremental transmission loss

In this work, we formulate P_{Loss} as a function of line flow as will be seen in the next section.

3.3 Heuristic Formulation for Line-Losses

Start with the general Lagrangian formulation for UC as seen below

$$\mathcal{L}(P, U, \lambda) = \sum_{t=1}^{T}\sum_{i=1}^{NG}(a_i + b_i P_i + c_i P_i^2)U_{it} + \sum_{t=1}^{T}\lambda^t(P_{\text{load}}^t - \sum_{i=1}^{NG} P_i U_{it}) \tag{3.17}$$

Note that the start-up and shutdown costs are not considered in this chapter. Instead of using the actual AC line-loss formulation, a heuristic is formulated to penalize the line flow.

If a generator is far away from a load center, a closer generator might be committed even if it is a more expensive generator. In equation 3.18 the term $(L^t_{\text{flow}}(P_i))^2 R_k$ is added to the load (P^t_{load}) to estimate the line losses.

$$\mathcal{L}(P, U, \lambda) = \sum_{t=1}^{T} \sum_{i=1}^{NG} (a_i + b_i P_i + c_i P_i^2) U_{it} + \sum_{t=1}^{T} \lambda^t (P^t_{\text{load}} + \sum_{k=1}^{NK} (L^t_{\text{flow}}(P_i))^2 R_k - \sum_{i=1}^{NG} P_i U_{it}) \quad (3.18)$$

where

NK = the total number of lines that are online in a time period

R_k = the line resistance for line k

The term $(L^t_{\text{flow}}(P_i))^2 R_k$ is proportional to the square of the generation shift factor (GSF) multiplied by the resistance (R_k) and can be expressed as

$$\sum_{k=1}^{NK} (L^t_{\text{flow}}(P_i))^2 R_k \quad \propto \quad \sum_{i=1}^{NG} GSF_{k-i}(P_i - D_i) \cdot R_k \cdot \sum_{i=1}^{NG} GSF_{k-i}(P_i - D_i) \quad (3.19)$$

where

D_i = the load at bus i

$P_i - D_i$ = the injected power at bus i

$\boldsymbol{P_{inj}} = \boldsymbol{P} - \boldsymbol{D}$ is the vector of the net injected power at each bus

The loss term from equation 3.19 can be generalized as

$$\sum_{k=1}^{NK} (L^t_{\text{flow}}(P_i))^2 R_k \quad \propto \quad \boldsymbol{P_{inj}^T} \cdot \boldsymbol{W} \cdot \boldsymbol{P_{inj}} \quad (3.20)$$

where $\boldsymbol{W}$ is a weighting factor and it is a symmetric matrix that is derived by multiplying a diagonal matrix of the resistance $\boldsymbol{R}$ on both sides by the $\boldsymbol{GSF}$ as shown below

$$\boldsymbol{W} = \boldsymbol{GSF^T} \cdot \boldsymbol{R} \cdot \boldsymbol{GSF} \quad (3.21)$$

The new Lagrangian function is then approximated as shown below

$$\mathcal{L}(P,U,\lambda) = \sum_{t=1}^{T}\sum_{i=1}^{NG}(a_i + b_iP_i + c_iP_i^2)U_{it} + \sum_{t=1}^{T}\lambda^t(P_{\text{load}}^t + \boldsymbol{P_{inj}^T}\cdot\boldsymbol{W}\cdot\boldsymbol{P_{inj}} - \sum_{i=1}^{NG}P_iU_{it}) \quad (3.22)$$

Decoupling equation 3.22 and taking the partial derivatives with respect to P_i and λ^t, we have the following expressions

$$\frac{\partial\mathcal{L}(P,U,\lambda)}{\partial P_i} = [b_i + 2c_iP_i + 2\lambda^t(\boldsymbol{P_{inj}^T}\cdot\boldsymbol{W}\cdot\frac{\partial\boldsymbol{P_{inj}}}{\partial P_i}) - \lambda^t]U_{it} \quad (3.23)$$

$$\frac{\partial\mathcal{L}(P,U,\lambda)}{\partial\lambda} = P_{\text{load}}^t + \boldsymbol{P_{inj}^T}\cdot\boldsymbol{W}\cdot\boldsymbol{P_{inj}} - \sum_{i=1}^{NG}P_iU_{it} \quad (3.24)$$

From equation 3.23 the term $\frac{\partial\boldsymbol{P_{inj}}}{\partial P_i}$ will be a vector with all zeros except at the location i where the value is 1. Although the generators are not decoupled from each other since the term $\boldsymbol{P_{inj}^T}$ couples all the generators, the problem in equation 3.23 is simplified and linear. P_i can be expresses as a linear combination of the *coordination equation* (CE) [79] and the heuristic (h) as shown in equation 3.26 and equation 3.27 respectively.

$$P_i = [\frac{(\lambda - b_i)}{2c_i}] - [\frac{\lambda}{c_i}\cdot\boldsymbol{P_{inj}^T}\cdot\boldsymbol{W}\cdot\frac{\partial\boldsymbol{P_{inj}}}{\partial P_i}] \quad (3.25)$$

$$CE = [\frac{(\lambda - b_i)}{2c_i}] \quad (3.26)$$

$$h = [\frac{\lambda}{c_i}\cdot\boldsymbol{P_{inj}^T}\cdot\boldsymbol{W}\cdot\frac{\partial\boldsymbol{P_{inj}}}{\partial P_i}] \quad (3.27)$$

The power of the heuristic from equation 3.27 is seen when it is scaled appropriately to the system. One method of scaling the heuristic is by normalizing it such that the maximum penalty is less than the capacity of the smallest unit during iterations. A second approach is to multiply directly by a carefully chosen scaling factor.

3.3.1 Formulation and Code Implementation

Figure 3.2 shows the general concept of the LR algorithm. During the data-loading process, the PTDF is generated from the network data using the makePTDF command in **MATPOWER** [103]. At the initialization stage, all starting values are set including λ(s) and the step sizes. Parameters, such as, ramp-up, ramp-down, minimum-up time, and maximum-down time, are set using the generation output values from the previous period. With all constants in place, the UC (U_i) and the generator output values (P_i) are initially updated by equation 3.14. The estimated P_i values and the bus load D_i are combined to calculate the injected power at each bus. The modified line flow is then updated as seen in equations 3.19 to 3.21. Using the above values a final P_i estimate for the iteration process is obtained as seen in equation 3.25. The dual value q^* is calculated from the values of P_i and the commitment U_i. The ED is solved using quadratic programming function in **MATLAB** [90]. The required parameters for solving the ED are the UC values (U_i), minimum output limits ($P_i^{\min}$), maximum output limits ($P_i^{\max}$), ramp-up limits, ramp-down limits, minimum-up time, and maximum-down time. The duality gap is calculated during each iteration using the objective (J^*) of the ED and the dual value (q^*) as seen in equation 3.1. If the relative duality gap meets the acceptable tolerance or the maximum number of iterations is reached, the iteration process is terminated.

3.3.2 Modified PJM 5 Bus System

A modified PJM 5 bus system is used for testing the above UC formulation [31, 52]. In this case, there are 4 generators instead of 5 generators and for simplicity only one generator is connected to bus 1 as shown in Figure 3.3. To understand how generators with similar parameters contribute to over commitment as well as over generation, generator 1 and 3 are made similar generators with all parameters identical except that the maximum capacity of generator 1 is 170 MW while that of generator 3 is 200 MW. Parameters of generators 2 and 4 are similar and they are the cheaper generators as shown in Table 3.1. Generators 2 and 3 are closer to the load center while generators 1 and 4 are further away from the load center.

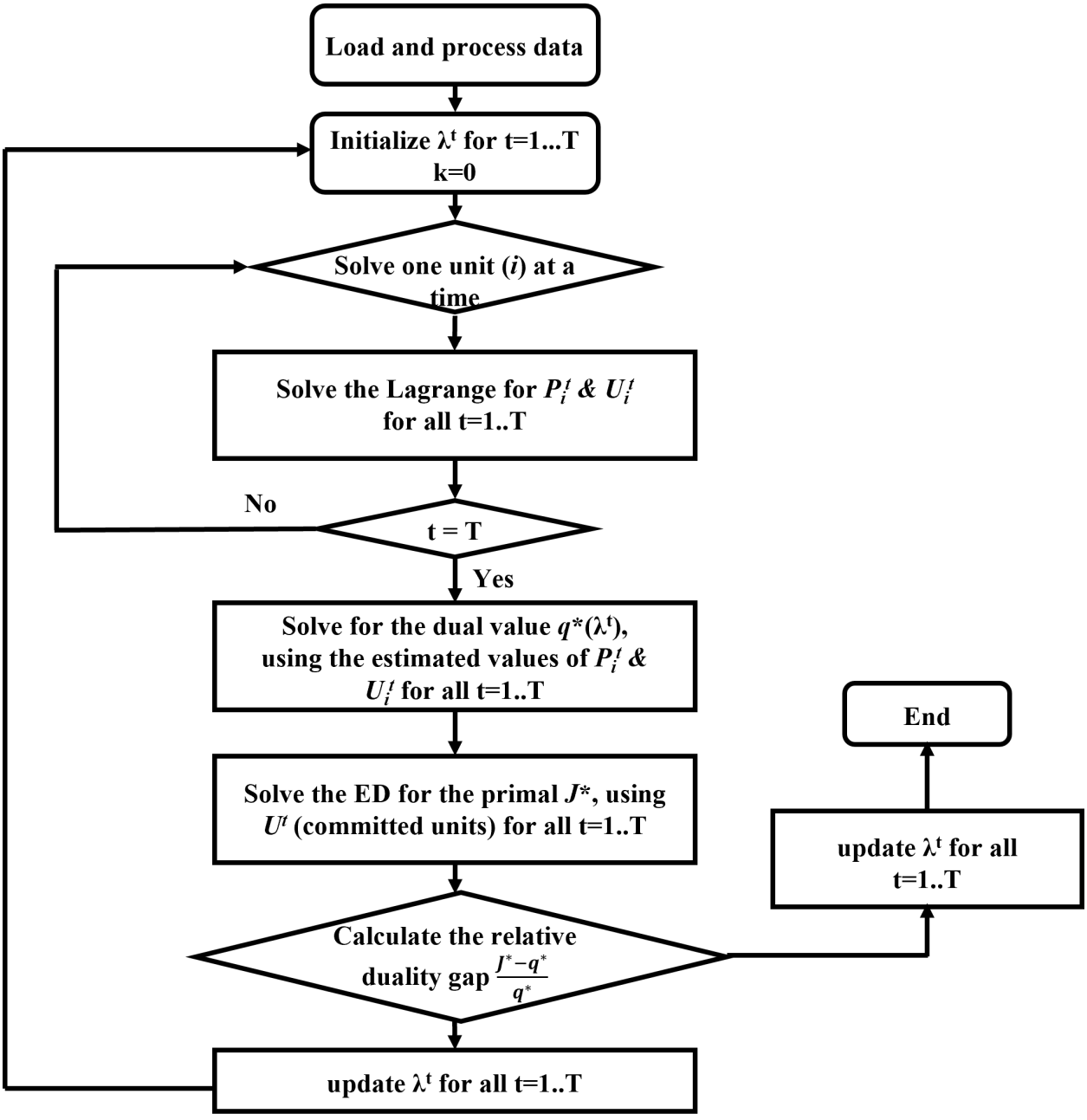


Figure 3.2: Lagrangian Relaxation Optimization Approach

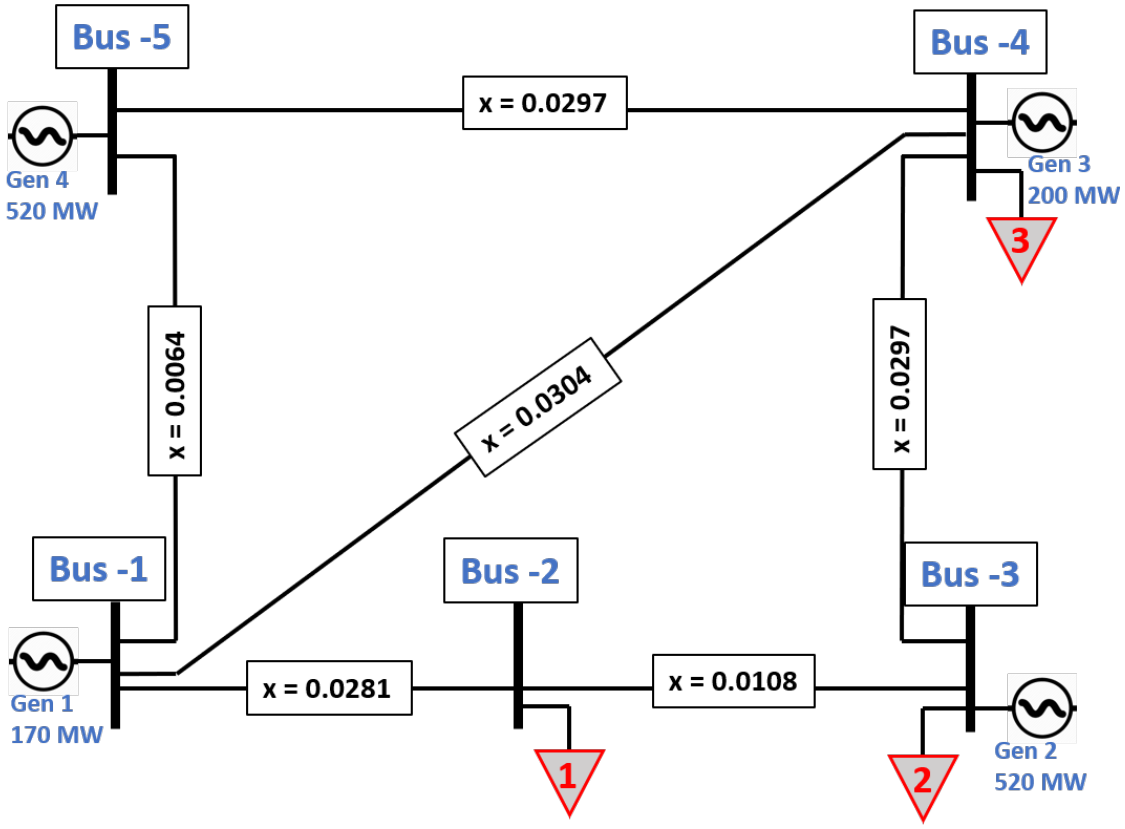


Figure 3.3: Modified PJM 5-bus system

Table 3.1: Generator parameters

Gen \Parameter	Gen-1	Gen-2	Gen-3	Gen-4
a	150	500	150	500
b	9	7	9	7
c	0.0045	0.005	0.0045	0.005
Max (MW)	170	520	200	520
Min (MW)	50	150	70	150
Ramp-up (MW/hr)	150	45	150	45
Ramp-down (MW)	-150	-45	-150	-45

The relationship between the impedance and the resistance, and the load data are shown in Table 3.2 and Table 3.3 respectively. For further simplification, all lines have unlimited flow capacity. A PJM 5 bus base case system is implemented with generator capacity and ramp rate limits. The formulation uses the heuristic from equation 3.27 added to the coordination equation and P_i is estimated at every stage of iteration by equation 3.25.

3.3.3 Test Result for the Base Case and Heuristic Formulation

The base case system is a modified PJM 5 bus system. It checks for generator ramp-rate limits without considering the network in any way. For the base case which is a lossless system, similar generators would have similar dispatch at all times except when the ramp-rate limit or the generator capacity limit is binding. To highlight the effect of the ramp-rate limit, two similar units, unit 2 and unit 4, have different *initial commitments*, 1 and 0 respectively as seen in Table 3.4.

The new Lagrangian formulation applies the heuristic as shown in equation 3.22. The modified P_i is updated during each step of iteration by equation 3.25. When solving the UC problem, the DC load flow is used for estimating the real power flow only. The reactive power is not considered during this process.

The simulation for both cases was performed for a 12-hour time horizon, using the load data from Table 3.3. After scheduling the units, the ED is solved for the real power output only, using the quadratic programming. This does not consider bus voltages or reactive power limits.

From Figure 3.4a below, it can be seen that unit 1 (blue) overlaps very well with unit 3 (yellow) except when unit 1 reached its maximum at 170 MW. Similarly, unit 2 (red) and unit 4 (purple) have equal values except during the periods when unit 4 is limited by the ramp rate. By penalizing the line flow, using the GSF, Figure 3.4b shows that the commitments at unit 1 differ from unit 3 at hours 2,5, and 10. Hence, the proposed UC formulation can differentiate between similar units when they are the marginal generators, selecting the unit with a shorter electrical distance from the load center. Unit 2 and unit 4 have outputs similar to Figure 3.4a because they are not the marginal generators in this scenario.

Table 3.2: Network parameters

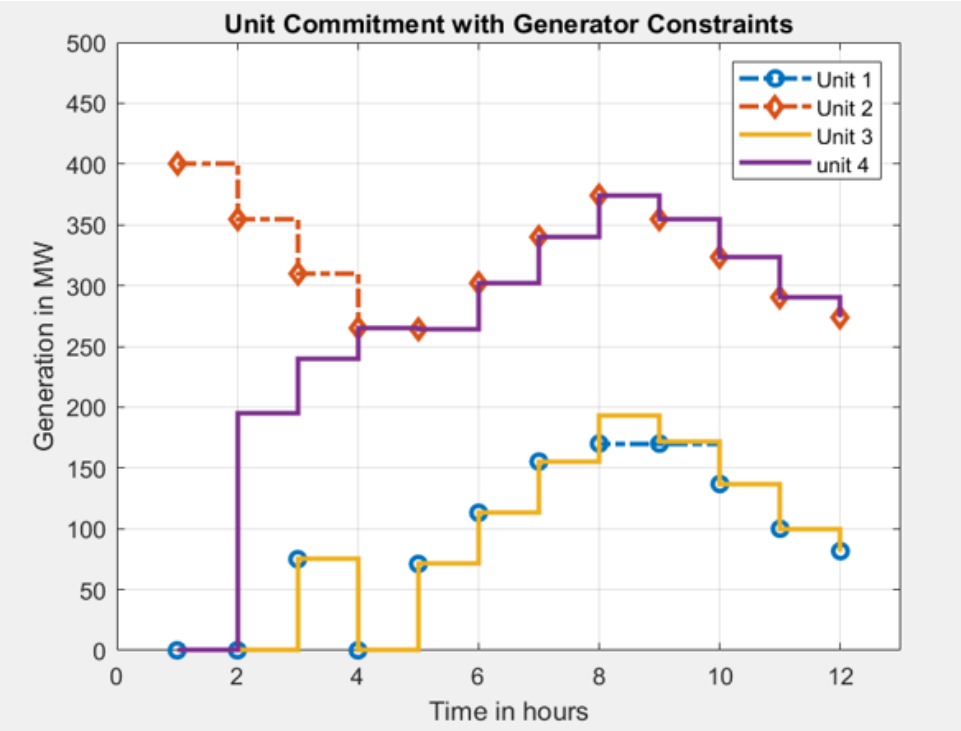
Line \Parameter	1-2	1-4	1-5	2-3	3-4	4-5
R	0.00281	0.00304	0.00064	0.00108	0.00297	0.00297
X	0.0281	0.0304	0.0064	0.0108	0.0297	0.0297
Line	999	999	999	999	999	999

Table 3.3: System bus load for a 12-hour period

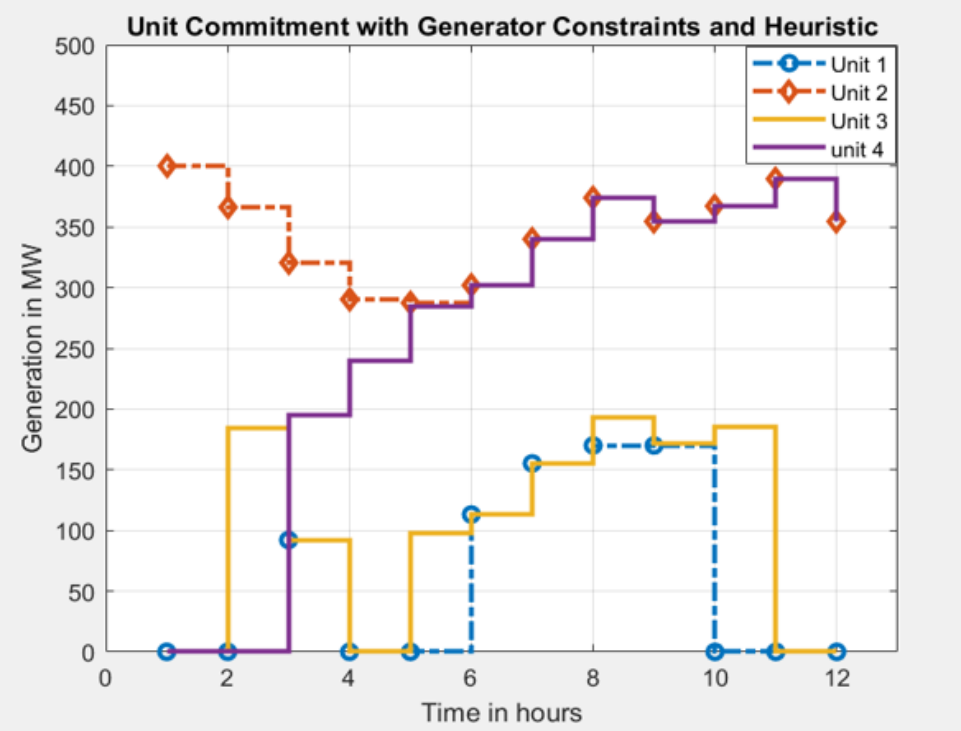
Period \Bus Number	Bus-1	Bus-2	Bus-3	Bus-4	Bus-5
Hour-1	0	50	150	200	0
Hour-2	0	100	200	250	0
Hour-3	0	150	250	300	0
Hour-4	0	90	190	250	0
Hour-5	0	150	230	290	0
Hour-6	0	200	290	340	0
Hour-7	0	250	340	400	0
Hour-8	0	300	360	450	0
Hour-9	0	300	350	400	0
Hour-10	0	250	320	350	0
Hour-11	0	200	280	300	0
Hour-12	0	160	250	300	0

Table 3.4: Generator and load data at Hour zero (Hour-0)

Hour-0 \Bus Number	Bus-1	Bus-2	Bus-3	Bus-4	Bus-5
Initial-Load	0	100	175	140	0
Initial-Commitment	0	0	1	0	0
Initial Gen-Output	0	0	415	0	0
Gen-Max-Capacity	170	0	520	200	520
Gen-Min-Capacity	50	0	150	70	150
Ramp-up-limit	150	0	45	150	45
Ramp-down-limit	-150	0	-45	-150	-45



(a) Base case system



(b) System with heuristic

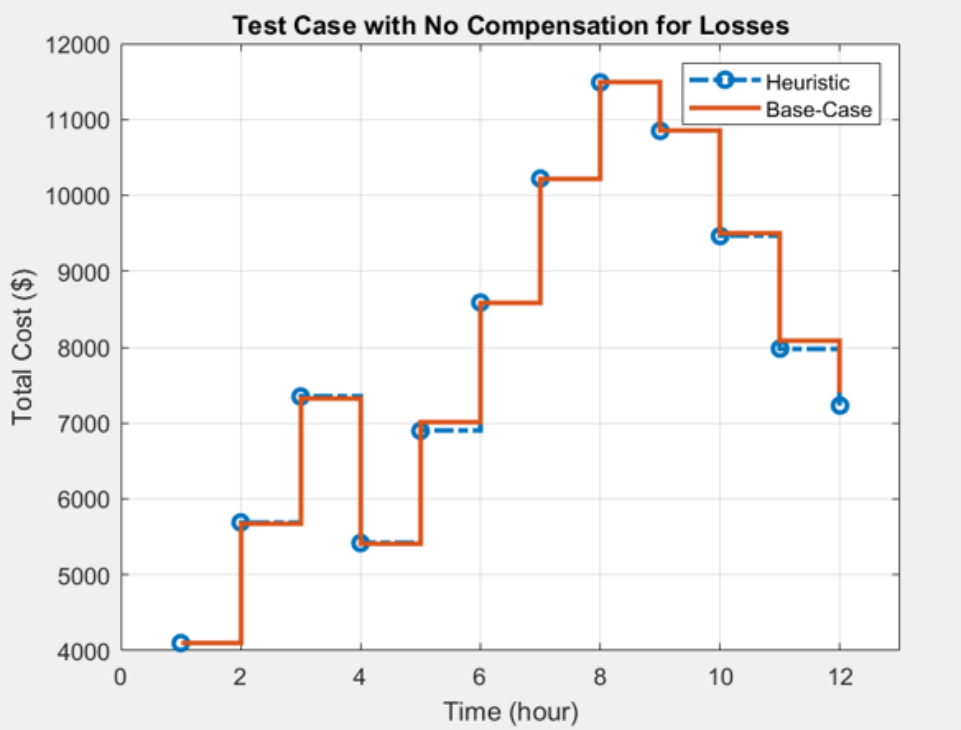
Figure 3.4: Comparing the base case system with the heuristic case for a 12-hour time horizon

The security constraint and convergence of the UC and ED result are verified by solving the Optimal Power Flow (OPF) using the **runopf** command in **MATPOWER** [103]. The hourly maximum generator limit ($P^{\max}$) and minimum generator limit ($P^{\min}$) for each unit as well as the hourly bus load (P^{t}_{load}) data are updated in the MATPOWER case data (case5 in this scenario). The unit status (1 or 0) in the case data is also updated periodically via the commitment parameter U_{it} from equation 3.22. All other bus, branch, and generator cost (gencost) data remain fixed. Figure 3.5a compares the hourly cost of the base case and heuristic without running the OPF. Figure 3.5b compares the hourly cost of the base case and heuristic after solving the OPF. In both cases, the heuristic resulted in a lower cost of generation as can be seen in hours 5 and 11. During hours 2 and 3 when the heuristic seems to underperform, the differences are minor. In Figure 3.6, the additional power output after compensating for losses is compared. The heuristic also performed better as the overall additional power required is less than that of the base case. At hour 12, the loss compensation for the heuristic is higher but the overall hourly cost is cheaper. The algorithm chose the farther but cheaper unit (unit 4) over the closer but expensive one (unit 3). The real and reactive losses were compared for each time period in Figures 3.7a and 3.7b and the results show that the heuristic is superior.

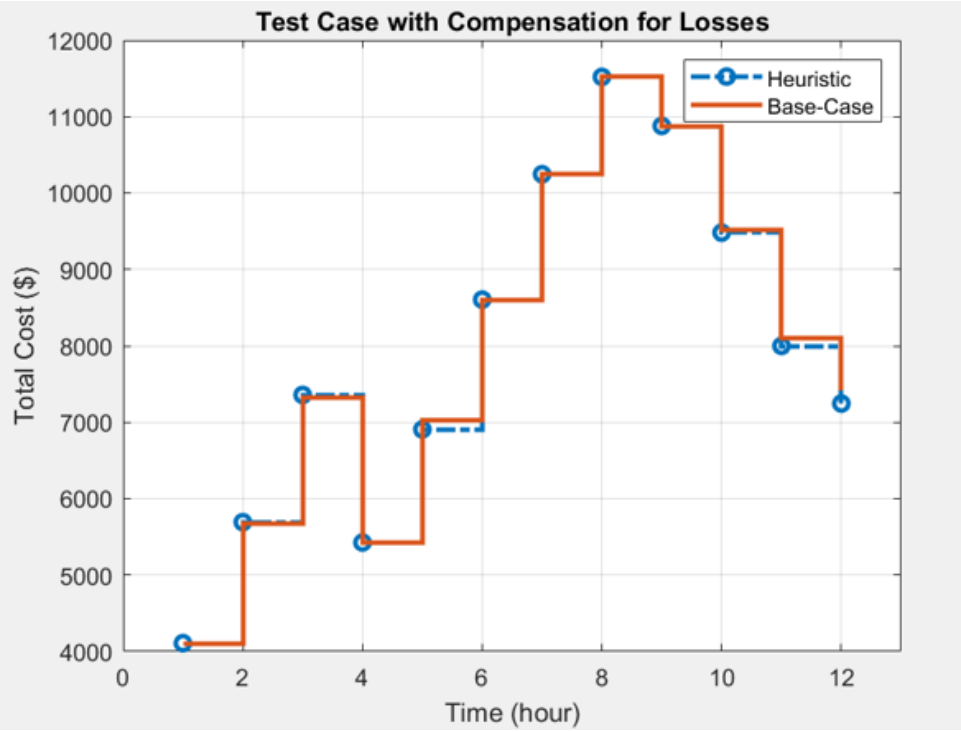
3.3.4 Discussion of Simulation Results

A. The effect of heuristic on the marginal units

As shown from Figure 3.4a (base case), generator 4 is the marginal unit at hour 2 while generators 1 and 3 are the marginal units at hours 3 and 5. The simulation selected unit 4 which is less expensive over units 1 and 3 as expected. One can also observe that units 1 and 3 are not distinguishable when they are the marginal units for the base case. Figure 3.4b on the other hand shows the effect of the heuristic on the UC process, when the generation costs of the marginal units are about the same or equal. At hour 2, generator 3 was selected ahead of generator 4 even though the former is more expensive. Since unit 4 is farther away from the load center, unit 3 which is closer to the load center is preferred. The identical units 1 and 3 are the marginal units at hours 5 and 10. The proposed formulation selected unit 3 ahead of unit 1 at hour 5 and de-selected the latter at hour 10. This helps mitigate



(a) Total cost without considering losses (no OPF solved)



(b) Total cost with losses compensated for (OPF solved)

Figure 3.5: Losses are calculated by solving OPF using MATPOWER

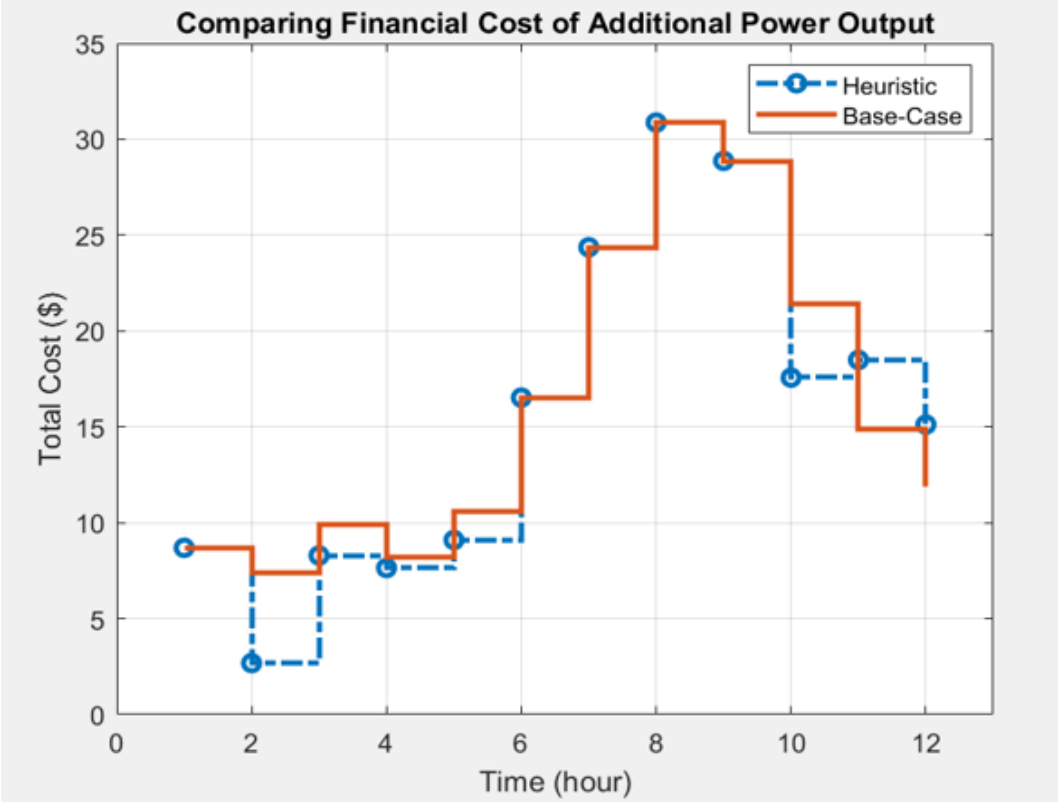
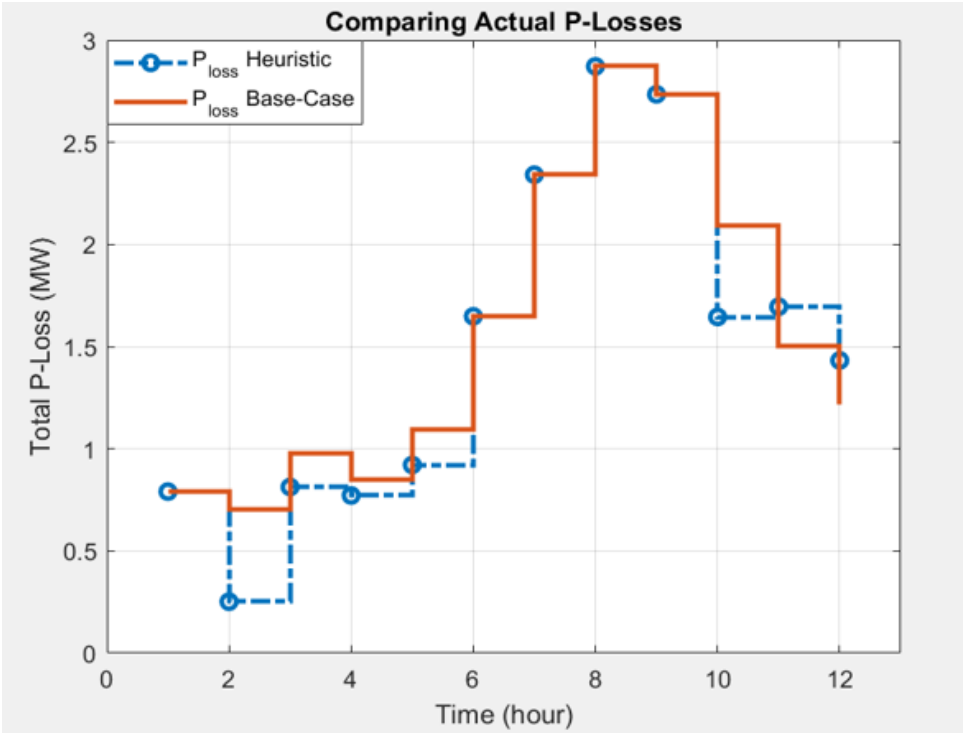
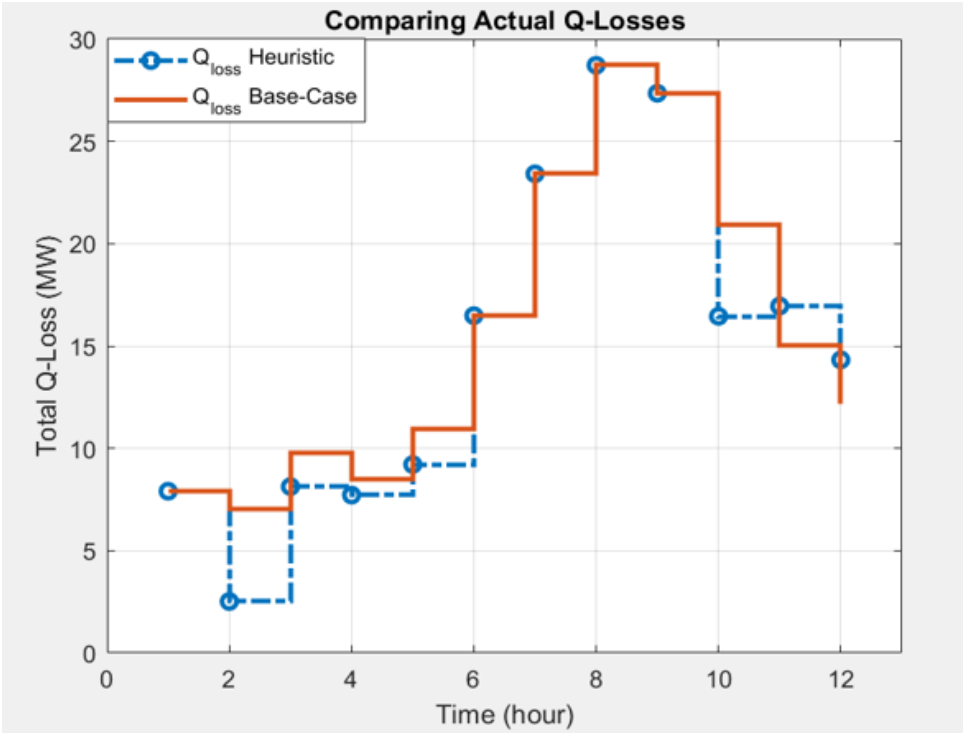


Figure 3.6: Additional power output obtained from solving OPF using MATPOWER



(a) Real losses calculated from OPF



(b) Reactive losses calculated from OPF

Figure 3.7: Real and reactive losses obtained from solving OPF using MATPOWER

the over-commitment problem normally associated with LR when similar or identical units are present.

The formulation with the heuristic is able to differentiate between similar generators by taking advantage of the transmission network. The formulation can also commit a more expensive generator over a cheaper one when the cheaper generator is far away from the load center. The algorithm incorporates the effect of losses in the UC process and improves the overall simulation result as expected.

B. The effect of heuristic on the solution and objective

The UC solutions from Figures 3.4a and 3.4b are considerably different. The base case does not consider the system network and solves the optimization problem as a single bus. On the other hand, the heuristic considers the system network to some extent. The latter adds an additional cost to the nodal injection as a function of the electrical distances from the load center. For example, at hour 2, the overall cost of committing unit 4 exceeds that of unit 3 even though unit 3 is more expensive. This also has some impact on the method of distinguishing between the identical units 1 and 3. The hourly cost of commitments in case 1 and case 2 after solving the ED and OPF is shown in Table 3.5. Figure 3.5a compares the primal for the base case and that of the heuristic after solving the ED. Figure 3.5b compares the primal for both the base case and the heuristic after solving the OPF. The base case performed better for hours 2,3 and 4 as can be seen by the negative signs, while the heuristic performed better at hours 5,10,11, and 12. When considering the differences resulting from the ED and OPF, one can observe that the hourly differences from the OPF solution are smaller when the base case does better. Table 3.6 further highlights the effect of losses on the hourly costs. Since the heuristic is an approximation, the algorithm could sometimes overestimate the losses at the expense of cost. This can lead to higher costs but lesser losses as seen in hours 2,3 and 4 and vice versa for hours 11 and 12. Improvements to the overestimation issue will be further discussed in Section 5.3.2. Table 3.7 shows that the heuristic performed better overall with reduced losses and lower objective cost. MIP optimization technique will be used to benchmark the solution quality and the simulation time of the proposed formulation in the next chapter.

Table 3.5: Hourly Generation Cost Difference for ED and OPF solutions

(a) Solution for ED

Primal (Base)	Primal. (Heuristic)	Diff. (ED)
4,100	4,100	0
5,670.3	5,690.1	-19.9
7,319.1	7,349.4	-30.3
5,412.3	5,418.5	-6.3
7,016.3	6,897.2	119.1
8,589	8,589	0
10,222.2	10,222.2	0
11,488.7	11,488.7	0
10,850.3	10,850.3	0
9,500.2	9,464.6	35.6
8,091	7,981	110
7,403.8	7,230.3	173.6

(b) Solution for OPF

Primal (Base)	Primal (Heuristic)	Diff. (OPF)
4,108.7	4,108.7	0
5,677.7	5,692.8	-15.2
7,329	7,357.7	-28.7
5,420.5	5,426.1	-5.7
7,027	6,906.3	120.6
8,605.5	8,605.5	0
1.0,246.6	10,246.6	0
11,519.6	11,519.6	0
10,879.2	10,879.2	0
9,521.6	9,482.2	39.5
8,105.9	7,999.5	106.4
7,415.7	7,245.4	170.3

Table 3.6: Hourly Generation Cost Difference and P loss Difference

Primal Base Case ($)	Primal with Heuristic ($)	Cost diff. ($) (Base - Heu.)	P loss diff. (MW) (Base - Heu.)
4,108.7	4,108.7	0	0
5,677.7	5,692.8	-15.2	0.4506
7,329	7,357.7	-28.7	0.1661
5,420.5	5,426.2	-5.7	0.0805
7,027	6,906.3	120.6	0.1765
8,605.5	8,605.5	0	0
10,246.6	10,246.6	0	0
11,519.6	11,519.6	0	0
10,879.2	10,879.2	0	0
9,521.6	9,482.2	39.5	0.4478
8,105.9	7,999.5	106.4	-0.1943
7,415.7	7,245.4	170.3	-0.2138

Table 3.7: Total Cost and Losses

	Base-Case	Heuristic
Gen. Cost ($) (Lossless)	95,663.2	95,281.3
Gen. Cost ($) (With Losses)	95,856.8	95,469.5
Cost of Added Power ($)	193.6	188.2
Total P-Losses (MW)	18.8	17.9
Total Q-Losses (MW)	188.3	179.2

C. Impact of heuristic weighting factor on losses

To compare with the simulation result from Figure 3.4, a smaller heuristic was applied by scaling down the weighting factor $\boldsymbol{W}$ in equation 3.27 (reduced $\frac{1}{2}$ for this example). In this scenario, the UC only differs in two time periods (hours 5 and 12). In both cases, the heuristic performed better than the base case as seen in Table 3.8. Unlike the original case, the hourly generation cost of the new weighting factor never exceeds the hourly cost of the base case. Still, it can be seen that the aggressive weighting factor performs better in the overall cost of production as seen in Table 3.9.

D. Over-generation and duality gap

One known challenge of LR optimization is that the algorithm over-commits units when similar units are present, leading to over-generation. The proposed formulation is able to select one of two similar units when they are the marginal generators. A marginal unit is usually more expensive than the already committed units when the load is increasing. When the sum of the lower limits of the selected (similar) units exceeds the needed additional power, the marginal units will be running at their lower limits, leading to over-commitment. Every time the algorithm chooses between similar units, we can observe the positive effect on the overall generation cost. The reduction in the generation cost is directly related to the reduction in the duality gap.

3.3.5 Impact of 24-hour Horizon at 5-minute intervals

The modified PJM 5 bus system from Figure 3.3 was used to simulate a 5-minute time period for a 24-hour horizon. Hourly load data with a minimum of 593 MW and a maximum of 781 MW is distributed across buses 2,3,4, and 5. For a 5-minute period, the ramp-up limits of generators 2 and 4 which are the cheaper generators are reduced to 7 MW and 5 MW respectively. Generator 3 which is more expensive and a faster generator can ramp up to a maximum of 75% of its maximum capacity in 5 minutes. The most expensive unit, which is generator 1 can ramp up to its maximum capacity in 5 minutes. The load pattern includes some initial downward ramping and two peaks to strain the ramping capability of

Table 3.8: Effect of the conservative weighting factor on generation cost and losses

Primal Base Case ($)	Primal with Heuristic ($)	Cost diff. ($) (Base - Heu.)	P loss diff. (MW) (Base - Heu.)
4,108.7	4,108.7	0	0
5,677.7	5,677.7	0	0
7,329	7,329	0	0
5,420.5	5,420.5	0	0
7,027	6,906.3	120.6	0.1660
8,605.5	8,605.5	0	0
10,246.6	10,246.6	0	0
11,519.6	11,519.6	0	0
10,879.2	10,879.2	0	0
9,521.6	9,521.6	0	0
8,105.9	8,1058.7	0	0
7,415.7	7,3045.8	111.1	0.2051

Table 3.9: Original and reduced weighting factors considered

	$\frac{1}{2}$ Weight (Reduced)	Full Weight (Orginal)
Gen. Cost ($) (No OPF)	95,434.7	95,281.3
Gen. Cost ($) (with OPF)	95,625.1	95,469.5
Cost of Added Power ($)	190.4	188.2
P-Compensation (MW)	18.5	17.9
Total P-Losses (MW)	18.5	17.9
Total Q-Losses (MW)	184.6	179.2

the generators and the algorithm. The simulation is implemented with the heuristic from Section 3.3. The generation output plot is shown in Figure 3.8.

Comparing the simulation time of Figure 3.4, which is simulated for a 12-hour horizon and 12-time steps to Figure 3.8 which is simulated for a 24-hour horizon and 288-time steps, we see that our formulation scales well. Table 3.10 shows that the computation time increases approximately linearly with the number of scheduling intervals (at an approximate rate of 1.9 seconds per interval).

3.4 Discussion

The proposed formulation differentiates between similar units by selecting units with the aim of reducing line losses. A line-flow penalty is added to equation 3.26, thereby, discouraging large power injections from buses that are far away from load centers. The penalty slightly increases the generation cost for a unit that is far away from the load center. Hence, the algorithm treats similar units at different buses differently depending on their electrical distances from the load center. The algorithm only has an impact when the similar units in question are the marginal units. Note that selecting an appropriate weighting factor can play a crucial role in the overall energy production cost. As seen in Table 3.6 and Table 3.8, using a conservative weighting factor may reduce the effectiveness of the heuristic but it certainly improves the overall performance when compared to the base case. Simulations show that the weighting factor will be system specific and should be carefully selected. It should be noted that this chapter does not focus on methods of updating lambda (λ) between iterations.

In this chapter, we started by formulating a new linear loss factor that differentiates similar units during UC and scales linearly for an increasing time horizon. The effect of the losses is distributed evenly using the Generation Shift Factor (GSF). We used a small test case with a 12-hour horizon to show that the algorithm can identify and differentiate between similar units and commit or de-commit them depending on distances from the load center. The effect of losses and generation production cost were compared when considering committing or de-committing certain units from their similar counterparts. The

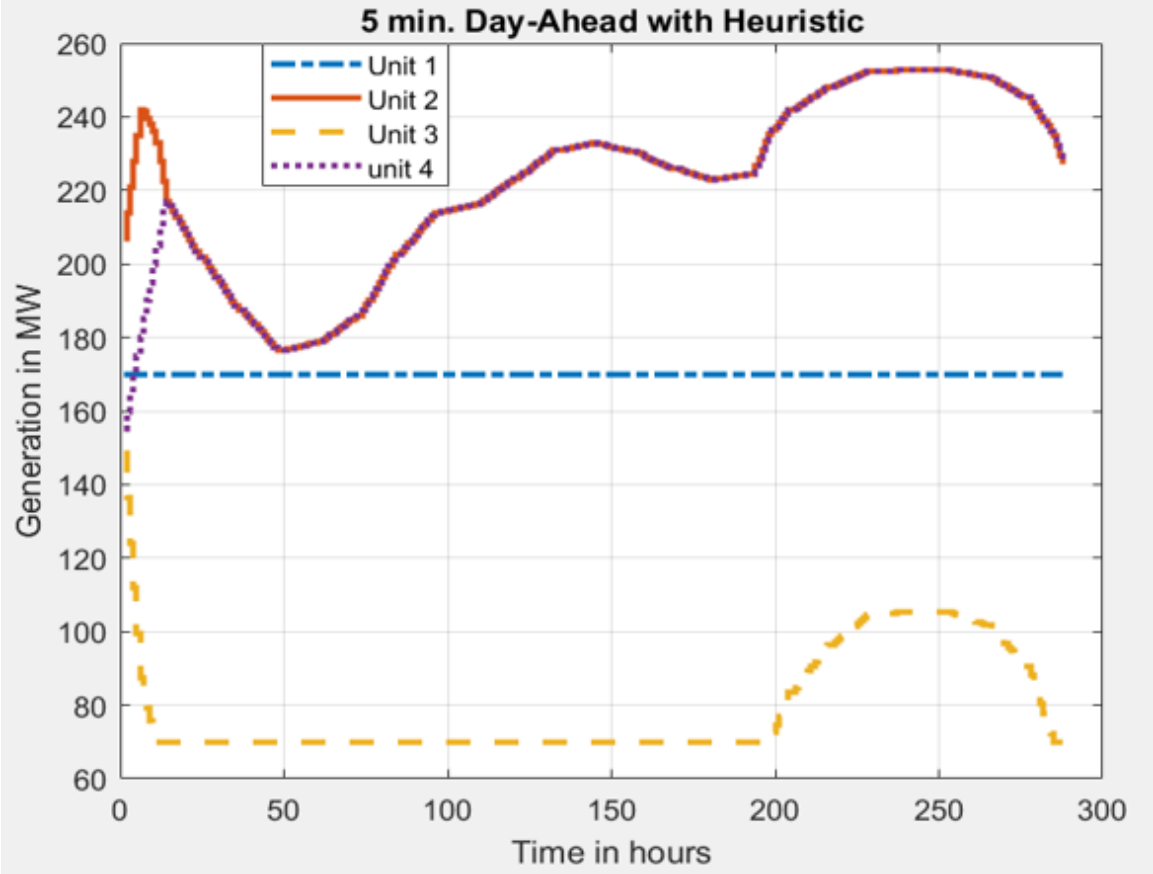


Figure 3.8: A Day-Ahead UC and ED with 5-minute interval and 288 time periods

Table 3.10: Scalability test for hourly vs 5-minute time periods and 288 time periods

	12-periods	288-periods
Ave. Run Time	0.23 s	5.41 s

approach reduced the overall line losses and the overall cost of generation without increasing simulation time. Finally, using a longer time horizon with 288-time steps, we showed that the formulation scales linearly with increasing time horizon.

Chapter 4

LR Algorithm and Implementation

The proposed work here is to formulate and implement optimization techniques using Lagrangian Relaxation (LR) and heuristics to enhance a high penetration of distributed energy resources (DER). In continuation of the work from Chapter 3, the solution quality and simulation time are studied, using MIP as a benchmark.

4.1 Formulate a Benchmark for Solution Quality using MIP

MIP is a state-of-the-art optimization program that guarantees optimal solutions (with some caveats) and, hence, a good tool for a benchmark on the solution quality. We verified the quality against a MIP solution using Egret, an open-source software which is a Python-based optimization tool [46]. The tool is built on the Pyomo optimization modeling language for the power grid. The PJM 5 bus system from subsection 3.3.2 was modified and the benchmark was performed for a day ahead UC and ED. For simplicity, constraints such as start-up and shutdown costs, and minimum up and down time were not added. Two test cases with identical units are considered below.

4.1.1 Case 1

The two identical generators are unit 1 and unit 3. Unit 2 is less expensive than the identical units while unit 4 is the most expensive. The system is lightly loaded with the load distributed at buses 3, 4, and 5. The LR algorithm commits the profitable units for each period and then solves the ED using quadratic programming function in **MATLAB** [90]. A DC power flow model is used. This can be observed in the solution as the power output of unit 1 and unit 3 are always equal whenever they both get selected. Table 4.1 compares the UC and ED results for both optimization methods. It can be seen that the LR formulation tends to select unit 3 over unit 1 most of the time even though they are identical units. The formulation does this by distributing the effect of the penalties as a function of the individual electrical distance of each generator from the load center. The MIP algorithm also does a good job of selecting only one of the identical units when necessary. However, since the algorithm does not consider the effect of line losses, the selection of either identical unit is arbitrary. This can be observed as the farther unit 1 does get selected over the closer unit 3 during periods 2 through 8.

In order to see the effect of line losses on the overall objective function, using the UC solutions of both LR and MIP, the Optimal Power Flow (OPF) was solved by **MATPOWER**. Figure 4.1 compares the solutions of the OPF for both LR and Egret. The OPF tends to prioritize the identical unit (unit 3) with the shorter electrical distance from the load center, even when both units get selected as it is in periods 1 and 9 through 24. This is in line with the LR algorithm and hence, the output from unit 3 is always greater than or equal to the output of unit 1. The MIP solution on the other hand could be arbitrary in the UC process which could be due to the occurrence of multiple optimal solutions (flat bottom). Hence, the generation output of unit 3 is not always prioritized as it is the case in the LR algorithm. Table 4.2 shows the periodic cost of generation for both algorithms while Table 4.3 shows the total costs of production after solving with DC and AC Power Flow. For both the DC and AC load flow solutions, there are insignificant differences between LR and Egret solutions. It should be noted that the quadratic cost function was used in both LR and MIP formulation. The MIP algorithm converts the cost functions into piecewise linear cost

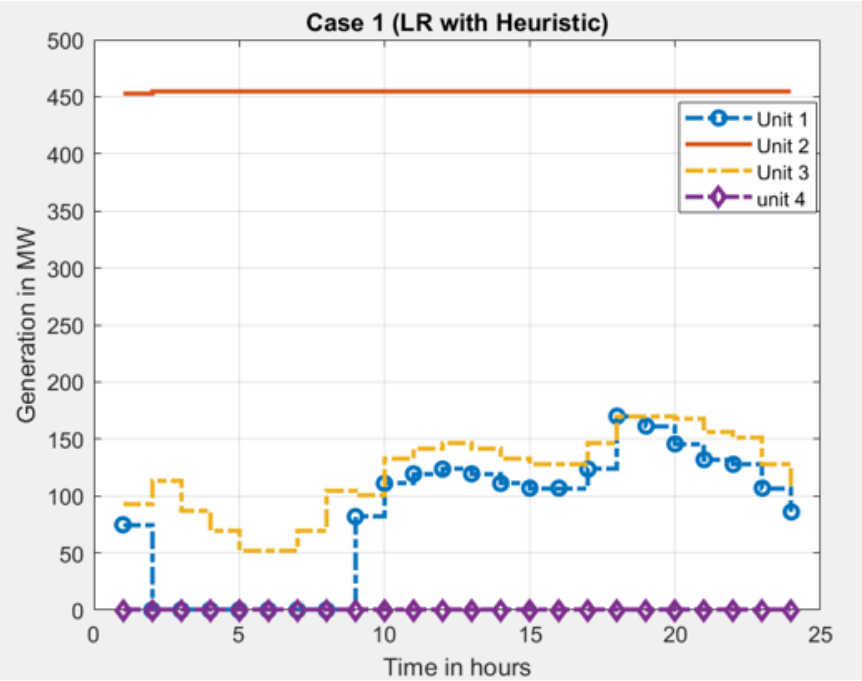
Table 4.1: Comparing UC and ED results for LR with Heuristic and Egret Case 1

(a) LR with Heuristic Case 1

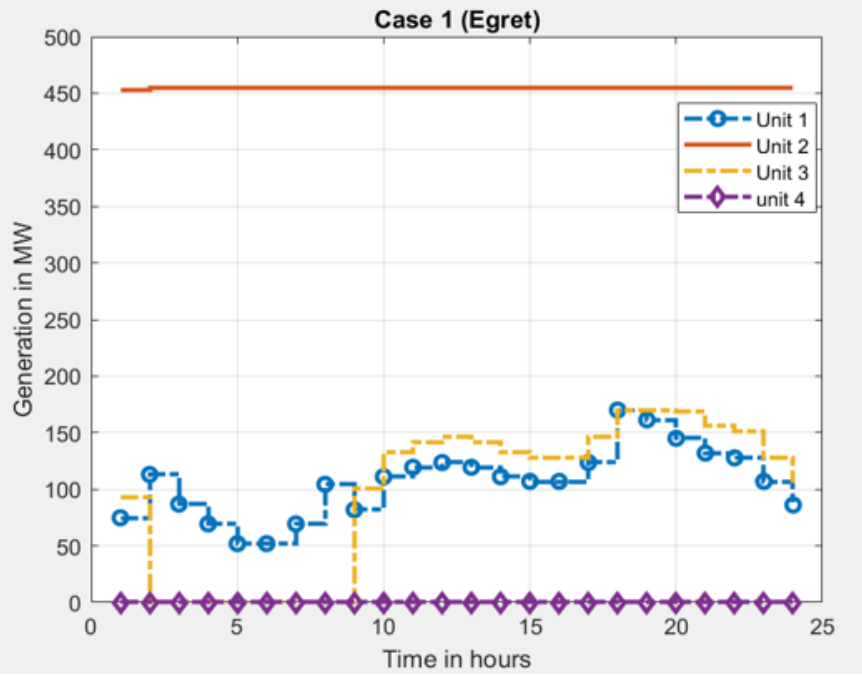
	Gen_1	Gen_2	Gen_3	Gen_4
1	83.64	452.5	83.64	0
2	0	455	112.41	0
3	0	455	86.22	0
4	0	455	68.76	0
5	0	455	51.30	0
6	0	455	51.30	0
7	0	455	68.76	0
8	0	455	103.68	0
9	91.12	455	91.12	0
10	121.68	455	121.68	0
11	130.41	455	130.41	0
12	134.77	455	134.77	0
13	130.41	452.5	130.41	0
14	121.68	455	121.68	0
15	117.31	455	117.31	0
16	117.31	455	117.31	0
17	134.77	455	134.77	0
18	169.69	455	169.69	0
19	165.32	455	165.32	0
20	156.59	455	156.59	0
21	145.50	455	145.50	0
22	139.13	455	139.13	0
23	117.31	455	117.31	0
24	95.49	455	95.49	0

(b) Egret Case 1

	Gen_1	Gen_2	Gen_3	Gen_4
1	72.29	452.5	95	0
2	112.41	455	0	0
3	86.22	455	0	0
4	68.76	455	0	0
5	51.30	455	0	0
6	51.30	455	0	0
7	68.76	455	0	0
8	103.68	455	0	0
9	87.25	455	95	0
10	148.35	455	95	0
11	95	455	165.81	0
12	170	455	99.54	0
13	95	452.5	165.81	0
14	95	455	148.35	0
15	139.62	455	95	0
16	95	455	139.62	0
17	170	455	99.54	0
18	170	455	169.37	0
19	160.64	455	170	0
20	143.19	455	170	0
21	117.00	455	170	0
22	108.27	455	170	0
23	95	455	139.62	0
24	95	455	95.97	0



(a) LR with Heuristic plot for Case 1



(b) Egret plot for Case 1

Figure 4.1: Plots of UC and ED results for LR with Heuristic and Egret for Case 1

Table 4.2: Periodic cost of production for Case 1

Period	Cost for LR ($)	Cost for Egret ($)
1	12128.15	12128.34
2	10642.16	10642.16
3	9937.14	9937.14
4	9467.67	9467.67
5	8998.63	8998.63
6	8998.63	8998.63
7	9467.67	9467.67
8	10407.05	10407.05
9	12572.17	12572.19
10	14217.84	14218.86
11	14688.52	14690.31
12	14923.94	14925.71
13	14688.52	14690.31
14	14217.84	14218.86
15	13982.58	13983.29
16	13982.58	13983.29
17	14923.94	14925.71
18	16809.26	16809.26
19	16573.41	16573.44
20	16101.86	16102.12
21	15394.95	15395.95
22	15159.42	15160.77
23	13982.58	13983.29
24	12807.11	12807.11

Table 4.3: Total cost of production for Case 1

Power Flow Method	Total Cost for LR ($)	Total Cost for Egret ($)
DC Power Flow	315,073.6	315,087.7
AC Power Flow	315,451.4	315,451.5

functions (approximation) which slightly affect the solution quality when compared with the LR solution.

4.1.2 Case 2

In Case 2, the identical generators are units 1 and unit 3, and they are both more expensive than unit 2 and unit 4. As in Case 1, unit 2 remains the most economical unit. The system is heavily loaded when compared to Case 1 with the load distributed at buses 3, 4, and 5.

The UC and ED results for the scenario in Case 2 are shown in Table 4.4. One can see that both methods committed the same number of units during each period. It should be noted that whenever the identical units are the marginal units, the LR algorithm tends towards selecting the unit with the shortest electrical distance from the load center as determined by the system network. Hence, unit 3 is preferred to unit 1 most of the time. Figures 4.2a and 4.2b show the degree of the differences in output between the identical units. It can be seen that the MIP algorithm is also able to differentiate between identical units but the choice of selection can be arbitrary.

The effect of selecting unit 3 can be easily seen in Table 4.5 when comparing the DC power flow and AC power flow. It should be noted that the algorithm is designed to reduce over-commitment that is associated with LR when solving problems with similar and identical units. When considering all other constraints, MIP is expected to outperform in the quality of the solution.

4.2 Implementation of Network Constraints, System Reserve and LMP

Additional system characteristics, including system reserves, transmission line limits, and Locational Marginal Pricing (LMP) are investigated in this section using the proposed formulation. A varying load pattern with two peaks is considered for testing the approach for flexibility and robustness. The load distribution is set up in a way to activate at least one of the two reserve units. Line 1, which is the line from bus 1 to bus 2 requires the most

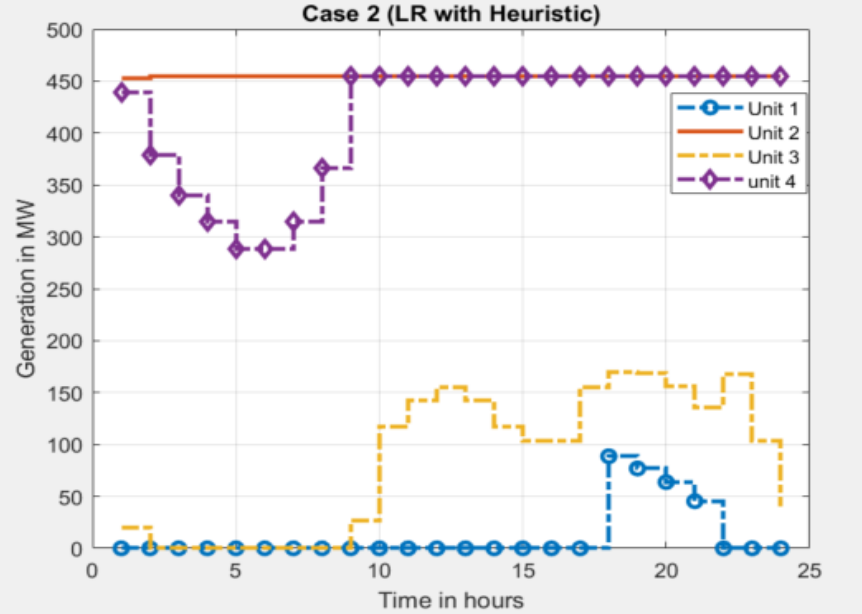
Table 4.4: Comparing UC and ED results for LR with Heuristic and Egret Case 2

(a) LR with Heuristic Case 2

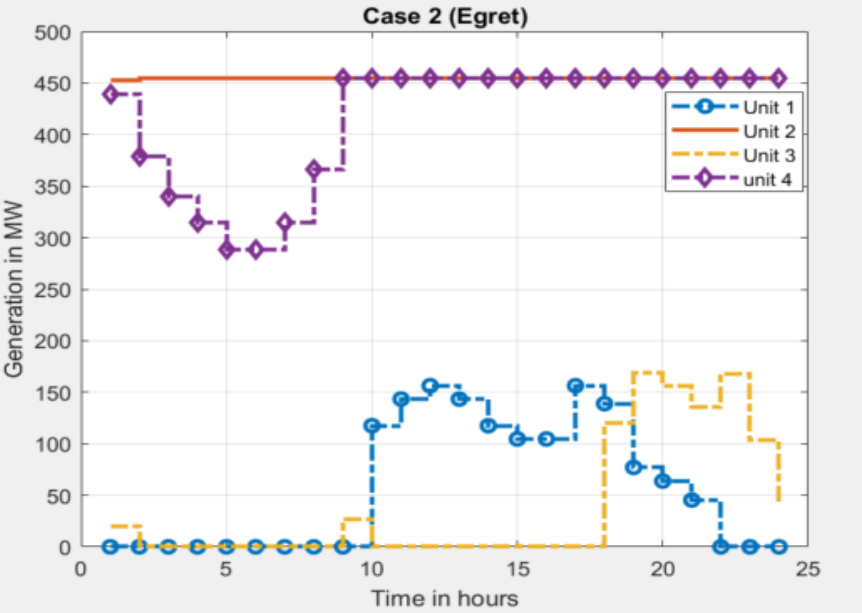
	Gen_1	Gen_2	Gen_3	Gen_4
1	0	452.5	20	436.46
2	0	455	0	377.14
3	0	455	0	338.74
4	0	455	0	313.13
5	0	455	0	287.53
6	0	455	0	287.53
7	0	455	0	313.13
8	0	455	0	364.34
9	0	455	24.56	455
10	0	455	114.18	455
11	0	455	139.78	455
12	0	455	152.58	455
13	0	452.5	139.78	455
14	0	455	114.18	455
15	0	455	101.37	455
16	0	455	101.37	455
17	0	455	152.58	455
18	120	455	135	455
19	121.10	455	121.10	455
20	108.30	455	108.30	455
21	89.10	455	89.10	455
22	0	455	165.38	455
23	0	455	101.37	455
24	0	455	37.36	455

(b) Egret Case 2

	Gen_1	Gen_2	Gen_3	Gen_4
1	0	452.5	20	436.46
2	0	455	0	377.14
3	0	455	0	338.74
4	0	455	0	313.13
5	0	455	0	287.53
6	0	455	0	287.53
7	0	455	0	313.13
8	0	455	0	364.34
9	0	455	24.56	455
10	114.18	455	0	455
11	139.78	455	0	455
12	152.58	455	0	455
13	139.78	452.5	0	455
14	114.18	455	0	455
15	101.37	455	0	455
16	101.37	455	0	455
17	152.58	455	0	455
18	95	455	160	455
19	147.20	455	95	455
20	121.60	455	95	455
21	83.19	455	95	455
22	0	455	165.38	455
23	0	455	101.37	455
24	0	455	37.36	455



(a) LR with Heuristic plot for Case 2



(b) Egret plot for Case 2

Figure 4.2: Plots of UC and ED results for LR with Heuristic and Egret for Case 2

Table 4.5: Total cost of production for Case 2

	Total Cost for LR ($)	Total Cost for Egret ($)
DC Power Flow	446,407.7	446,410.4
AC Power Flow	447,929.7	448,056.4

power flow since it is connecting the distant generators 1 and 5 to the load center. A 200 MW line flow limit is imposed on line 1 as shown in Figure 4.3. Generators 5 and 6 are dedicated reserve units and are connected to buses 3 and 4 respectively. Since the estimated power output and the heuristic only capture the effect of losses, the algorithm is set up to track the line flows and activate the appropriate reserve unit. The iterative optimization scheme for the system setup is shown in Figure 4.4.

The modified PJM 5 bus system has 3 pairs of similar generators. These are generators 1 and 3, 2 and 4, and 5 and 6. Two simulation cases are considered for this study. The base case is a classical LR algorithm and the generation MW output over a 12-hour time period is seen in Figure 4.5. It can be observed that the outputs of similar units 1 and 3 and 2 and 4 differs from period 7. This is a result of line flow violation prevention. The power outputs of the farther units 1 and 4 are reduced when compared to their similar counterparts. A reserve unit (unit 5) is activated at hour 8 where the spinning reserve capacity is not sufficient to prevent the line flow violation in line 1.

A second test case is implemented with the proposed heuristic from Chapter 3. Figure 4.6 shows the generation MW output over a 12-hour time period. When comparing the UC for both cases, it can be observed that the similar units are mostly indistinguishable in case 1. The only time unit 3 got committed over unit 1 is due to the difference in their maximum capacities (170 MW and 200 MW respectively). The heuristic case on the other hand is able to distinguish between similar units. The difference in outputs of similar units 1 and 3 in period 5 is a result of their electrical distances from the load center. As expected, the heuristic case performed better with a lower cost of production. The increase in the number and type of constraints impacts how the heuristic affects the UC solutions. One advantage of the proposed formulation is that it is only meant to be in effect for similar or identical units when they are the marginal units, thus, the additional computational burden is minor.

The LMP of the buses can be seen in Figures 4.7 and 4.8. As expected, bus 2 has the highest LMP followed by bus 3 where the reserve unit (generator 5) is committed.

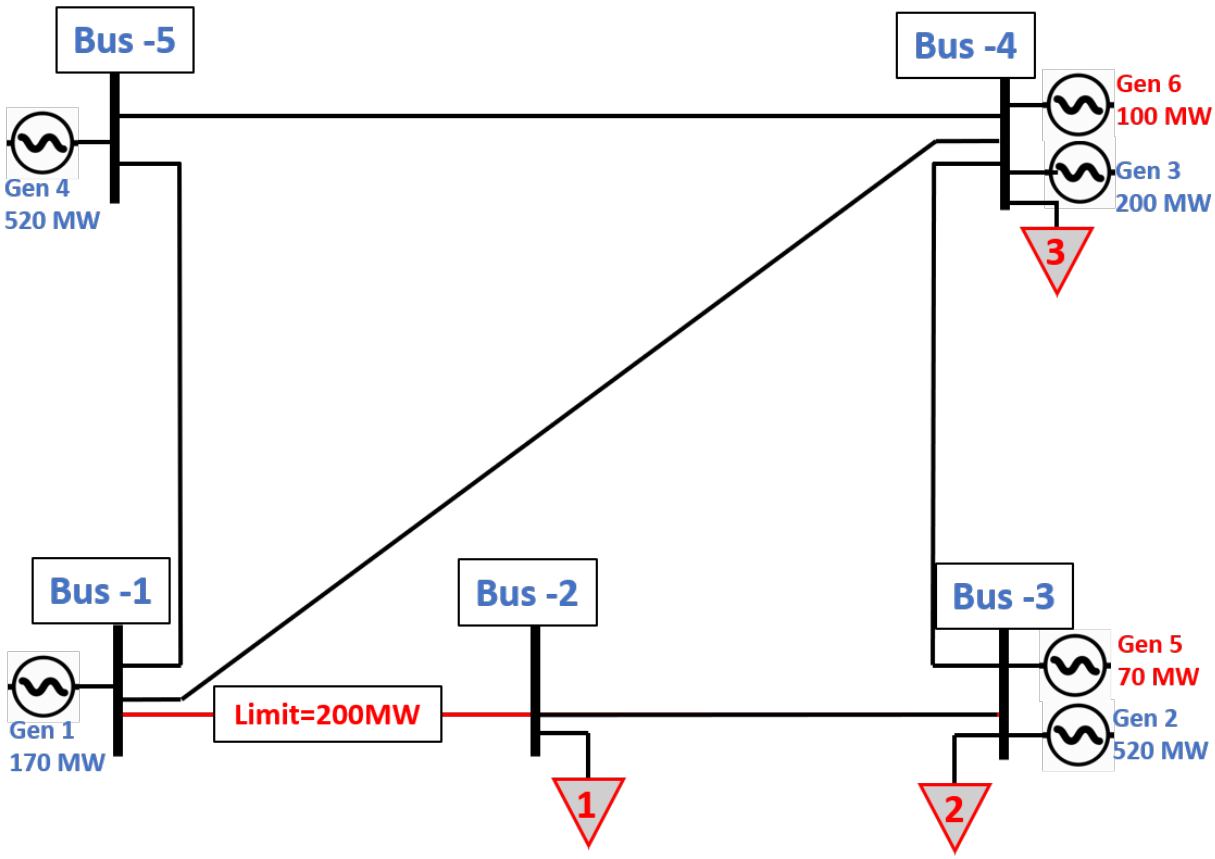


Figure 4.3: Modified PJM 5 bus system with 4 main units and 2 reserve units

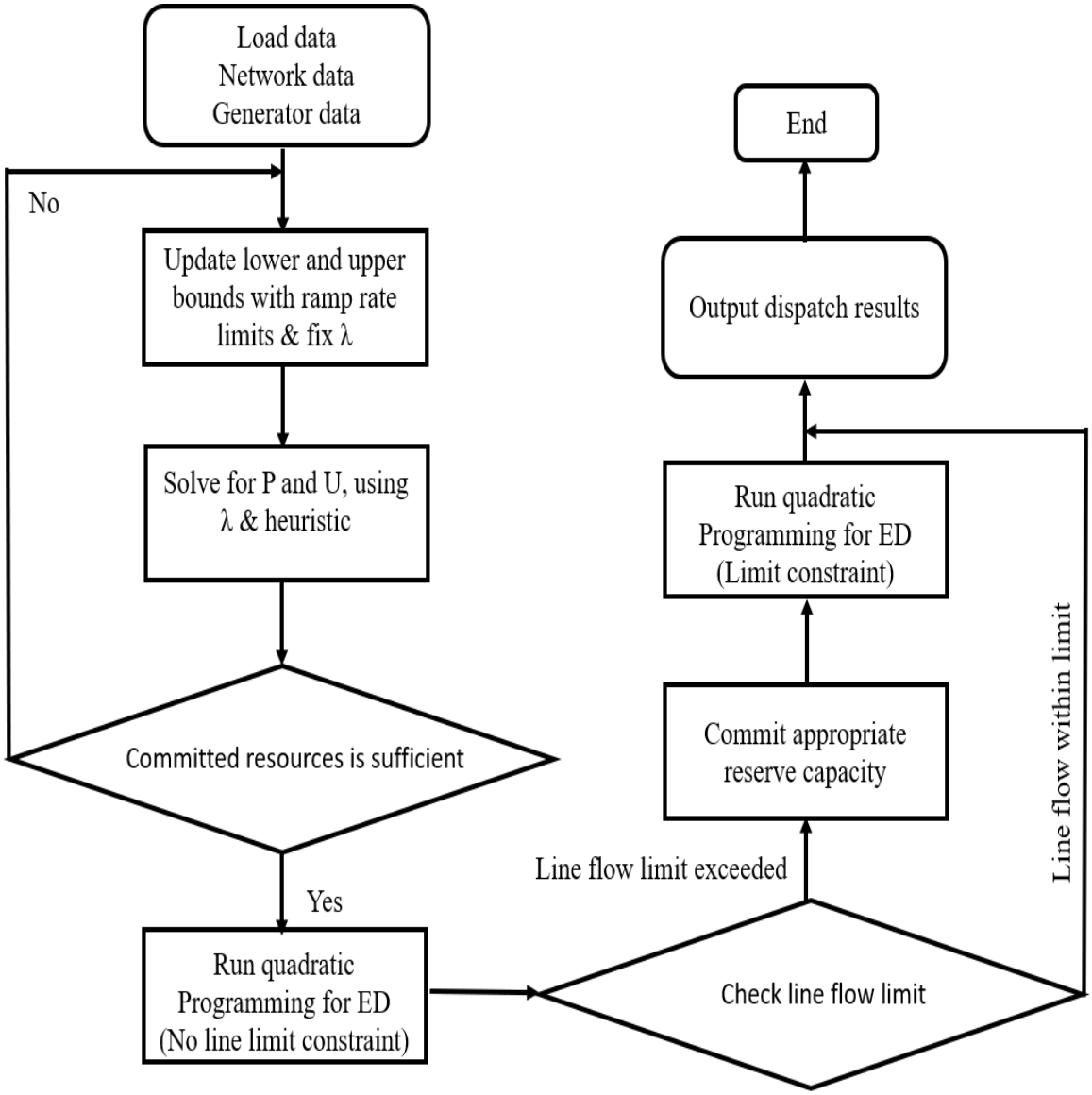


Figure 4.4: Iterative Optimization Approach

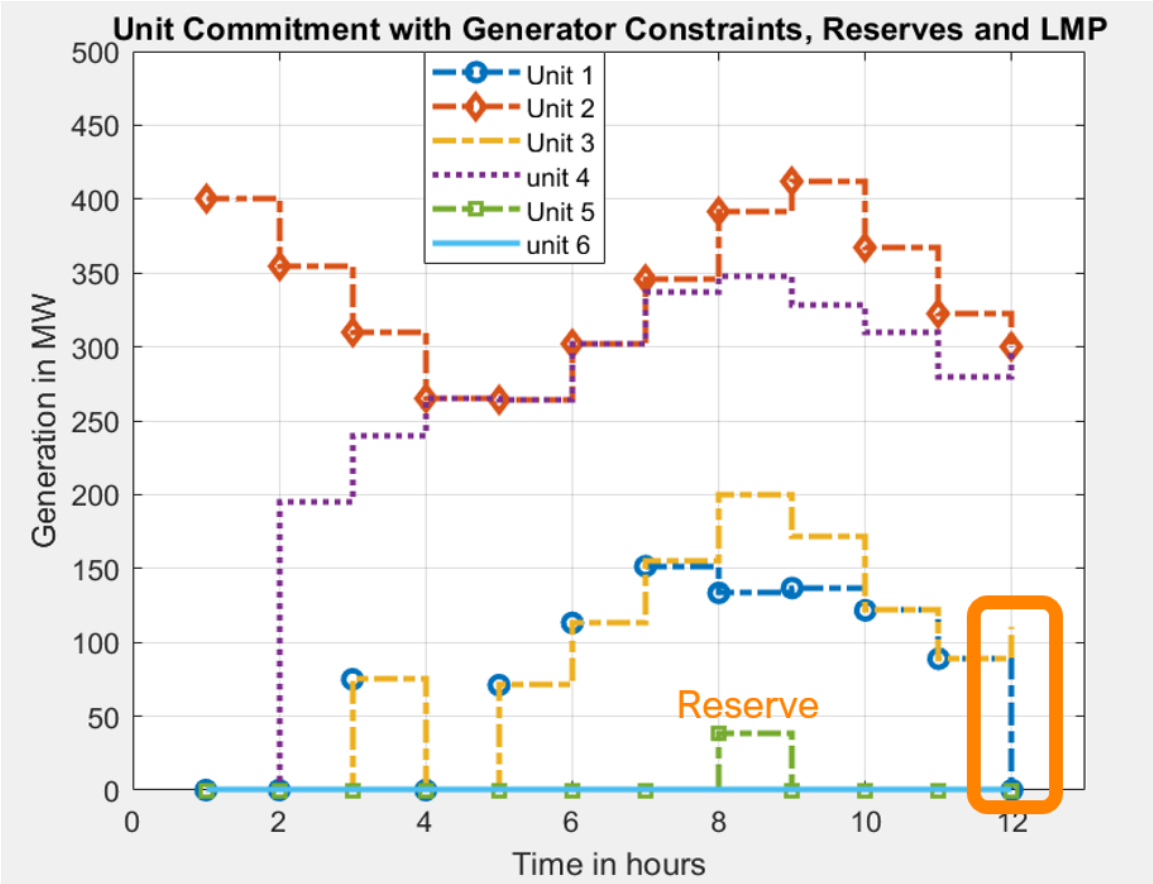


Figure 4.5: Network constraint UC considering reserves and LMP

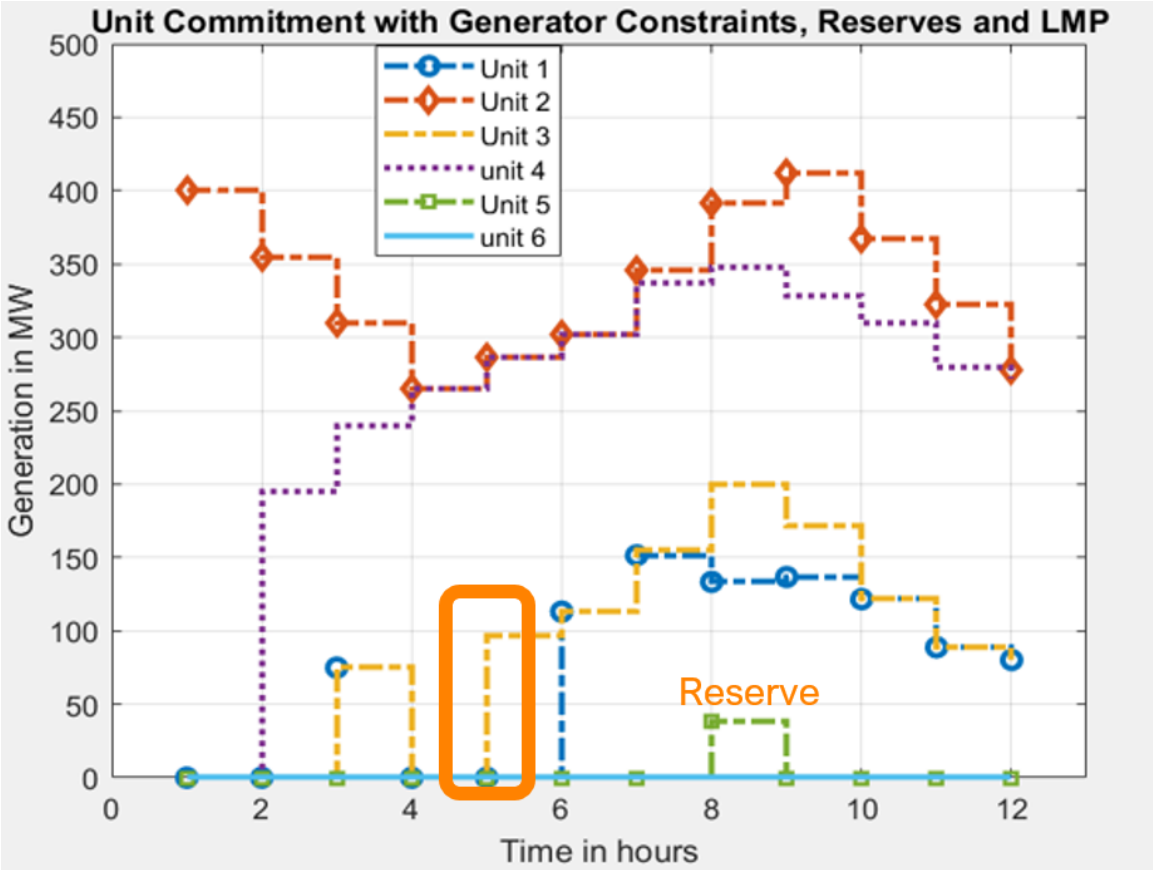


Figure 4.6: Network constraint UC considering reserves and LMP with heuristic

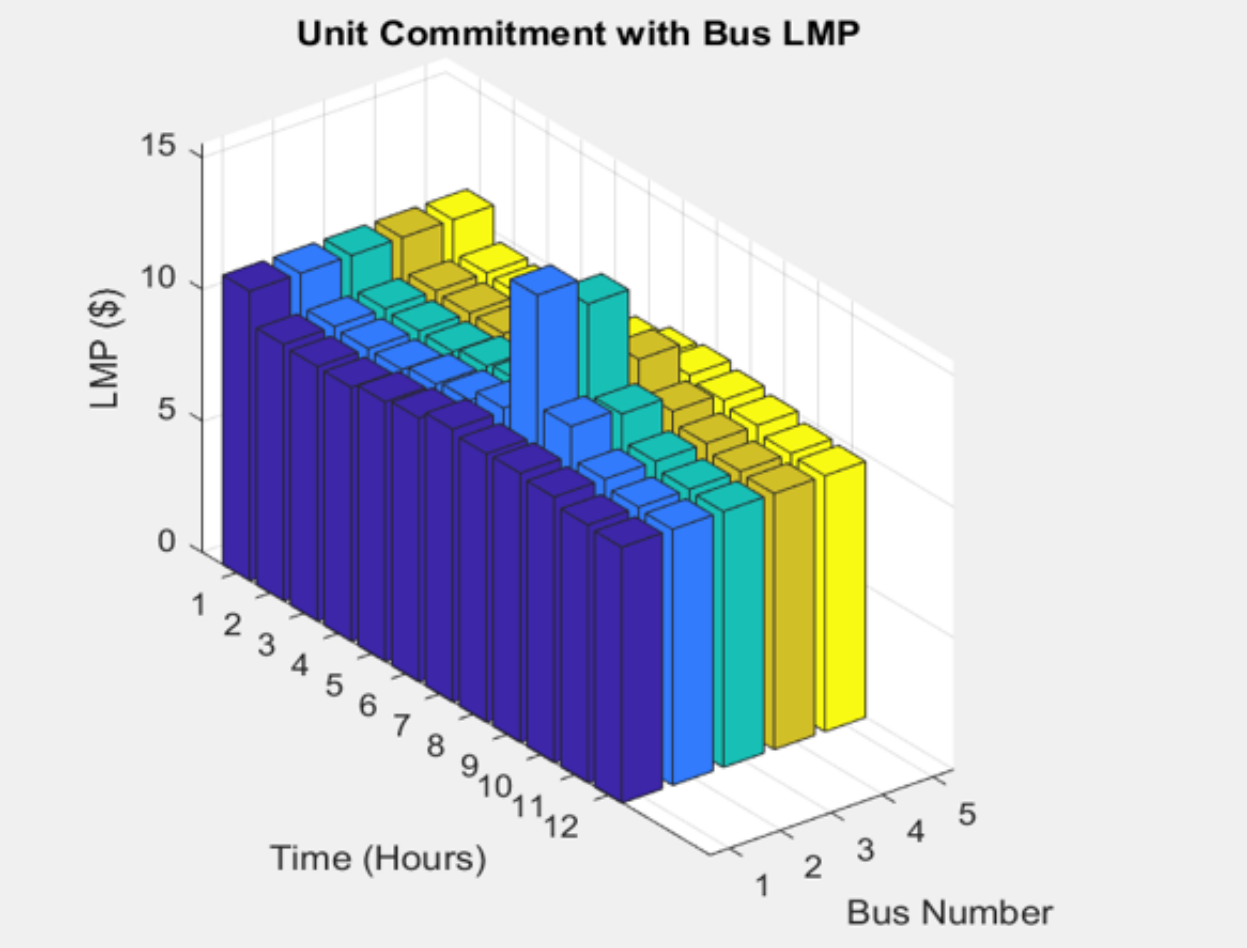


Figure 4.7: Modified PJM 5 bus LMP result considering line limit and reserve (3D)

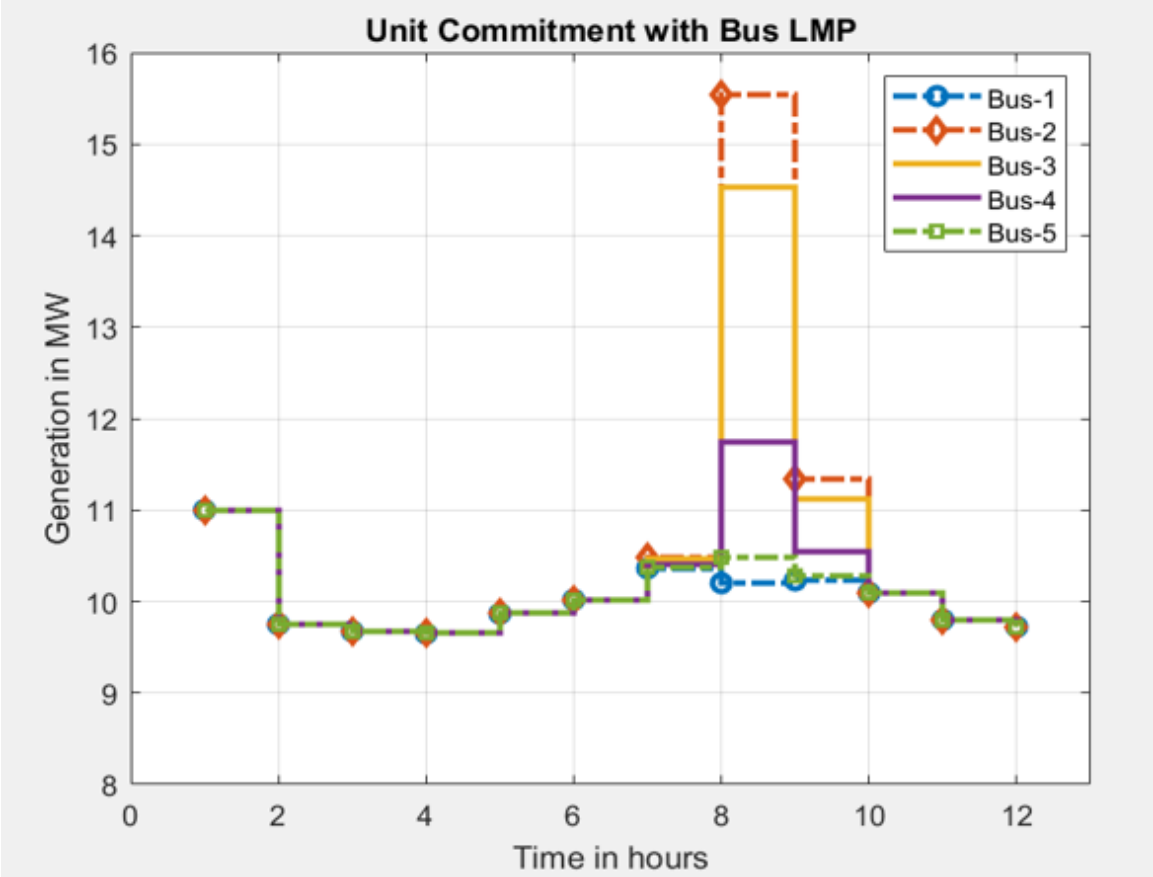


Figure 4.8: Modified PJM 5 bus LMP result considering line limit and reserve (2D)

4.3 LR and Scalabilty

The classic LR formulation scales linearly while the simulation time for MIP increases exponentially with increasing problem size as seen in Figure 2.4. This section focuses on the impact of the problem size on the simulation time and solution quality.

4.3.1 Modified RTS-GMLC 73 Bus System

Following the formulation and solution quality verification from Chapter 3 and Chapter 4 respectively, we study a more interesting system for scalability. The well-studied Reliability Test System (RTS) was originally created in 1979 and has been a useful tool for studying UC and ED [87]. Table 4.6 shows the energy mix for the RTS. Over the years, as power systems continue to modernize, some important updates have been made to the RTS in order to keep up with the challenges that come up with the modernization. In 2019, Barrows et al. made several updates to the RTS and they called the new model RTS-Grid Modernization Laboratory Consortium (RTS-GMLC) [7]. The system is a 73-bus system and is designed to be complicated enough to show the effect of changes in power systems modernization and small enough to enhance research in the area of UC and ED. Some examples of the updates include replacing several conventional units with gas units, adding renewable resources, and changing bus load capacity to create congestion on transmission lines. In this work, a modified RTS-GMLC 73 bus system is analyzed for different time horizons. The solution from the proposed formulation is compared with that of Egret for solution quality and computational time.

The RTS-GMLC bus data, shunt data, and branch data are unaltered for this investigation. To include identical units, generators 101_CT_1, 115_STEAM_1, 123_STEAM_2, 201_STEAM_3, 216_STEAM_1, 223_STEAM_1, 316_STEAM_1, and 323_CC_1 were all replaced with the parameters of generator 113_CT_1. The first 3-digit number in the generator name points to the bus location while the last digit indicates the position of the unit on the bus. To increase the chance of committing the somewhat expensive identical units, the cheap renewable resources and the only Nuclear plant were removed. Other modifications

Table 4.6: RTS-79 Generation Mix

Prime Mover	Fuel	Capacity-MW (MW)	(%)
Steam	Fossil-Oil	951	28
Steam	Fossil-Coal	1,274	37
Steam	Nuclear	800	24
Combustion Turbine	Fossil-Oil	80	2
Hydro	Hydro	300	9
Total	----	**3,405**	**100**

include removing of the reserves resources and system requirements like flexible ramp up and down requirements, and regulation up and down requirements.

4.3.2 Benchmark for Simulation Time using MIP

The study is done by running simulations for 3 cases with different time horizons. The simulation time horizons are 48 hours, 168 hours (1 week), and 336 hours (2 weeks) for Case 1, Case 2, and Case 3, respectively. Constraints such as generator minimum and maximum limits, ramp up and down limits, and minimum up time and down time limits are considered during the simulation. For each time horizon, three sets of simulations are performed using three formulations. These formulations are (1) Egret, (2) Heuristic only (Heuristic-1), and (3) Heuristic with iteration over lambda (Heuristic-2).

4.3.3 Test Result for Case 1

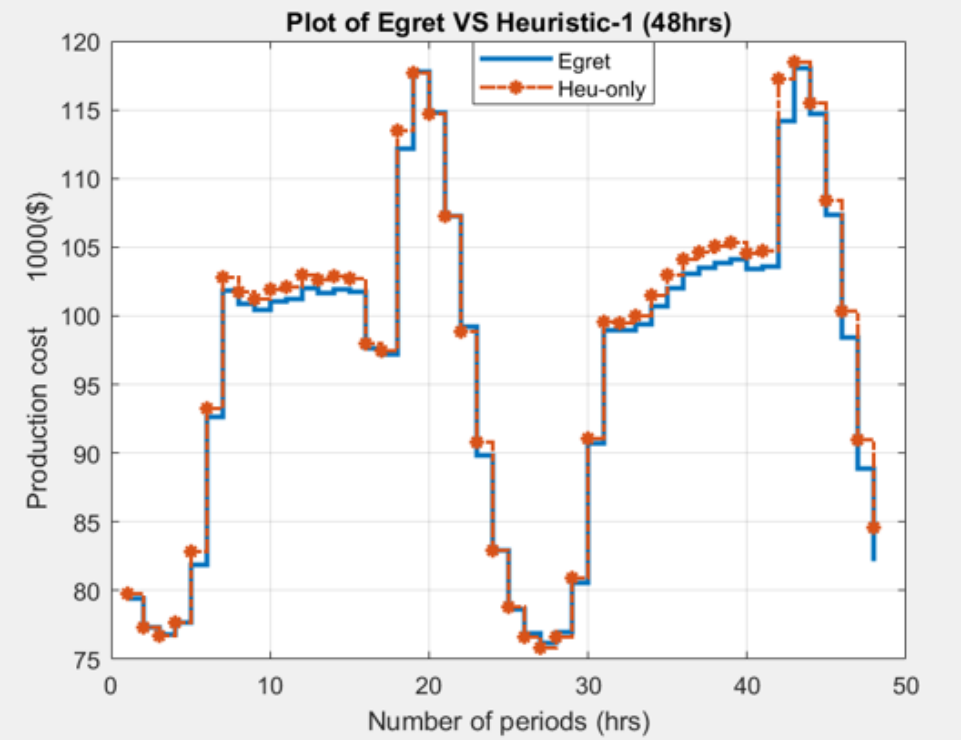
The RTS-GMLC 48 hours load data for Case 1 is time stamped "2020-02-04 00:00:00","2020-02-06 00:00:00", and can be found in the SourceData folder. This time stamp points to the time periods from February 4, 2020, at 12:00 AM to February 6, 2020, at 12:00 AM. Table 4.7 clearly shows that the Egret formulation has the best solution but not the best run time. Comparing the other two solutions (Heuristic-1 and Heuristic-2), it can be observed that further iteration over price can improve the solution quality but at the expense of run time. The improvement in the solution quality is well highlighted in Table 4.8. The percentage difference was reduced from 0.7% to 0.01% when compared to Egret. Figures 4.9a and 4.9b compare the hourly cost of Egret to Heuristic-1 and Heuristic-2 respectively. The hourly cost of Heuristic-2 closely follows that of Egret when compared to Heuristic-1. It is important to note that even though Egret outperformed overall, it does underperform during certain periods. Figure 4.10 shows the hourly performance of Heuristic-2 and Egret by plotting the hourly cost difference. A positive relative cost difference implies that Egret has a cheaper cost (superior) of production and a negative value means that it has a higher production cost (performs poorly). A general trend here is that Egret performs better (positive relative cost) when the hourly load increases and the reverse when the hourly demand decreases.

Table 4.7: Production cost for Case 1

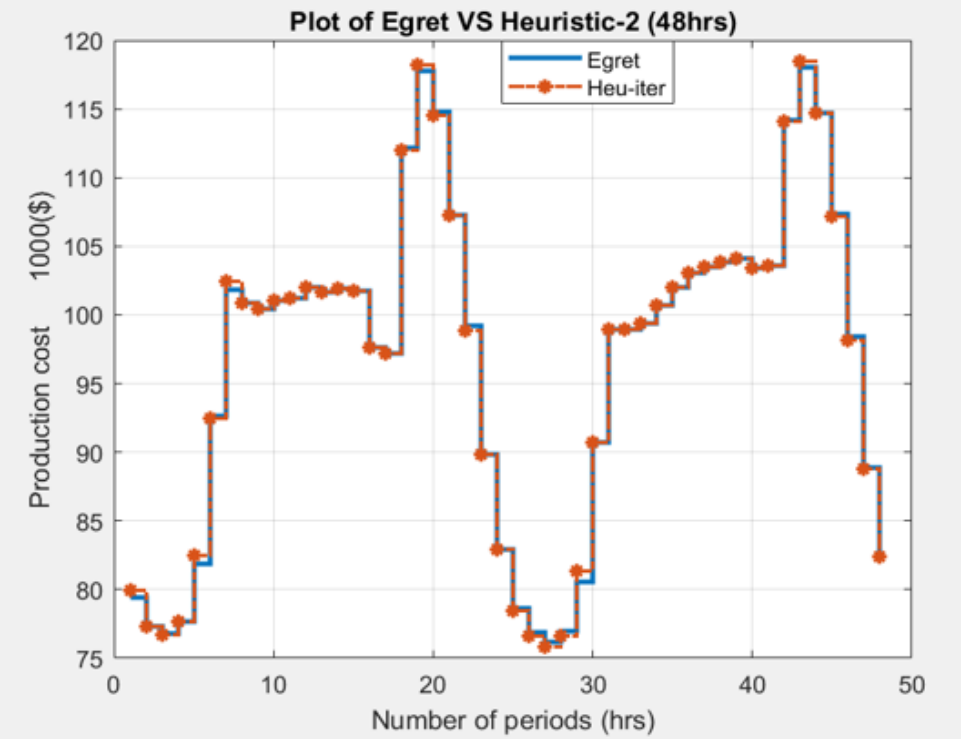
	Egret	Heuristic-1	Heuristic-2
Total Cost	$ 4,642,377.36	$ 4,676,697.22	$ 4,642,938.77
Run Time	2.32 sec.	0.64 sec.	1.17 sec.

Table 4.8: Cost Benchmark w.r.t Egret for Case 1

	Difference	Ratio	% difference
Heuristic-1	$ 34,319.9	0.007	0.7
Heuristic-2	$ 561.41	0.0001	0.01



(a) A benchmark of the hourly cost of the heuristic only using Egret



(b) A benchmark of the hourly cost of the heuristic with iteration using Egret

Figure 4.9: Solution benchmark for Case 1

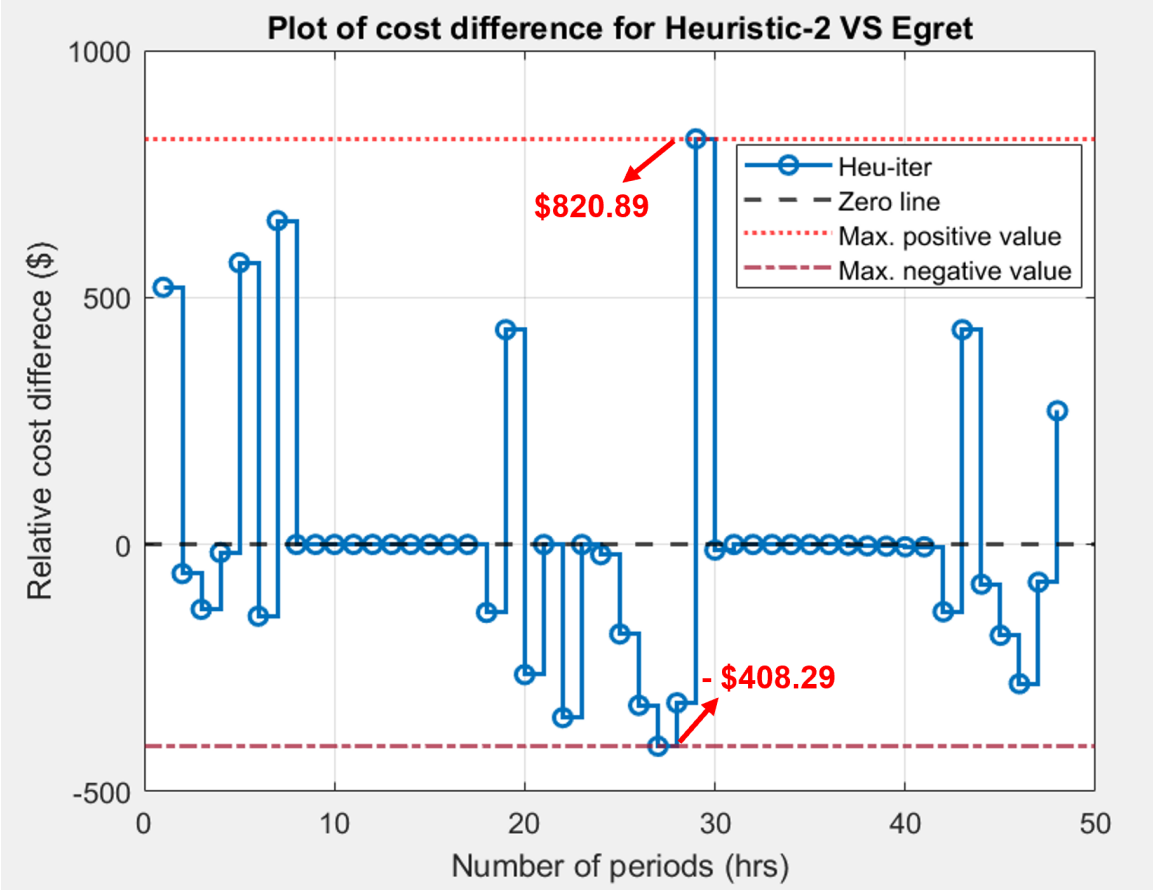


Figure 4.10: Hourly cost difference between Heu-iter and Egret for Case 1

Larger spikes in hourly cost difference can be seen at periods when Egret performs better. The largest spike in hourly cost is positive $820.89. There are smaller but many more spikes when Heuristic-2 performs better (negative relative cost).

LR compares the hourly demand with the committed resources during each iteration and modifies λ (estimated price) as needed for the next iteration. Once enough energy capacity is committed, the UC process stops and the ED is solved. The number of units committed might not be the optimum number of units for the demand. This is where iterating over price could be helpful. Committing too few resources could result in some generators running at or close to their maximum capacities. In contrast, committing too many units could result in expensive units running at their minimum capacities. It is economically appealing for units with quadratic cost functions to run at optimum capacities rather than at the minimum or maximum capacities.

During the λ iteration process, two fixed δ values are selected. δ_1 is the maximum allowed difference between the estimated price (lambda) and the actual price after solving the ED. δ_2 is the maximum allowed number of iterations. The smaller the value of δ_1 and the larger the value of δ_2, the better the solution quality. The above δ combinations, however, could lead to a longer simulation time. Hence, the values of δ_1 and δ_2 should be selected in such a way that the result is improved in a meaningful way and the simulation time is not seriously impacted. For this system, the acceptable range of δ_1 is found to be between 2.5 and 3 while the acceptable range of δ_2 is between 2 and 4.

4.3.4 Test Result for Case 2

In Case 2, the simulation time horizon is set to 168 hours (1 week). The RTS-GMLC load data is time-stamped "2020-02-01 00:00:00","2020-02-8 00:00:00", and can be found in the SourceData folder. This time stamp points to the time periods from February 1, 2020, at 12:00 AM to February 8, 2020, at 12:00 AM. As seen in Case 1, MIP has the best solution but the largest run time (Table 4.9). Heuristic-1 has the best simulation run time but the worst solution. Although the solution quality for Heuristic-2 is of lower quality when compared to Egret, it is a significant improvement over Heuristic-1.

Table 4.9: Production cost for Case 2

	Egret	Heuristic-1	Heuristic-2
Total Cost	$ 15,633,093.6	$ 15,723,283.5	$ 15,636,502.7
Run Time	5.42 sec.	2.16 sec.	3.63 sec.

Performing extra iteration over price as in Case 1 above improved the solution quality with some additional increase in simulation run time. Using Eret as a benchmark, the improvement in the solution quality from Heuristic-1 to Heuristic-2 is seen in Table 4.10. The percentage difference from Heuristic-1 to Heuristic-2 was reduced from 0.5% to 0.02%. The spikes in hourly cost difference are observed in Figure 4.11. Unlike Case 1, the larger spikes in prices occurred at periods when Egret performed poorly (negative relative cost) and the largest price spike of $-\$778.62$ is seen at hour 95.

4.3.5 Test Result for Case 3

In Case 3, the simulation time horizon is set to 336 hours (2 weeks). The RTS-GMLC load data is time-stamped "2020-02-01 00:00:00","2020-02-15 00:00:00", and can be found in the SourceData folder. This time stamp points to the time periods from February 1, 2020, at 12:00 AM to February 15, 2020, at 12:00 AM. In line with the results from Case 1 and Case 2, the MIP solution quality is superior to LR as seen in Table 4.11. Iteration over price improved the solution quality of the heuristic formulation (Heuristic-1 to Heuristic-2) from a percentage difference of 0.5% to 0.05% as seen in Table 4.12. It is also worth noting that as scalability is being considered, increasing the problem time horizon directly increases the solution run time for all 3 formulations as seen in Tables 4.7, 4.9, and 4.11. The system scalability will be further discussed in the following sections. A large positive cost difference of $\$2,168.99$ is observed in favor of Egret while the largest negative cost difference observed in favor of the LR formulation is $-\$1,100.14$ (Figure 4.12). A further investigation of the hourly cost difference can give a good insight into new methods of solution quality improvements in LR formulations.

4.3.6 Scalability Considering System Size

In the previous subsections, the system scalability was studied by increasing the time horizon of the optimization problem. Another way of understanding system scalability and solution run time is by increasing the number of decision variables in the optimization problem. The system size is scaled up by increasing the number of units (binary variables) and load by

Table 4.10: Cost Benchmark w.r.t Egret for Case 2

	Difference	Ratio	% difference
Heuristic-1	$ 90189.9	0.005	0.5
Heuristic-2	$ 3409.1	0.0002	0.02

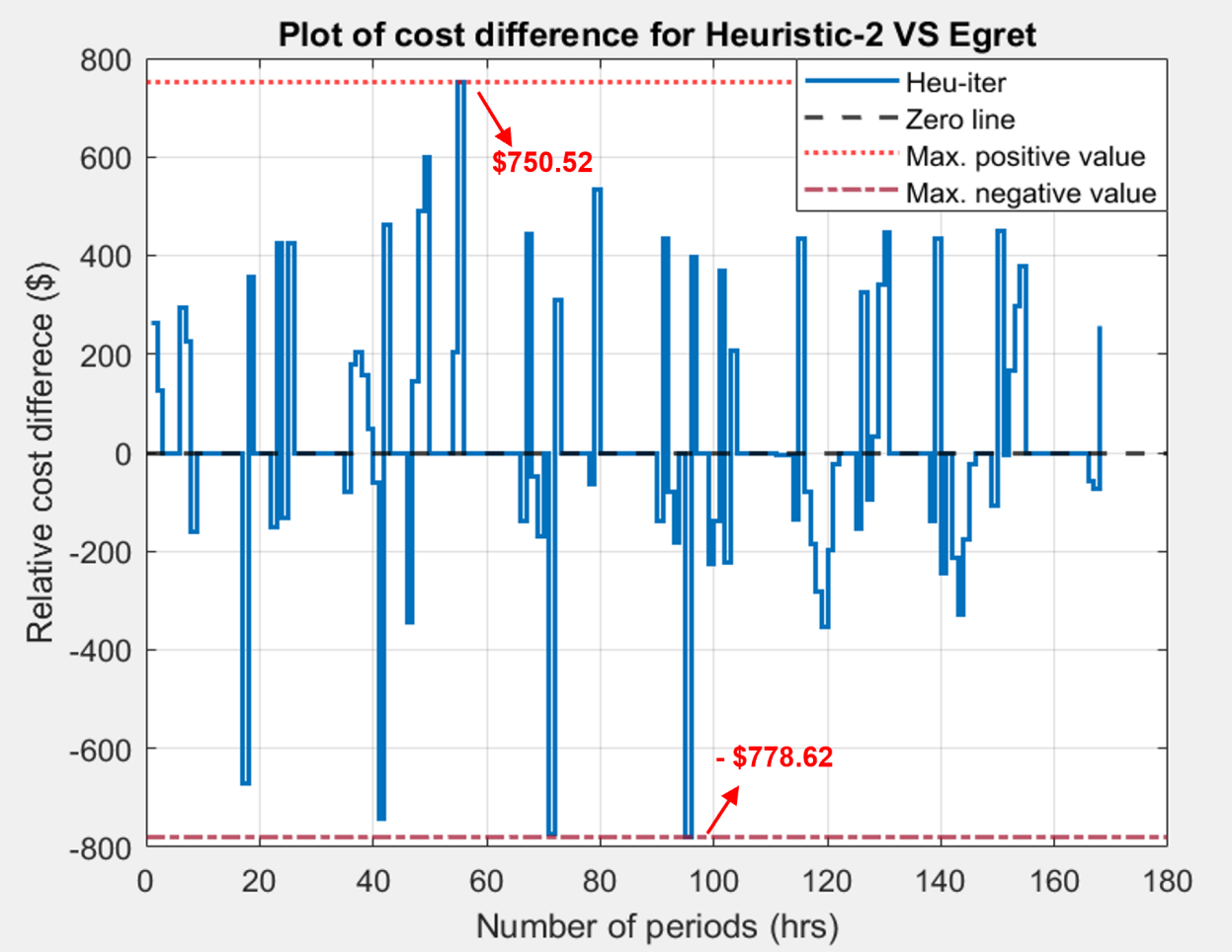


Figure 4.11: Hourly cost difference between Heu-iter and Egret for Case 2

Table 4.11: Production cost for Case 3

	Egret	Heuristic-1	Heuristic-2
Total Cost	$ 31,292,617.3	$ 31,464,022.7	$ 31,307,552.0
Run Time	12.89 sec.	4.36 sec.	7.63 sec.

Table 4.12: Cost Benchmark w.r.t Egret for Case 3

	Difference	Ratio	% difference
Heuristic-1	$ 171,405.318	0.005	0.5
Heuristic-2	$ 14,934.6	0.0005	0.05

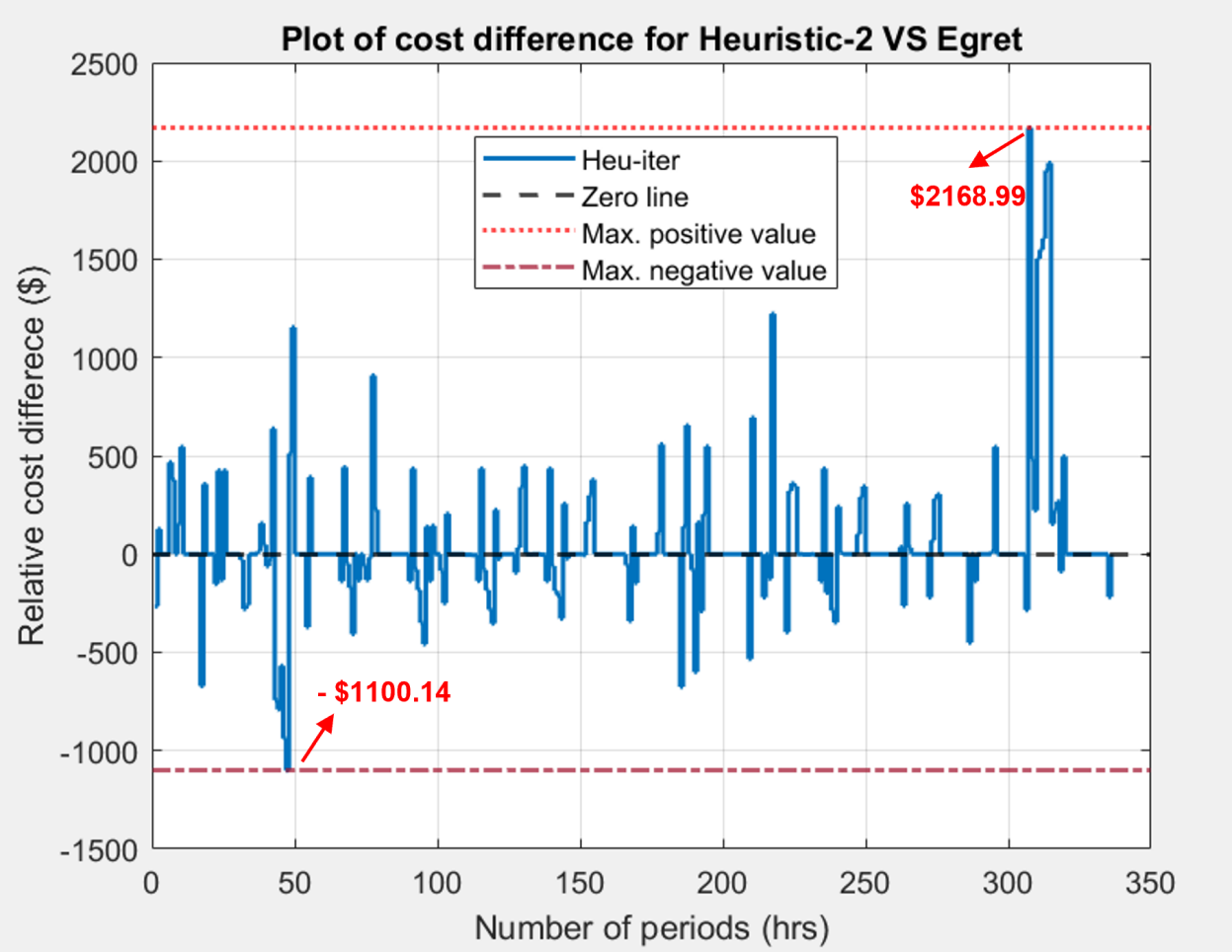


Figure 4.12: Hourly cost difference between Heu-iter and Egret for Case 3

factors of 2, 3, and 4, making 144, 216, and 288 units respectively. The demand is increased to match the increase in the number of units for each scenario. The increase in the total load size and the number of units per problem is shown in Figure 4.13. Investigating this setup by using the above Heuristic-2 model only, 3 sets of simulations are performed for 48, 168, and 336 hours. It can be seen that the cost of production is linearly proportional to the increase in the number of units and demand size (Figure 4.14).

4.3.7 Discussion

This research considered 3 simulation cases with different time horizons (48 hours, 168 hours, and 336 hours). In order to find a balance between solution quality and scalability, 2 heuristic formulations were modeled (Heuristic-1 and Heuristic-2). Heuristic-2 requires additional iteration over λ in order to minimize the gap between lambda and the actual price. Using Egret as a benchmark for both models, a trade-off between solution quality and simulation run time can be determined. From all 3 cases, it can be easily observed that Heuristic-1 scales very well when compared with Egret but the solution quality might be too poor for real-world applications. A good trade-off between the highly scalable Heuristic-1 model and Egret is the Heuristic-2 model with λ and price iteration. The solution quality is improved in all 3 cases as seen in Tables 4.8, 4.10, and 4.12. The simulation run time does increase with this formulation but remains linear as seen in Figure 4.15. As expected, Egret's simulation run time increases exponentially.

An important aspect of this research is the spikes in the hourly cost differences between Egret and the proposed formulation. Depending on peak demand, very high hourly costs difference could be observed as seen in Figure 4.12 where the maximum difference is $2168.99. These spikes in cost difference point to the difference in the committed unit combinations and the number of selected units per time. Figures 4.16 shows the difference in the hourly number of units committed for Egret and Heuristic-2 as well as the load demand pattern. When load demand is low, Egret commits more units than LR, making the hourly cost of generation of the former larger. In contrast, Egret commits fewer units than LR at periods with high demands, making the hourly cost of generation for the latter larger. It can be seen that at hours 19 and 43 where the hourly demands are high, LR committed 22 units while

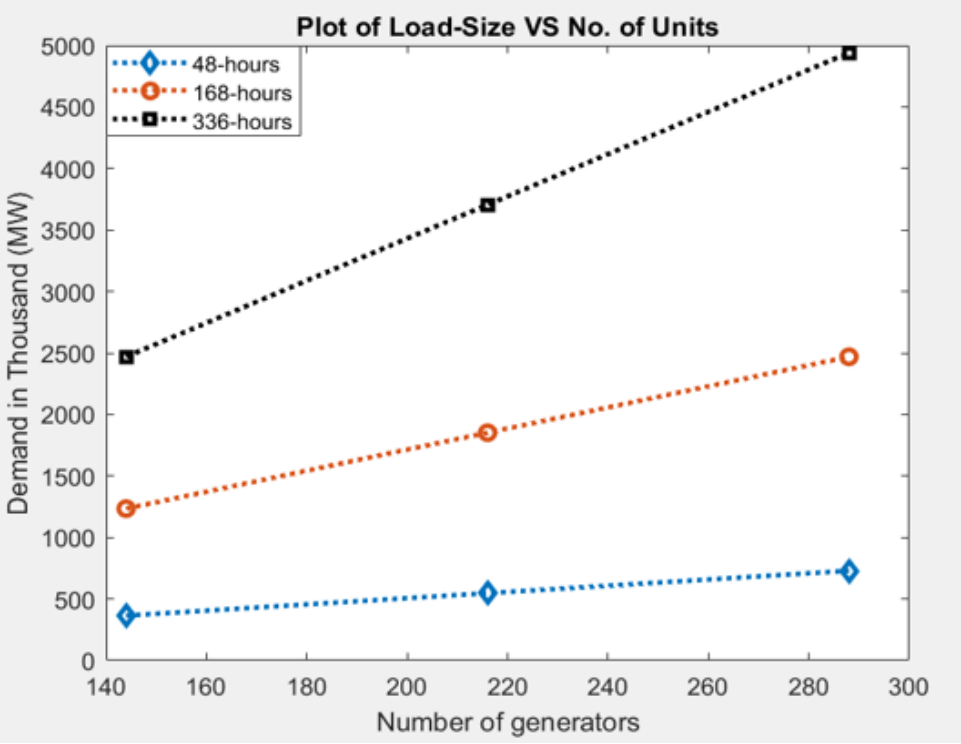


Figure 4.13: Linear increase in total load size and number of units

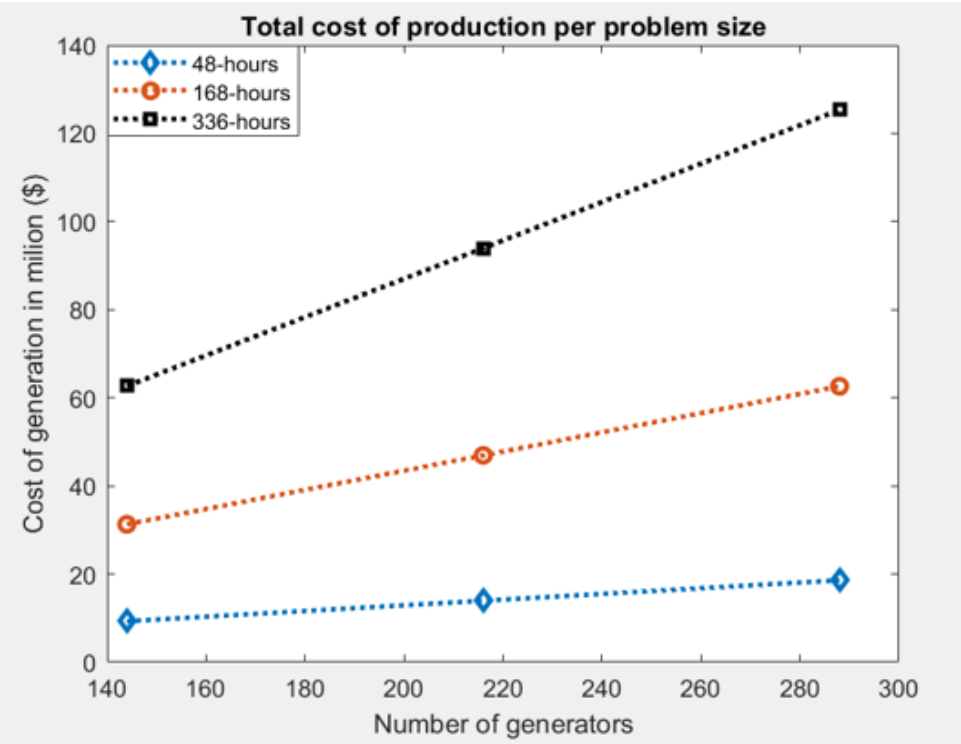


Figure 4.14: Increase in the total cost of production with increase in problem size

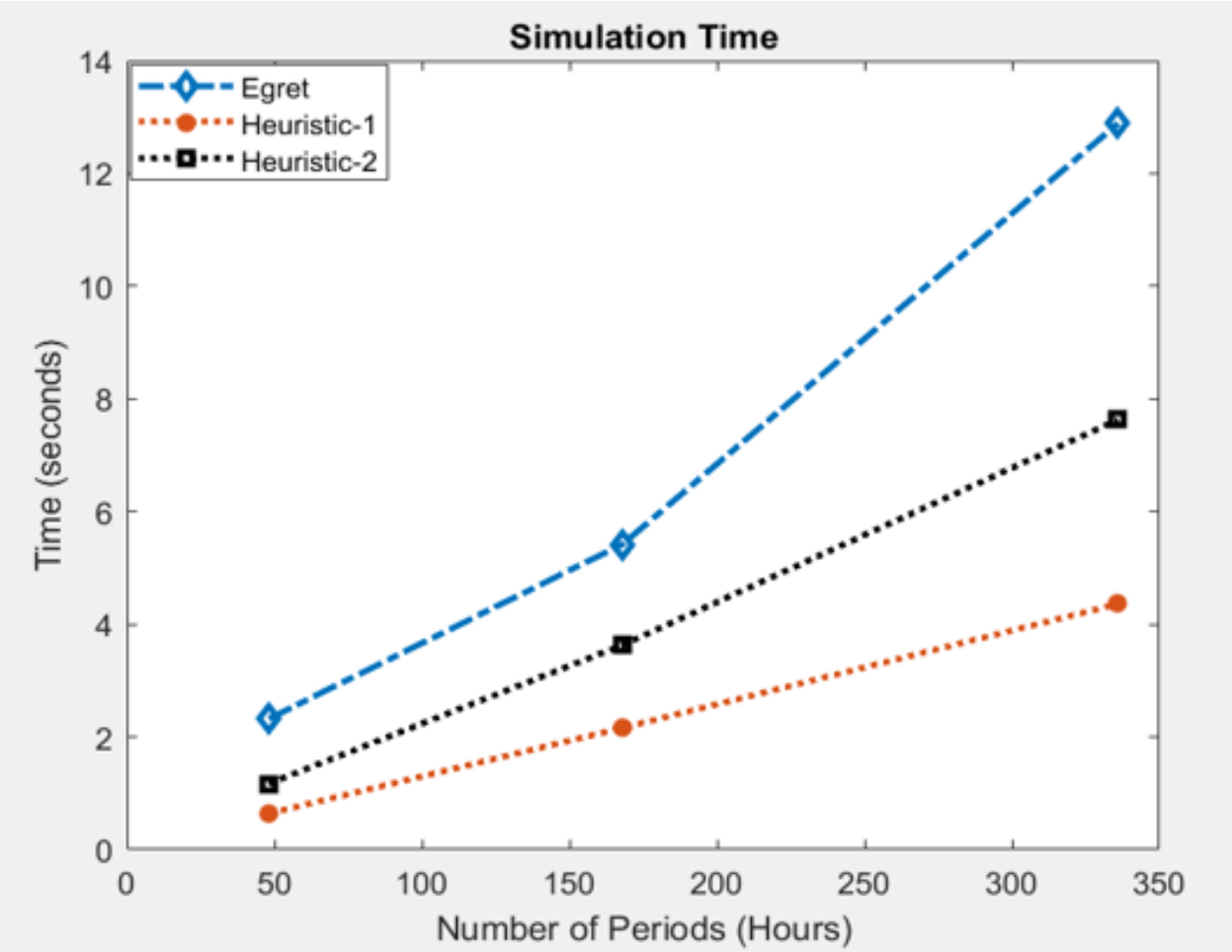


Figure 4.15: Plot of simulation run time for all 3 formulations and all 3 cases

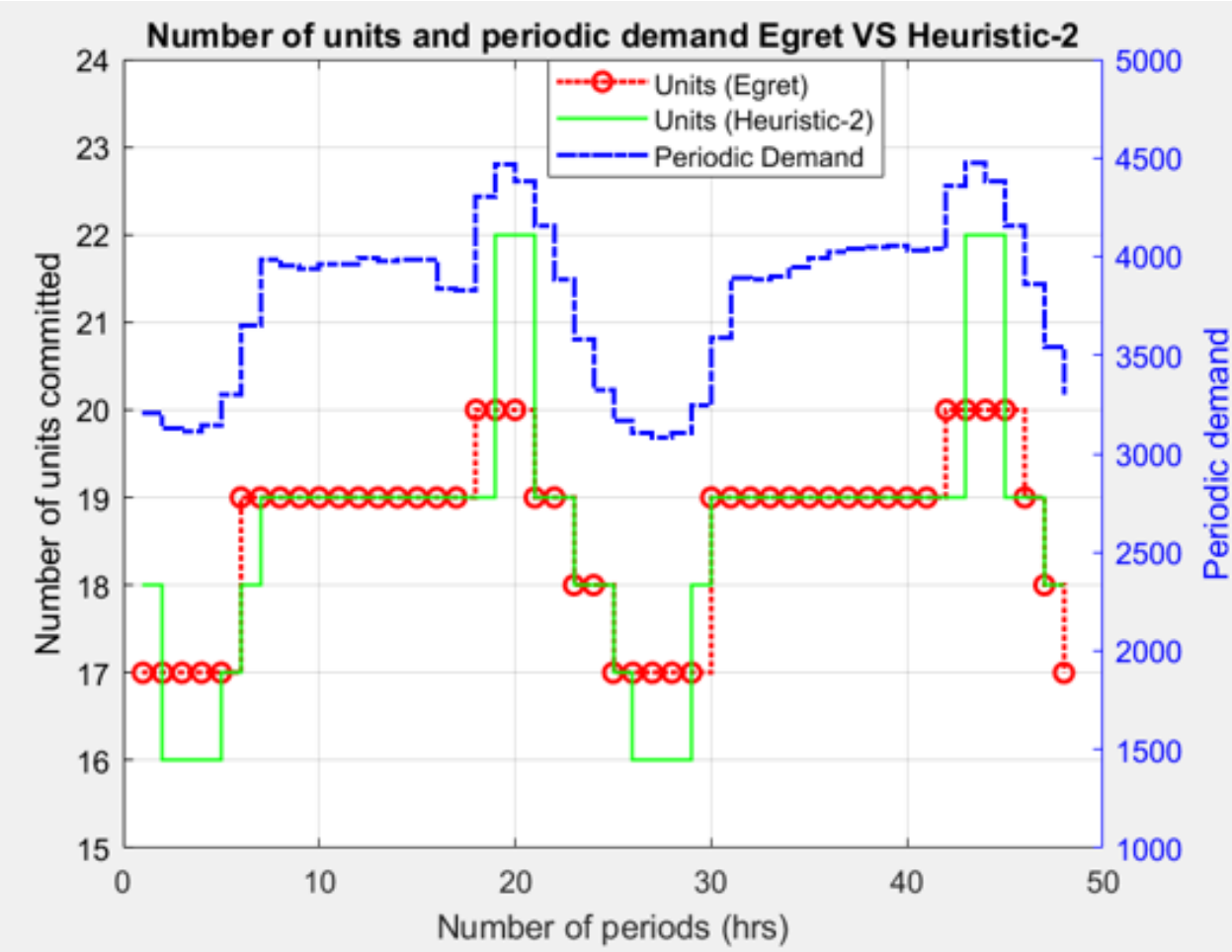


Figure 4.16: Total number of units committed per period

Egret committed 20 units. In contrast at hours 2 and 26 where the hourly demands are very low, LR committed 16 units while Egret committed 17 units. Heuristics can be formed around this pattern of UC to further improve the solution quality of LR in future research.

Following the above results, a second study involving increasing load size and the number of units (binary variables) was performed for 3 different time horizons (48hrs, 168hrs, and 336hrs). This investigation only focuses on the proposed Heuristic-2 as seen in Figures 4.13 and 4.14. It can be easily seen from Figure 4.17 that the solution run times for the proposed formulation and for all 3-time horizons are linear with the scaling of the decision variables and problem size. Overall, the proposed formulation scales considerably well and the solution quality is in an acceptable range when compared to MIP.

4.4 Scalability for DA UC with Different Time Intervals

The importance of the DA SCUC problem cannot be overemphasized in the optimum scheduling of resources and for reliably operating the power grid. Apart from solving the DA SCUC problem as a 1-hour interval problem, modern markets solve the same problem over smaller intervals in good time considering the increase of non-dispatchable resources in the power grid. Optimization solutions for 5-minute, 15-minute, and 30-minute time intervals can better capture the effect of uncertainties and the frequent changes in demand when compared to the 1-hour time interval. The solution quality and simulation run time for these time intervals are considered using Egret, heuristic-1, and heuristic-2 formulations. Each formulation is applied to solve the optimization problem in 1-hour, 30-minute, 15-minute, and 5-minute time intervals which directly translates to 24, 48, 96, and 288 periods respectively. Figure 4.18 compares the simulation run time for all 3 formulations and for all time intervals. Heuristic-1 scales linearly with the increase in the number of periods. Heuristic-2 and Egret have a considerable increase in the simulation times, especially for the 5-minute interval. However, when considering the solution qualities, Egret outperforms, while Heuristic-2 shows a good compromise between solution quality and simulation run

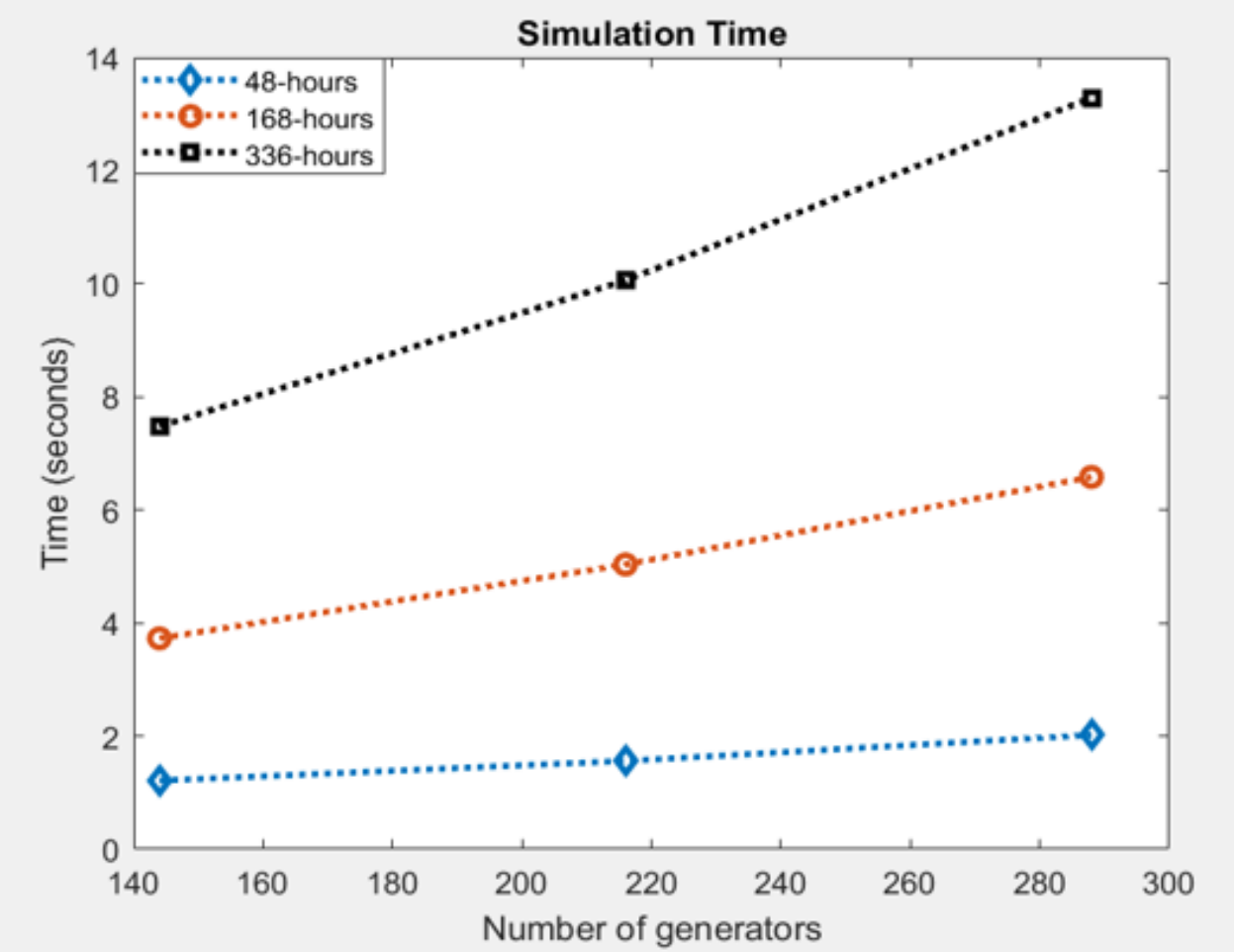


Figure 4.17: Simulation run time for increasing load and number of units

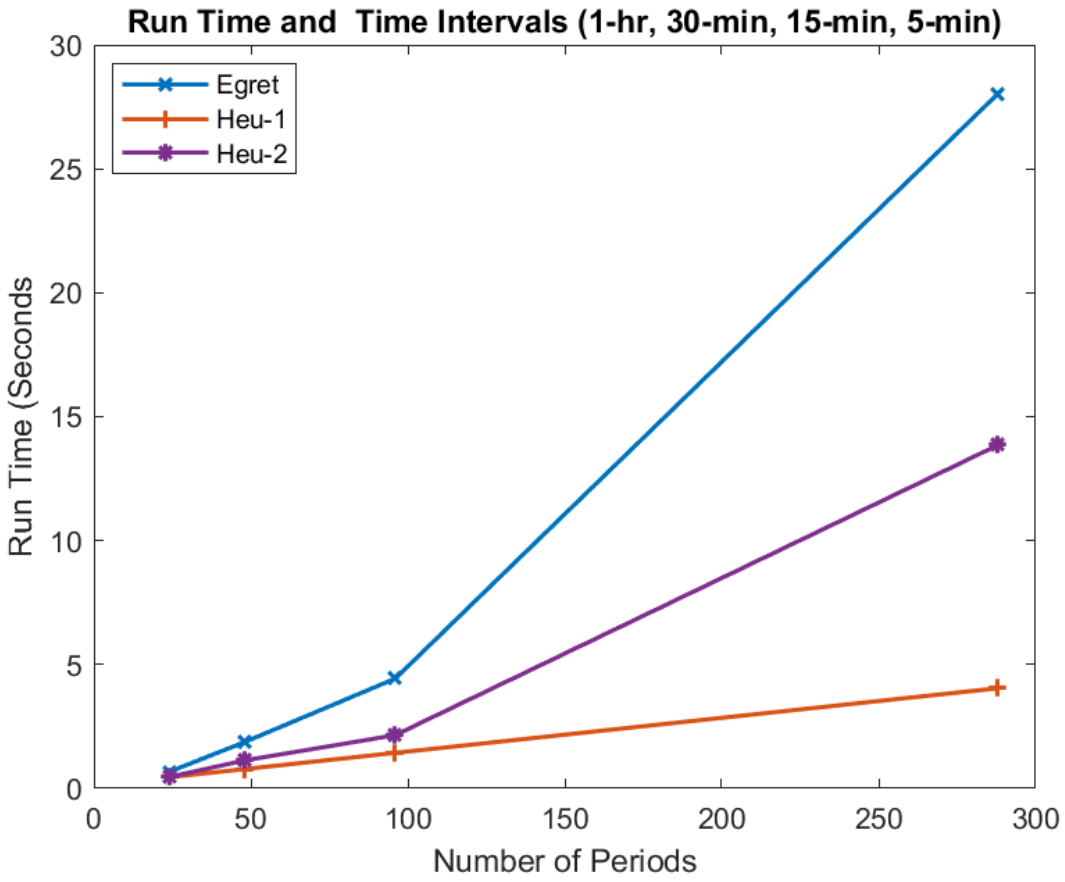


Figure 4.18: Simulation run time considering 1-hour, 30-minute, 15-minute, and 5-minute time intervals

time. Table 4.13 compares the solution quality of Heuristic-1 to Heuristic-2 for the 1-hour and 5-minute time intervals, using Egret as a baseline. The solution quality of Heuristic-2 for the 5-minute interval is well improved but with a considerable increase in simulation run time.

4.5 Conclusions

Following the formulations from the previous chapter, several benchmarks were performed using Egret. The presence of similar and identical units in the UC and ED problem is expected to have considerable impacts on the solution quality of the traditional LR technique. This chapter investigates the benefits of the proposed formulation (with the additional iteration of λ) on solution quality and simulation run time.

First, a study was performed on a small system to highlight the UC process and how identical units are differentiated and prioritized. A modified PJM 5 bus system is studied and Egret is used as a benchmark. The proposed algorithm can distinguish between similar and identical units on different buses using an estimate of the line losses and the units' electrical distances from the load center. Units are also committed in a way that can improve the AC power flow solution since line losses are considered in the UC process. The traditional LR formulation cannot distinguish between similar or identical units, hence, underperforms in solution quality.

Second, the solution quality and simulation run time of the proposed algorithm are investigated using RTS-GMLC. Heuristic-2 with additional iteration over λ improves the solution quality within a reasonable simulation run time when compared to Heuristic-1. The formulation also scales well overall as the number of units and load size increase when compared to Egret.

Third, an investigation is performed for a 24-hour model, using 4 different time intervals (1 hour, 30 minutes, 15 minutes, and 5 minutes). This is of interest because solving optimization problems with short time intervals can help track uncertainties and variabilities in renewable resources and load.

Table 4.13: Cost w.r.t Egret for 1-hour and 5-minute intervals

	% difference 1-hour Interval	% difference 5-minute Interval
Heuristic-1	0.52	0.54
Heuristic-2	0.042	0.067

Heuristic-1 has a linear simulation run time with an increasing number of periods but the solution quality might not be within an acceptable range. Heuristic-2 has a considerable increase in simulation run time, especially for the 5-minute (288 periods) time interval. The simulation run time is however reduced (about half) when compared to Egret. Finally, the solution quality of Heuristic-2 is in an acceptable range when compared to Egret and hence, can serve as a good alternative.

In conclusion, of the 3 formulations, Heuristic-1 is an improvement from the traditional LR. The simulation run time is barely impacted and the solution quality is a lot better when compared to the classic LR. Heuristic-2 could be a better trade-off between LR and Egret because it could improve the solution quality of Heuristic-1 by a factor of 10 with some limited impact on simulation run time.

Chapter 5

Computational efficiency using LR Formulations

MISO researchers have reported that the Day Ahead (DA) scheduling is the most challenging optimization problem because about 98% of the market resources get committed during this process. Since the start of the market in 2005, there have been continuous efforts on reducing the simulation run time and improving the solution quality for the current and anticipated challenges on the power grid. For example, system bottlenecks were observed during days with a high volume of virtual trading (a large number of small virtual transactions) coupled with a high volume of transmission constraints [15, 16, 18]. With further technological advancements, it is reasonable for power systems researchers to anticipate future grid challenges and prepare accordingly.

In this chapter, formulations and optimization techniques are further explored using Lagrangian relaxation to determine if it is feasible to include DER and renewables in the unit commitment. Considering the unique characteristics of the different generation resources, the limitations and advantages of these resources are investigated. The goal is to enhance market integration of Distributed Energy Resources (DER), Demand Response (DR), and concepts, such as virtual bidding. The task will be a continuation of the work from Chapter 4.

5.1 WECC 240 Bus System

In support of the effort for the bold target of renewable energy adoption by the California's administration, legislature and energy regulators, a reduced 240 bus model was created to better understand the impact of a high penetration of these resources on the CAISO and WECC regional markets [75]. The details of the reduced WECC system and network data are given as follows:

- The system generation resources from the transmission expansion planning are roughly for the 2015 to 2020 time frame.
- The renewable resources and base load (nuclear and coal plants) have the highest priority during the dispatch process. All 3 resource types have a heat rate of 1 for simplicity. The hydro resources are the next on the priority list with a heat rate of 5. The gas fired plants are the least on the priority list.
- The gas fired plants are the main dispatchable resources with most of the system flexibility. The cost functions are piecewise linear and are given in the form of incremental heat rates (Heat Rate Increments) and MW output points (Heat Points) for each gas fired plant. The minimum point of the MW output points is taken as the generator's minimum output limit for each unit. The ramp rate limits for the gas fired plants are set to 60% of the maximum capacity to make the UC problem somewhat more challenging.
- The coal units are set to run at 85% of their maximum capacity. This is easily enforced since the heat rate is set to 1.
- The nuclear plants are set to run at the maximum capacity with a lower limit of 90% of the maximum capacity.
- Hydro generation is limited by water availability (including seasonal changes), and environmental limitations such as irrigation and recreation. The hourly ramp rate limit is approximately 10% of the maximum capacity while the minimum output is set to 20% of the maximum capacity.

- For further simplification, the fuel cost for all unit types is \$5/GJ. This fuel cost is modified to reflect the current marginal energy cost in CAISO and WECC markets for this research.

Using the incremental heat rates and the MW output points the cost of generation between each pair of break points is calculated as follows:

$$c_{m+1} = (hp_{m+1} - hp_m)hr_m + c_m \tag{5.1}$$

$$sl_m = \frac{(c_{m+1} - c_m)}{(hp_{m+1} - hp_m)} \tag{5.2}$$

and the intercept to the x-axis (corresponding to sl_m) is given as,

$$int_m = c_m - (hp_m sl_m) \tag{5.3}$$

where

hp_m = The power output at Heat Point m

c_m = Cost when the power output is hp_m

sl_m = The slope between hp_{m-1} and hp_m

The general equation for each piecewise cost can be expressed as

$$c_m \geq sl_m hp_m + int_m \tag{5.4}$$

The heat rate increases with power output so that the piecewise linear bidding functions are convex and the economic dispatch (ED) can be solved using linear programming (LP). Using equation 5.4, a plot of the cost functions of the first few gas fired plants shows that the calculated cost functions are convex as can be seen in Figure 5.1. The cost functions for hydro and renewable resources are given or calculated as a constant slope that is equal to their heat rate increments (for simplicity).

A notable challenge with the 240 bus system data is that the conventional generators have piecewise cost functions with varying numbers of breakpoints. As can be seen from Figure 5.1, unit 3 has 8 break points while unit 4 has none. The megawatts range between each

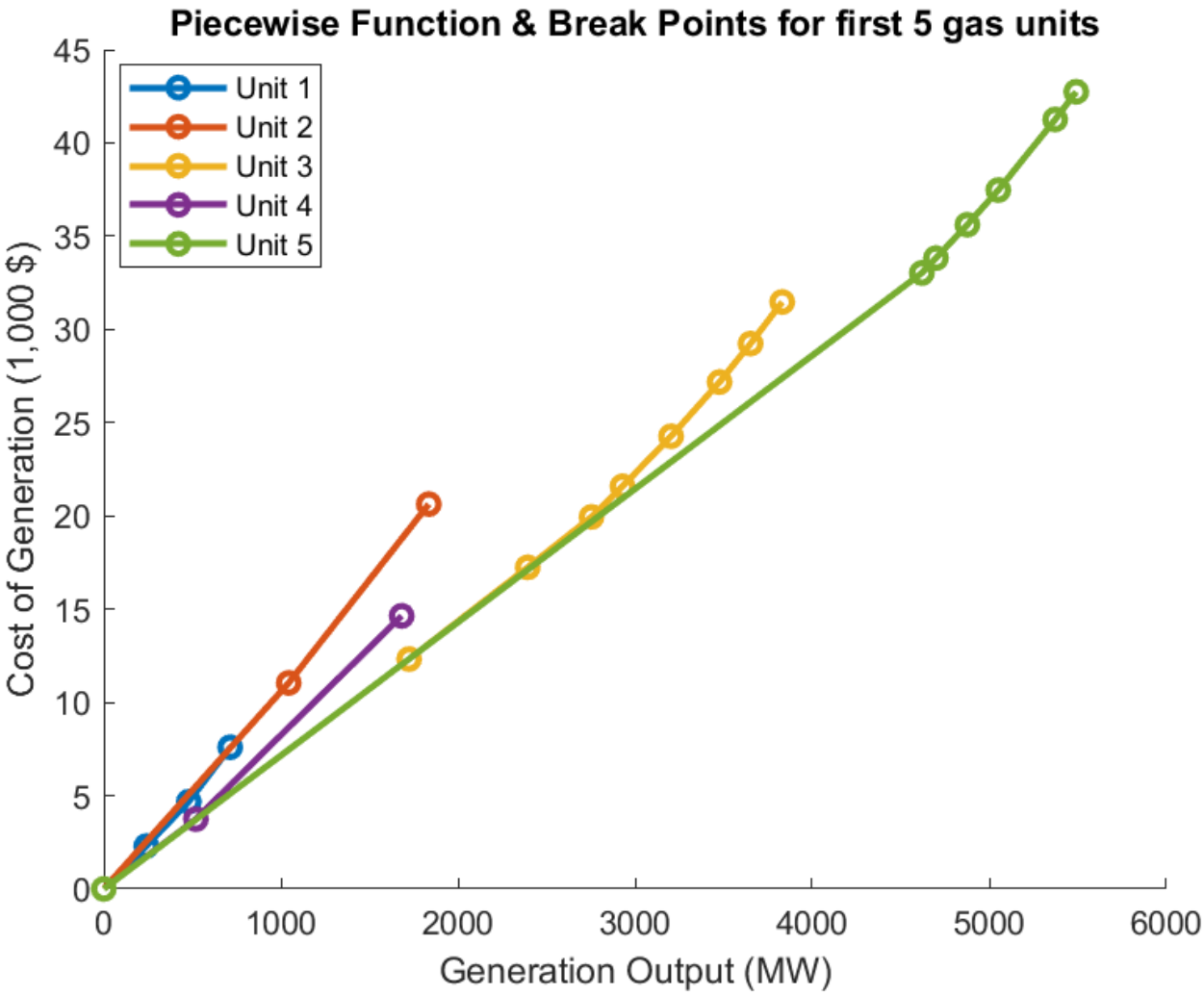


Figure 5.1: Fuel cost function for gas fired plants

pair of break points is also irregular both for individual units and when comparing between different units. For example, Unit 5 has most of its breakpoints bunched together at the tail end of the cost function. The maximum generator capacity could also vary considerably as seen in unit 5 and unit 1 with a ratio of 4.5 to 1 respectively. In practice, the number of breakpoints and the MW range between each pair are determined by market rules.

The data from the WECC system is processed for solving UC and ED, using LR. The formulation and simulations performed in Chapter 3, Section 4.1, and Section 4.2 above utilized a quadratic cost function for solving both the UC and ED problems. In Section 4.3, the quadratic cost function was calculated from the piecewise linear data and used for solving the UC problem, while the ED is solved using the piecewise linear cost function. The effect of the above conversion is minimal on the final solution because the Egret cost data have evenly distributed MW output break points. In this chapter, the WECC data for the piecewise cost functions are converted to quadratic cost functions for simplicity and to reduce the effect of the irregularities in the piecewise cost functions (see Figure 5.1).

5.2 System Flexibility Requirement with DR

The influx of PV solar resources in the CAISO market has continued to create some interesting load patterns. The Duck Curve trough continues to decrease, leading to an increase in the system flexibility requirement. Traditional fossil fuel generators are typically limited in their ability to ramp up and down as quickly as needed. A solution to this problem is utilizing grid technologies such as DR and virtual trading as flexible resources that reduce demand and allow slow units enough time to ramp up. These additional resources also imply an additional number of binary variables when solving UC problems, which directly translates to an increase in the solution computational time.

Considering a case where ISOs have access to a large number of small market resources from market participants who are enrolled in the DR program. These resources can be coordinated to reduce load during periods of high load demand or increase load during low demand periods. In this research, we are considering Type-II DR. The Type-II DR is of interest because of its flexibility and simplicity. While the Type-I DR can only supply

or curtail a fixed amount of load, the Type-II DR can continuously adjust the generation supply or load curtailment as needed. Hence, the Type-II DR can gradually reduce load consumption, flattening the load peak to match available capacity and give slow generators ample time to ramp to the needed levels. In this study, the Type-II DR is implemented by incrementally shifting some percentage of the peak load (the participating DR) to periods of low demand.

The WECC hourly load data from August 10, 2004, with a peak of 141,519.5 MW is modified for this study. The CAISO renewable resources data from July 2, 2022, is scaled and projected over the WECC load data to create a new load pattern with a high ramping requirement and a new net load peak of 185,728.9 MW (See Appendix A).

5.2.1 Impact of Load Peak on Market Price and LMP

The California ISO 2022 Summer Market Performance Report [3] highlights the relationship between daily load peaks and the daily average LMPs. The daily peak load data from August 1 to September 30, 2022, is considered for the report. Daily peak loads (including Operating Reserves) over 50,000 MW were observed for September 1st, 5th, 6th, 7th, and 8th and with the corresponding LMP spikes (see Appendix B). The average LMP for both months is less than \$100/MWh but the daily spikes in price on September 1st and 6th are \$420/MWh (4 times the average) and \$600/MWh (6 times the average) respectively. These large LMP spikes could even be more pronounced when individual buses are considered. In the next session, the effect of DR on LMP spikes is investigated.

5.2.2 Case Study of System Flexibility and LMP Spikes using DR

A base case (case 1) with 143 units, 240 buses, and 448 branches is modeled for the system flexibility requirement test. The load pattern for case 1 has a required ramping of approximately 55 GW in 5 hours (see Figure A.3). A quadratic cost function is generated for each unit, using the corresponding piecewise cost function. The renewable units (with linear cost functions) have the constant and quadratic parts of their cost functions equal to zero. The UC problem is solved using equation 3.17, with a_i, b_i, and c_i as the constant,

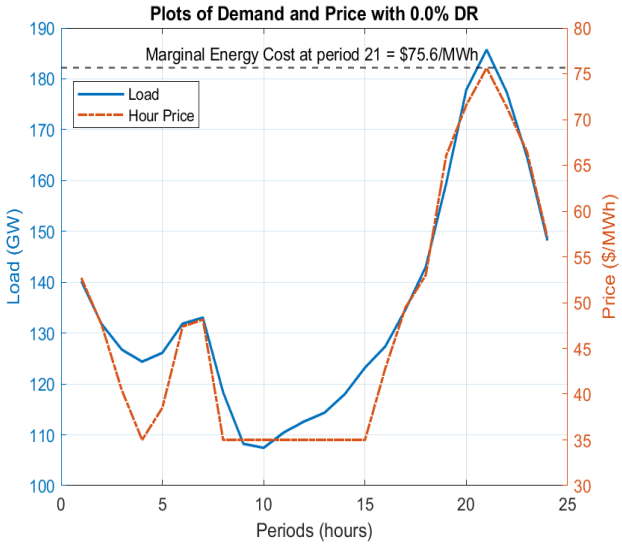
linear, and quadratic coefficients of the cost functions respectively. Once the committed units are identified for the period, the ED problem is solved via the same quadratic cost function for consistency. The ramp rate limits for the next period are updated for each unit, using the result of the ED from the previous period.

From the studies in [4], a 5% shift and a 10% reduction in the total load are considered good DR available capacities. For this investigation, a maximum of 4.5% shift in total load is considered with no load reduction. It should be noted that in reality, all participating customers might not respond to the request to reduce energy usage or to move activities to a time of low energy demand. With this in mind, a total of 10 simulations were performed with committed DR ranging from 0.0% to 4.5% of the daily peak load. The flexible load resources (DR) shifted from the high demand periods (20, 21, and 22) are evenly distributed across periods 8 to 15, thereby, keeping the total daily load constant. Figure 5.2 shows an inverse relationship between available DR and the marginal energy cost as calculated from the ED. As enrolled customers responded to the DR request by shift 0.0%, 1.5%, 3.0%, and 4.5% of the load, the corresponding marginal energy costs at hour 21 are \$75.6/MWh, \$73.9/MWh, \$72.6/MWh, and \$71.4/MWh respectively.

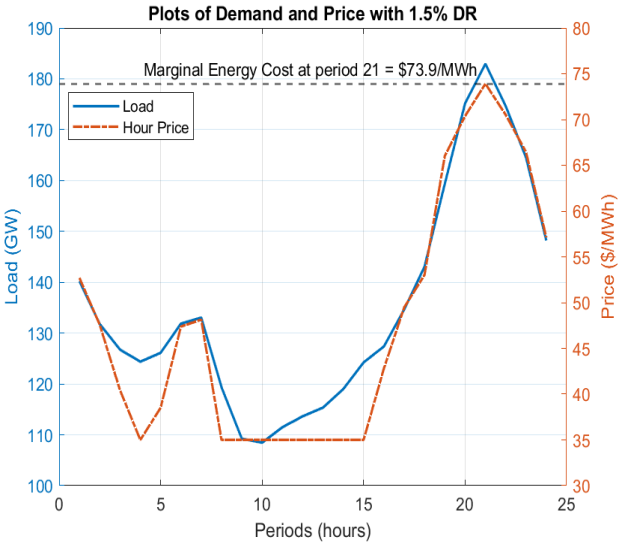
The network effect is investigated by solving the AC power flow **MATPOWER**. The data for solving the hourly OPF is updated from the ED result. These data include the hourly generator limits (as determined by the ramp rate limits) and the associated buses, the unit outputs, the hourly load and the associated buses, and the unit commitment data for updating the unit status. From the result of the AC Power Flow, the bus LMPs for hours 20, 21, and 22 are obtained and plotted as seen in Figure 5.3. As expected, the highest LMP is observed at hour 21 where the daily peak load is observed. The LMP spike at bus 198 reduces as the percent capacity of the DR increases. The LMP spike could be a function of committing a very expensive generator or due to system congestion.

5.2.3 Discussion

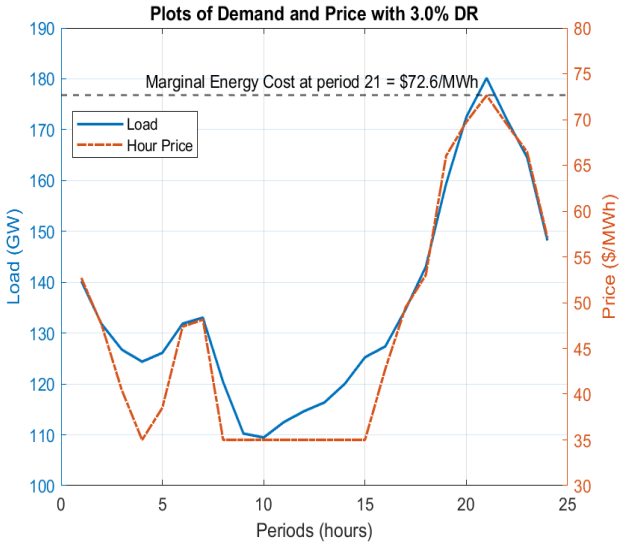
This chapter investigates the impact of peak load shaving via DR on UC solution, especially the marginal energy costs and LMP spikes. Research has shown that it could be beneficial to have 10% to 15% of the load available as DR resources. To understand the sensitivity of



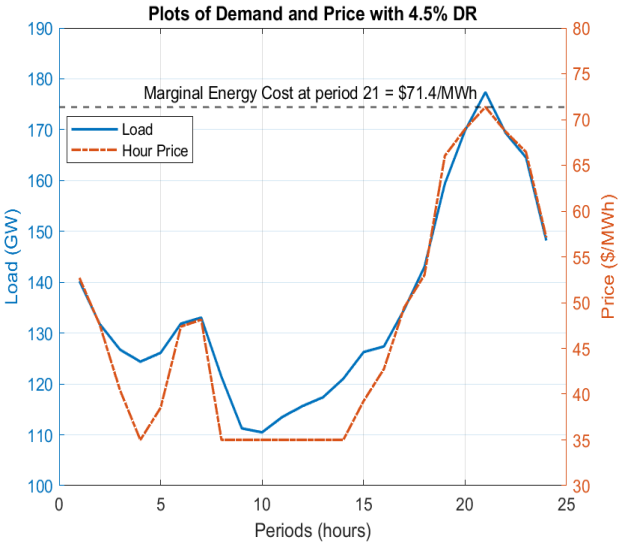
(a) 0% DR



(b) 1.5% DR

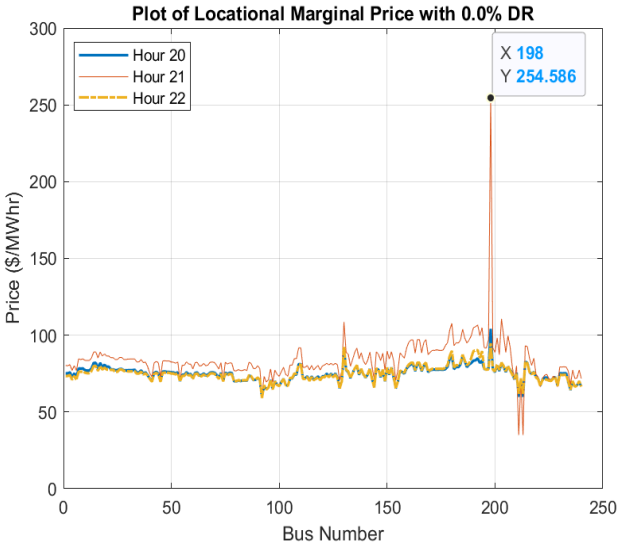


(c) 3% DR

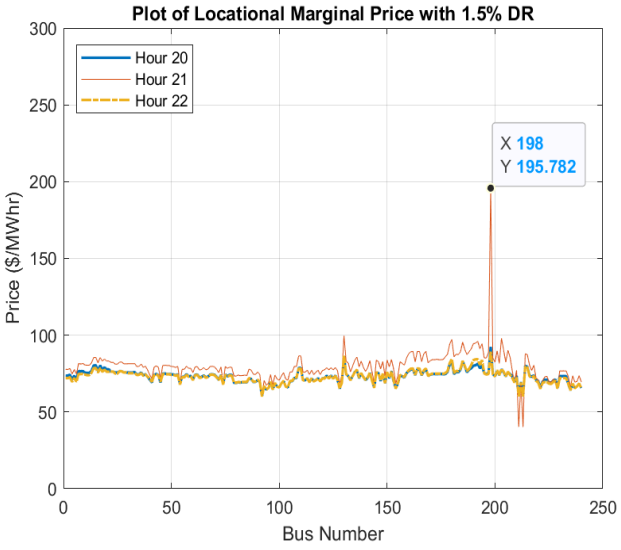


(d) 4.5% DR

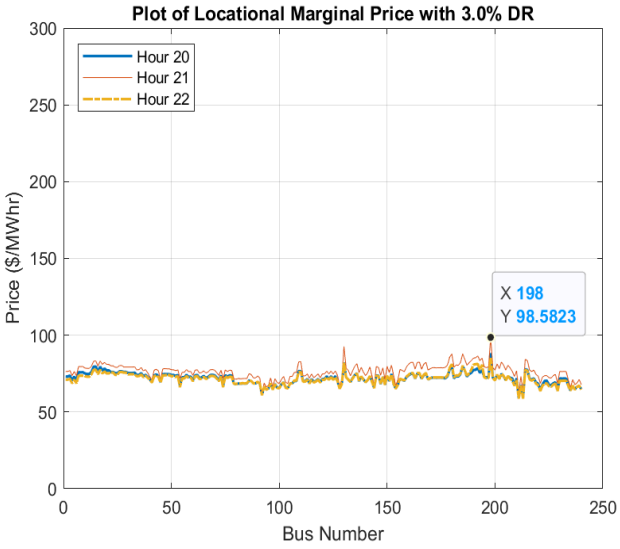
Figure 5.2: Modified demand and the effect on hourly marginal energy cost



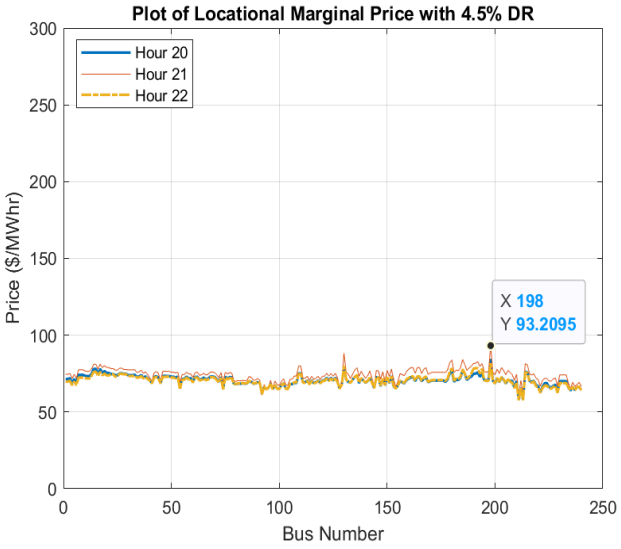
(a) 0% DR



(b) 1.5% DR



(c) 3% DR



(d) 4.5% DR

Figure 5.3: LMP spikes and available DR

the shift in load usage to periods of low demand, the load shift is done in steps of 0.5% of the daily peak load. To this effect, 10 simulations were performed to show a clear trend. Keeping the total overall daily load constant at $3,244,868$ MW, the highest daily peak of $185,728.9$ MW is observed at the base case (0.0% DR) while the lowest daily peak of $177,371.1$ MW is observed for the case with 4.5% DR. As expected, the increase in the percentage of DR resources (decrease in daily peak load) directly translates to a decrease in the number of units committed (Figure 5.4a) and decrease in the total generation cost (Figure 5.4b). The above-mentioned trends show that more expensive units do not get committed with increasing DR capacities. The total cost of generation and the marginal energy cost reduce linearly with the increase in the percentage of available DR. Figures 5.4d compares the available DR resources to the maximum LMP spike at hour 21. It can be observed that the price spike on bus 198 settles down to approximately \$100/MWh at 3% DR with minimal changes afterward.

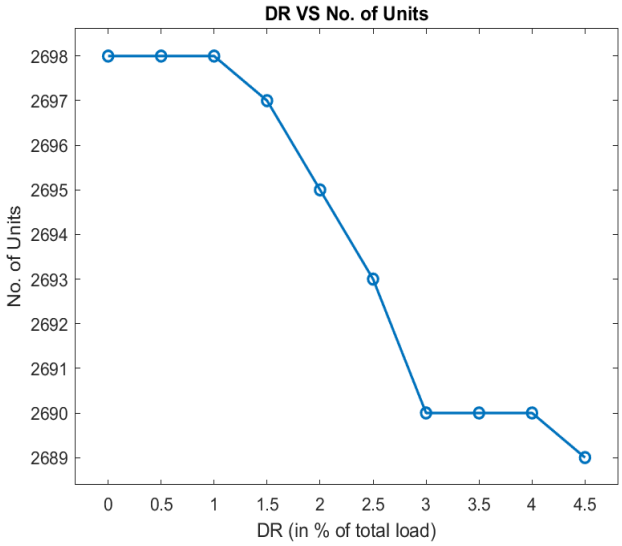
In conclusion, a 3% availability of DR is able to reduce the cost of generation considerably. Some major causes of the spike in bus prices are committing expensive units and system congestion during high system loading periods. Studies of this kind can help with future transmission planning and future unit locations.

5.3 Price Iteration Techniques using Augmented LR

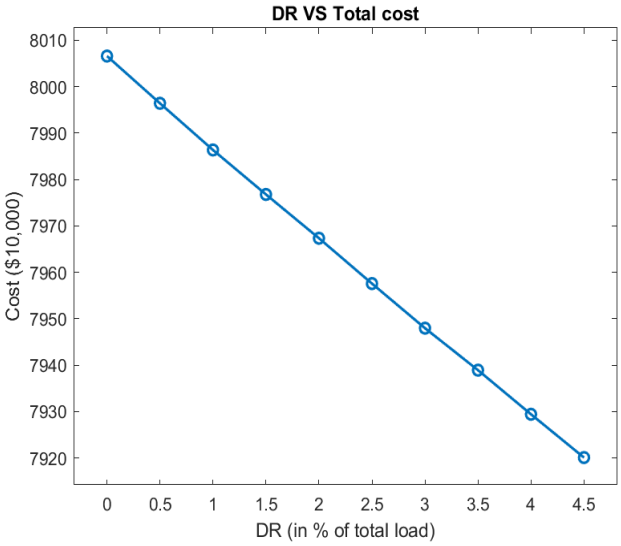
In Chapter 4, the optimization objectives were improved by iterating over λ (estimated price) and the actual price after solving the ED. Of course, the additional iteration over price (while solving the ED during each iteration) leads to an increase in computational resources as well as simulation run time. Hence, it is important to investigate methods of iteration over λ and price in ways that will have minimal impact on computational resources and simulation run time. Considering the challenges with LR convergence, Augmented LR (ALR) is considered.

5.3.1 Augmented LR and Coupling Constraints

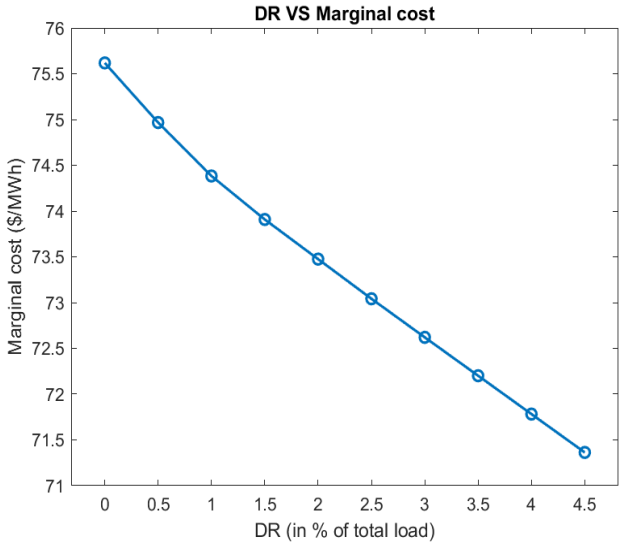
LR is well known for its ability to decompose optimization problems by relaxing the system constraints, using the Lagrangian multiplier (λ). The resulting subproblems are solved via an iterative process by continually updating λ. If the updating process of λ is not done right,



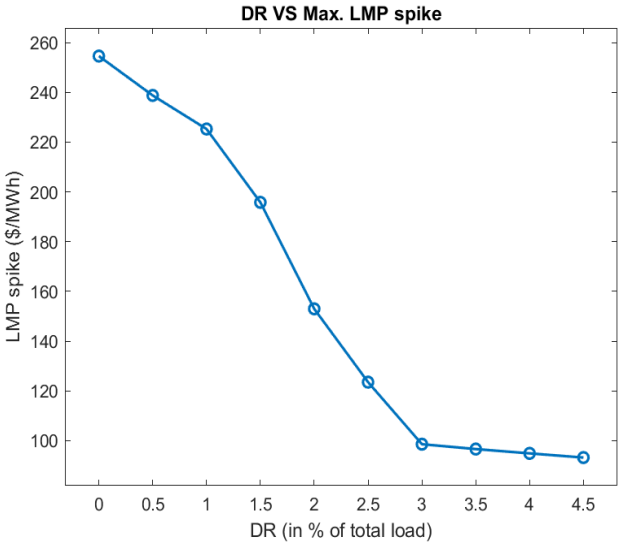
(a) Number of units w.r.t increasing % DR



(b) Total cost w.r.t increasing % DR



(c) Marginal cost w.r.t increasing % DR



(d) Max. LMP spike w.r.t increasing % DR

Figure 5.4: Effect of increasing % DR

the solution convergence could be slow and unsteady [96, 9, 92]. The Augmented LR (ALR) improves the solution convergence by adding a penalty term to the Lagrangian equation. The penalty term is derived from the energy balance coupling constraint. Expanding on equation 3.2, the ALR can be mathematically represented as

$$\mathcal{L}(P,U,\lambda) = \sum_{t=1}^{T}\sum_{i=1}^{NG}[F_i(P_{it})]U_{it} + \sum_{t=1}^{T}\lambda^t\left(P_{\text{load}}^t - \sum_{i=1}^{NG}P_iU_{it}\right) + \sum_{t=1}^{T}\frac{\gamma}{2}\left(P_{\text{load}}^t - \sum_{i=1}^{NG}P_iU_{it}\right)^2 \tag{5.5}$$

where

γ = the positive penalty coefficient of the system energy balance constraint.

Taking the partial derivatives of equation 5.5 with respect to P_i, we have the following expression

$$\frac{\partial\mathcal{L}(P,U,\lambda)}{\partial P_i} = b_i + 2c_iP_i - \lambda + \gamma\left(\sum_{i=1}^{NG}P_iU_i - P_{\text{load}}\right) \tag{5.6}$$

It can be easily seen from the penalty term that the units (subproblems) are no longer decoupled as observed in Section 3.2.2. P_i (power output for unit i) is given as

$$P_i = \frac{\lambda - b_i - \gamma\left(\sum_{\substack{j=1\\ j\neq i}}^{NG}P_jU_j - P_{\text{load}}\right)}{2c_i + \gamma} \tag{5.7}$$

It should be noted that summation in the term multiplying γ does not include P_i. λ is updated as follows

$$\lambda = \lambda + \gamma * \left(\sum_{i=1}^{NG}P_iU_i - P_{\text{load}}\right) \tag{5.8}$$

During the iteration process, the value of individual generator outputs (P_i) and λ are updated using the Alternating Direction Method of Multipliers (ADMM).

5.3.2 Test Results using WECC 240 Bus System

In this work, the ALR is implemented to investigate λ iteration techniques while focusing on the solution quality and convergence of optimization problems using three simulation cases. Case 1 (base case) with no additional iteration over λ or price is solved as a classical ALR problem. The algorithm updates λ and commits units appropriately until the required demand for the period is met and then solves the ED only once. Figure 5.5 shows the flow chart of the classical ALR. Case 2 (Heurisitic-1) has an added heuristic that prevents over-commitment of resources by attempting to commit the least possible number of units, turning off the most expensive (marginal) units until just enough generation capacity is online to meet the demand. As seen in Figure 5.6, once enough units have been committed (generation capacity is greater than or equal to demand), the heuristic continues to decrease the number of units by reducing the value of λ. This process is continued until a further decrease in λ would make the committed resources less than the demand. Like the base case, case 2 only solves the ED once. Case 3 (Heuristic-2) iterates over λ and price while monitoring the improvement in the hourly generation cost. Like the previous cases, case 3 also runs an inner loop that commits enough units to meet the demand. The outer loop implements the heuristic that iterates over λ and price as well as runs the ED multiple times as seen in Figure 5.7. Case 3 is expected to have the best solution quality but with some tradeoffs in the simulation run time since the ED is solved multiple times.

Both the solution and the simulation run times are compared for all 3 cases. This study uses the WECC load data from August 11, 2004. The load data is modified by scaling by a factor of 1.8, considering load growth over the years, and making the optimization problem somewhat interesting.

Figure 5.8 compares the number of units committed for all 3 cases (base case, Heuristic-1, and Heuristic-2). Case 2 attempts to avoid over-commitment at all costs, committing the fewest number of units during most of the periods. Case 3 on the other hand committed the most number of units, especially during periods of high system loading. It should be noted that committing the same number of units does not directly imply committing the same units with similar dispatch. This is because some units might have binding upward

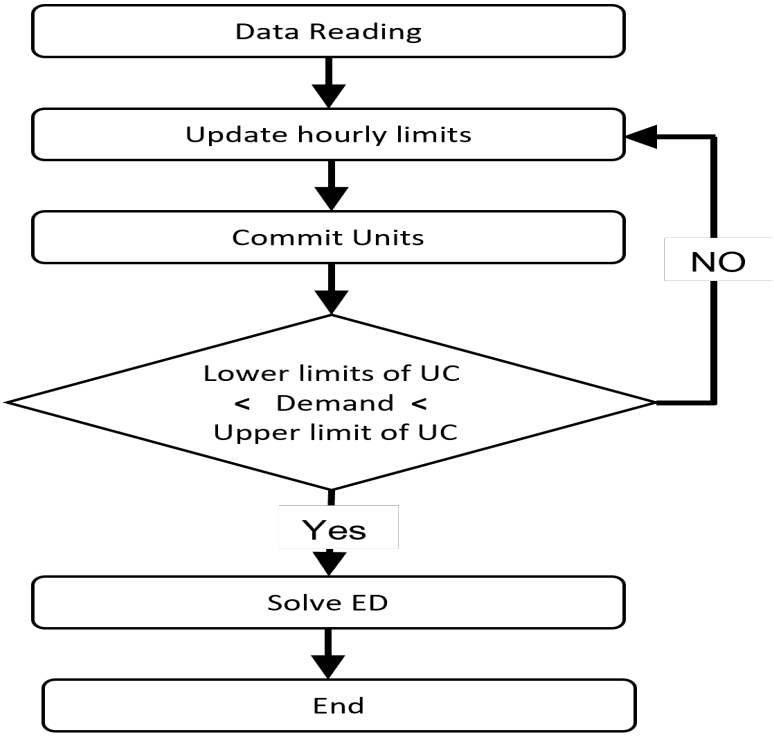


Figure 5.5: Base case flowchart

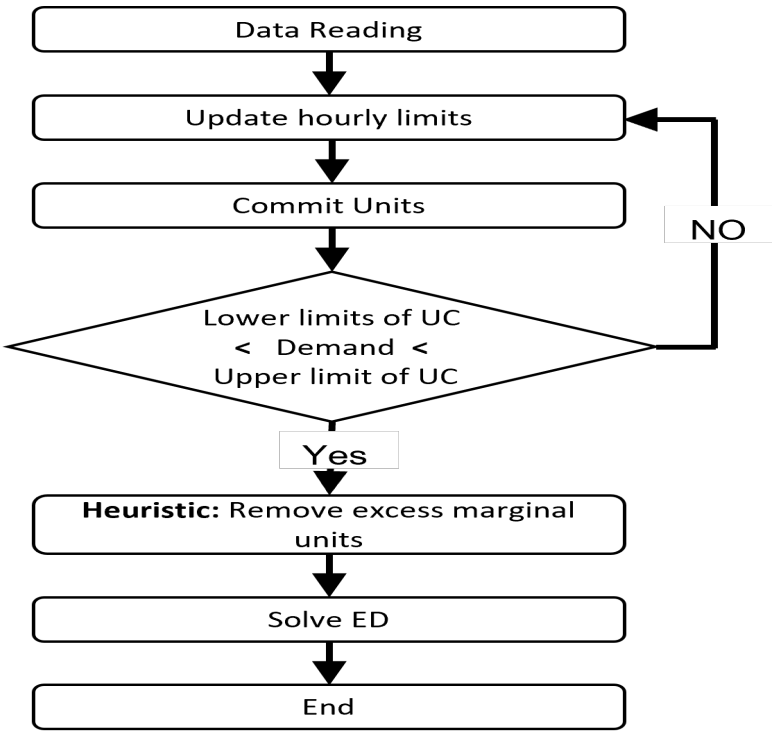


Figure 5.6: Heuristic for committing least number of units

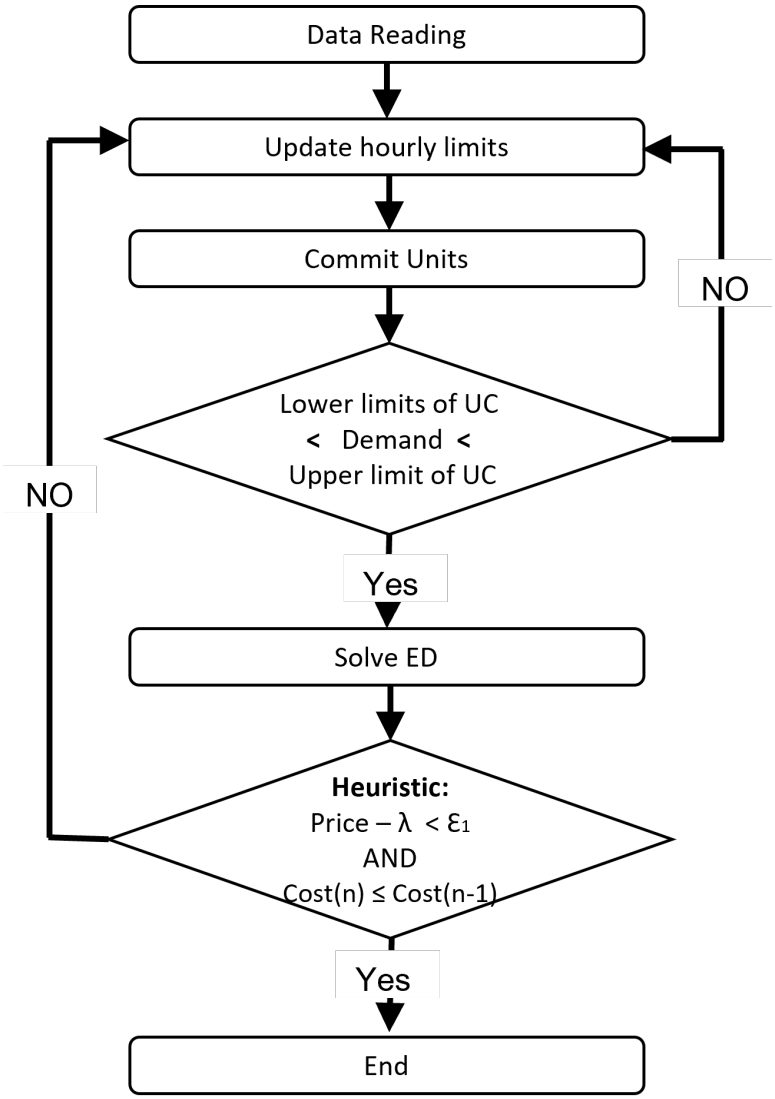


Figure 5.7: Heuristic for committing optimum number of units by iterating over λ

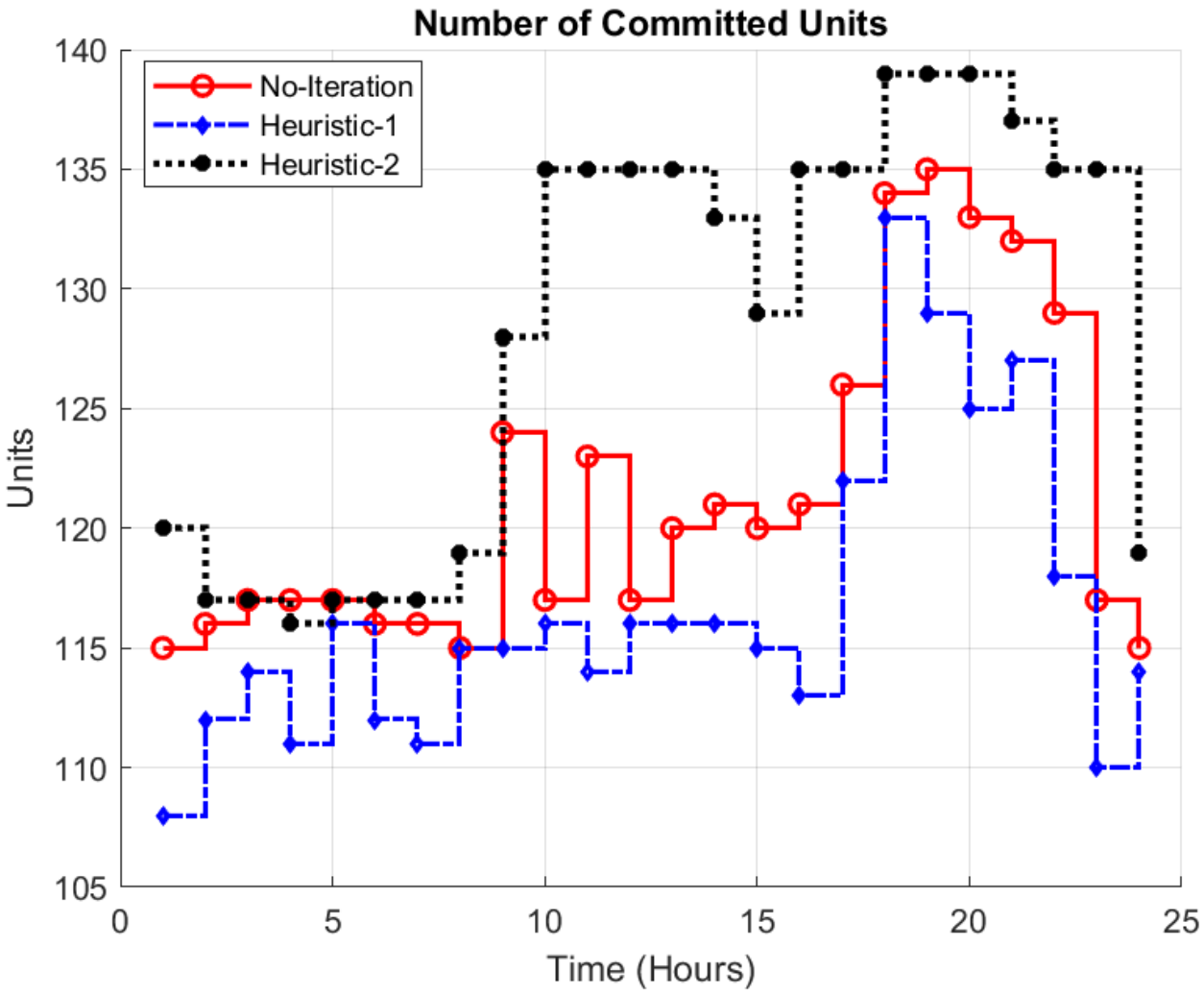


Figure 5.8: Number of units committed for case 1, case 2, and case 3

or downward ramping limits depending on their previous outputs. Figure 5.9 highlights the effect of both heuristics on the hourly marginal energy prices. The hourly marginal energy prices for case 3 are the lowest mostly during periods of high loading. During periods of low or light system loading, the marginal energy prices in cases 1 and 3 are similar for the most part. Figure 5.10 compares the hourly generation cost for all 3 cases, using case 1 as a reference. It can be easily seen that case 2 with the least number of committed units performed the worst, ending up with the highest hourly marginal energy prices and hourly generation costs. This shows that barely committing enough resources forces the algorithm to schedule many units to run at or close to their maximum capacities. Even though there is no occurrence of over-commitment in case 2, the classical ALR (case 1) can perform better than case 2. As expected, case 3 outperformed in solution quality. The algorithm tends to commit the optimum number of units during most periods, thereby scheduling most generators to run at their optimum levels and not at their minimum or maximum capacities. Committing the most number of units does not necessarily translate to the best solution as this could lead to a case of over-commitment. This is consistent with energy pricing and bidding as shown in Figure 3.1. This is also consistent with the fact that energy generation cost is usually cheaper when a unit runs at the optimum point and not at minimum or maximum capacity. In general, the classical ALR accepts the first instance of the UC result without considering other unit combinations while Heuristic-2 (case 3) goes an extra step to find other combinations.

Considering the simulation time, case 1 outperformed as expected while case 3 had the worst performance. Even though case 2 has a better simulation time than case 3, it has the worst solution overall. Table 5.1 shows a general summary of the results, highlighting the total number of units committed, the sum of the maximum marginal energy prices, the average simulation run time as well as the total generation cost for all 24-hour periods. The performance for each category is rated as red, black, and blue, with red indicating the worst and blue referring to the best performance.

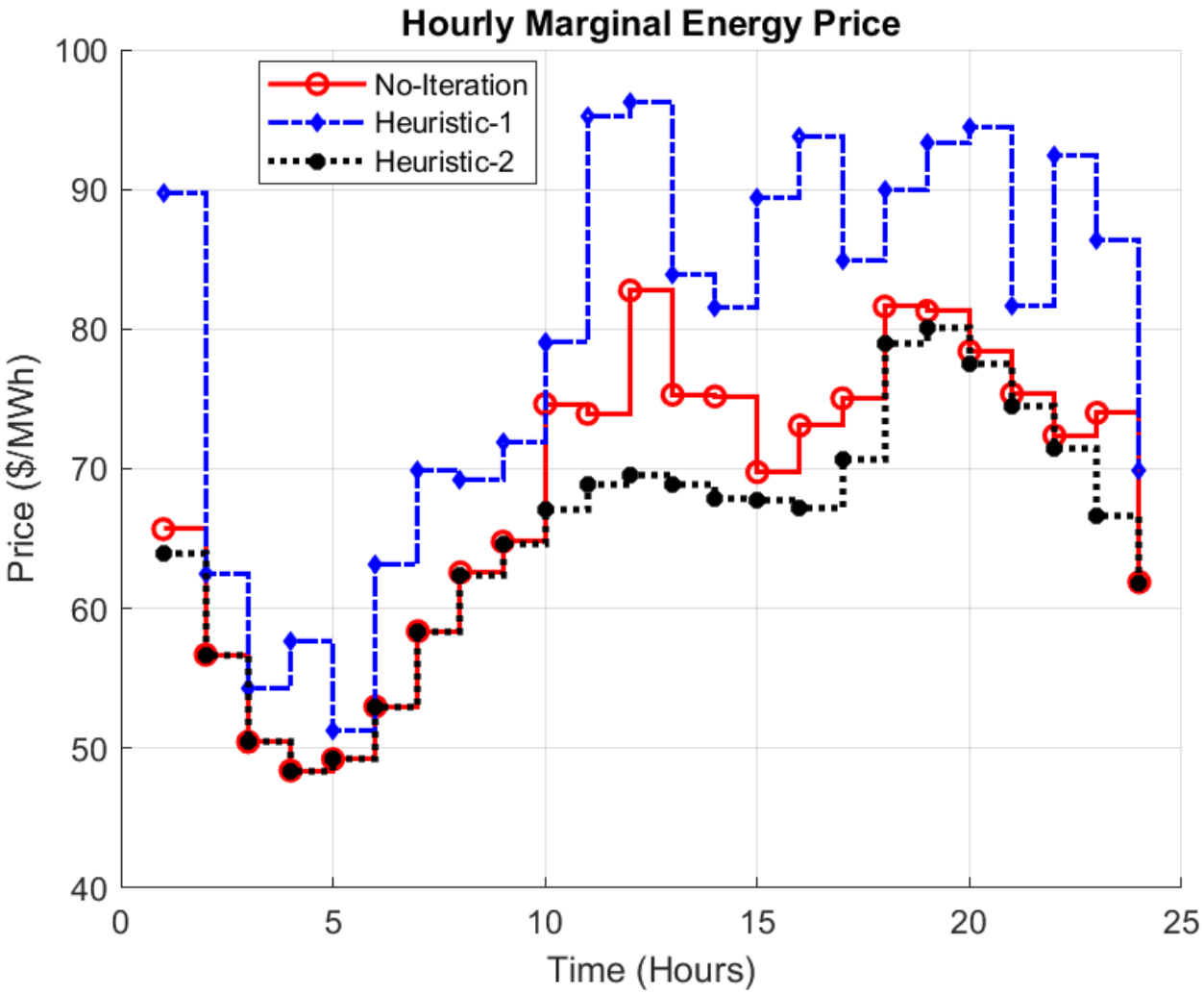


Figure 5.9: Hourly marginal energy price for case 1, case 2, and case 3

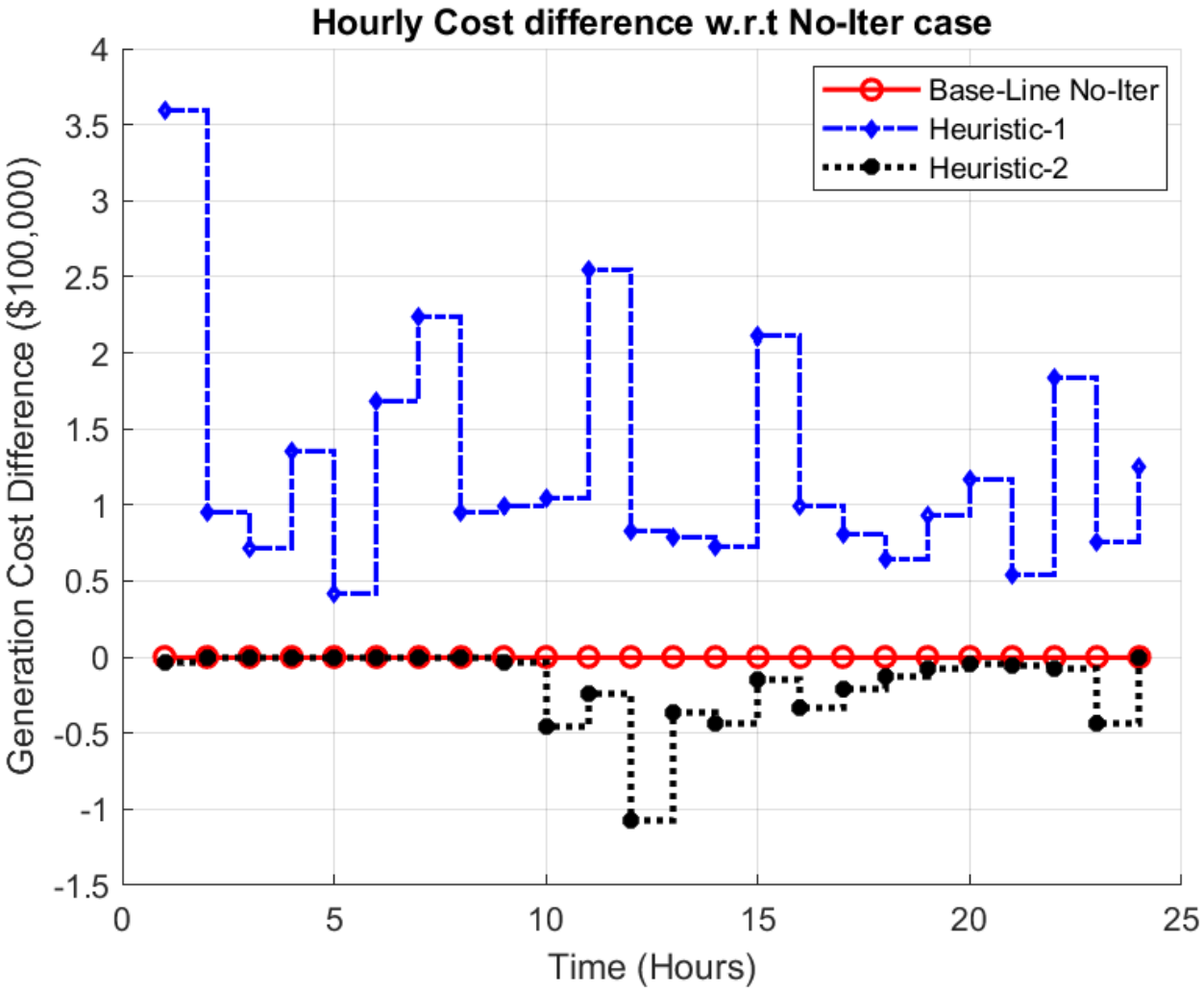


Figure 5.10: Plot of the hourly cost of generation for case 1, case 2, and case 3

Table 5.1: Summary of results

	Case 1	**Case 2**	**Case 3**
Total Load (GW)	3,931.1	3,931.1	3,931.1
Number of units	2,913	2,798	3,083
Max. Marginal Price ($)	82.8	96.3	80
Average Run Time (sec.)	0.41	0.59	1.31
Total Gen. Cost ($)	108,212,168	111,198,902	107,796,718

5.3.3 Discussion

Three cases, including a base case (classical ALR), a second case with a heuristic (Heuristic-1) to minimize the number of units, and a third case with a heuristic (Heuristic-2) to optimize the overall result by iterating over λ and price were compared. Heuristic-1 and Heuristic-2 were implemented to improve the solution quality in case 1 without considerably impacting the simulation run time. Heuristic-1 (case 2) attempts to prevent the over-commitment of units which is a well-known problem that is associated with LR and goes as far as committing the fewest possible units. The heuristic compares the committed resources to the hourly demand and turns off the most expensive unit(s) during every iteration process. This process is continued until it is no longer possible to turn off any unit and still have the committed resources equal to or greater than the demand. The advantage of Heuristic-1 is that it can prevent over-commitment with much less impact on the simulation run time since it only solves the ED once. However, since the ED is never solved during the iteration process, there is no way to know what the effect of the reduction in commitment is during each iteration. Hence, even though the impact on the solution run time is minimal, case 2 underperforms in solution quality as seen in Table 5.1. Heuristic-2 (case 3) on the other hand can compare the estimated price (λ) with the actual price from the ED, using the improvement in the solution (cost) during each iteration as a good stopping criterion. This produces an improved solution quality but with slightly more impact on the simulation run time when compared to Heuristic-1. A good balance between the solution quality and simulation run time can be implemented by adjusting the maximum number of times the ED can be solved in Heuristic-2. A fewer number of iterations over λ and price would normally imply a solution with slightly poorer quality and vice versa.

5.4 Effect of Transmission Limit on Optimization

As mentioned in section 5.3, solving optimization problems with a high volume of transmission constraints could be very challenging [15]. For example, since the MISO system requires monitoring a large number of transmission constraints, the complete network model is not used in solving the SCUC problem. One approach is to pre-identify and create a list of

transmission constraints using historical data and previous studies. This list of transmission constraints is partitioned into groups of 200 and is added to the SCUC problem in batches. The iteration process is continued until no new violations exist in the SCUC solution. This approach reduces the size of the SCUC problem by solving only 200 transmission constraints per time, instead of solving all identified constraints or the full network model [16].

5.4.1 Incremental Optimization

Studies have found that solving optimization problems incrementally can help speed up market clearing time and reduce the time spent on schedule solution verification [15]. The incremental problem solving in UC and ED is of great interest as the system increases in size and the volume of virtual trading and resources such as DR increases in the optimization problem. Researchers have implemented incremental optimization techniques as heuristics in MIP for alleviating transmission bottlenecks. The main concept is adding the transmission constraint to the problem incrementally and systematically checking for solution feasibility. Another approach combines the LR method with MIP by solving for and identifying the transmission constraint via LR. Significant progress was made when these incremental concepts were implemented on some unusually difficult optimization problems.

By default, LR is an incremental optimization technique because it commits units by iterating over price and schedules units starting from cheaper to more expensive ones. This study aims at taking advantage of the intuitive and incremental nature of the LR optimization technique. Both characteristics make tracking the progress of the solution possible while iterating over price and can help reduce the solution dispute and verification time. In addition, uncommitted units with costs lower than the MIP gap are easily identified since LR commits units by evaluating the cost in an incremental way.

5.4.2 Effect of Line Flow Penalty on Transmission Limit

In this section, a line penalty approach is proposed to alleviate transmission constraints and reduce excessive iterations that are associated with SCUC problems. The network model here is represented by the LR formulation with heuristic from Section 3.3. The heuristic

from Section 3.3 generally penalizes the branches and attempts to reduce the system line losses. The proposed approach targets transmission lines with binding line flow limits by scaling up the value of the reactance of the transmission line of interest. The idea is to discourage and reduce power injection at buses (which directly reduces the power outputs of generators) that directly contribute to flow increase on the specific line.

A modified WECC 240 bus system model is used to explore the effect of line penalty on transmission line flow limits. Transmission lines 125 and 325 have flow limits of 2,000MW and 2,500MW respectively. The base case from Figure 5.11 shows that the power flow in line-125 violates the line flow limit for all 24-hour periods while line 325 only violates the flow limit from periods 18 through 22. The UC for the base case was solved without the network data and the line flow limit violations were checked after solving the ED. For the proposed case, a penalty is added to lines with binding transmission limits by scaling up the values of the reactance at the identified branches. Using the modified LR formulation from equations 3.17 to 3.27, the new heuristic with penalty can be mathematically represented as

$$\mathcal{L}(P,U,\lambda) = \sum_{t=1}^{T}\sum_{i=1}^{NG}(a_i + b_i P_i + c_i P_i^2)U_{it} + \sum_{t=1}^{T}\lambda^t(P^t_{\text{load}} + \sum_{k=1}^{NK}(L^t_{\text{flow}}(P_i))^2 R_k Pn_k - \sum_{i=1}^{NG} P_i U_{it}) \tag{5.9}$$

where Pn_k is the penalty factor for line k. The term $(L^t_{\text{flow}}(P_i))^2 R_k Pn_k$ is proportional to the square of the GSF multiplied by the resistance (R_k) and the penalty (Pn_k) and can be expressed as

$$\sum_{k=1}^{NK}(L^t_{\text{flow}}(P_i))^2 R_k Pn_k \quad \propto \quad \sum_{i=1}^{NG} GSF_{k-i}(P_i - D_i) \cdot R_k \cdot Pn_k \cdot \sum_{i=1}^{NG} GSF_{k-i}(P_i - D_i) \tag{5.10}$$

The loss term with penalty factor from equation 5.10 can be generalized as

$$\sum_{k=1}^{NK}(L^t_{\text{flow}}(P_i))^2 R_k Pn_k \quad \propto \quad \boldsymbol{P^T_{inj}} \cdot \boldsymbol{W_p} \cdot \boldsymbol{P_{inj}} \tag{5.11}$$

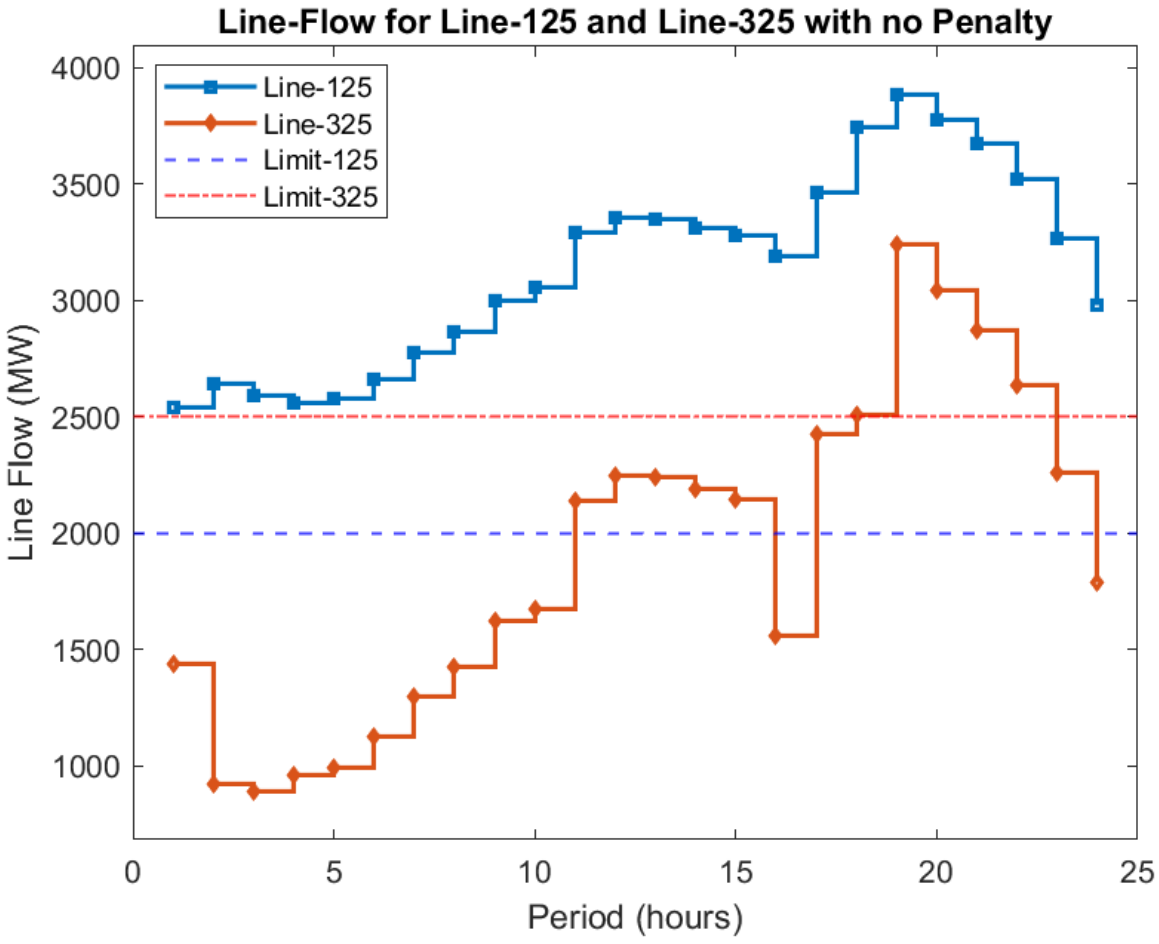


Figure 5.11: Base case with no line penalty

where $\boldsymbol{W_p}$ is the new weighting factor and it is a matrix that is derived by multiplying a diagonal matrix of the resistance $\boldsymbol{R}$ and a diagonal matrix of the penalty $\boldsymbol{Pn}$ on both sides by the $\boldsymbol{GSF}$ as shown below

$$\boldsymbol{W_p} = \boldsymbol{GSF^T} \cdot (\boldsymbol{R} \cdot \boldsymbol{Pn}) \cdot \boldsymbol{GSF} \tag{5.12}$$

The new Lagrangian function is then approximated as

$$\mathcal{L}(P, U, \lambda) = \sum_{t=1}^{T} \sum_{i=1}^{NG} (a_i + b_i P_i + c_i P_i^2) U_{it} + \sum_{t=1}^{T} \lambda^t (P_{\text{load}}^t + \boldsymbol{P_{inj}^T} \cdot \boldsymbol{W_p} \cdot \boldsymbol{P_{inj}} - \sum_{i=1}^{NG} P_i U_{it}) \tag{5.13}$$

For simplicity, both transmission lines are scaled equally and the effect of scaling by a factor of 10 is seen in Figure 5.12. Comparing both cases, it can be easily seen that the penalty was able to reduce the power flow in the required transmission lines by committing units that reduce the flow of power on the identified lines. In Figure 5.13, the optimization problem is solved for multiple iterations while increasing the scaling factor (penalty) for each iteration from 0 to 40. At period 19 where the peak load is observed, the maximum line flows for lines 125 and 325 are recorded and plotted against the penalty values. Point 0 (scaling factor = 0) represents the maximum line flow for the base case (during the first iteration) as observed in Figure 5.11. The inverse relationship between the penalty and the maximum line flow for both lines is easily seen. At a scaling factor of 6, the maximum line flows are either equal to or below their required line flow limits.

A second metric worthy of considering in measuring the performance of the proposed penalty method is its effect on solution quality. It is expected that every additional constraint that is added to an optimization problem would have some form of negative impact on the solution quality. Hence, it is important to find an optimum penalty value with the least impact on the solution quality. Figure 5.14 Shows that the additional constraint cost is about $\$48,000$ with no considerable change in cost as the penalty increases. One advantage of this penalty approach is that the impact on cost settles down quickly and stays flat for a wide range of scaling factors. In essence, no further calculation is needed to find a unique or optimum scaling factor. Therefore reducing both the computational resources and simulation

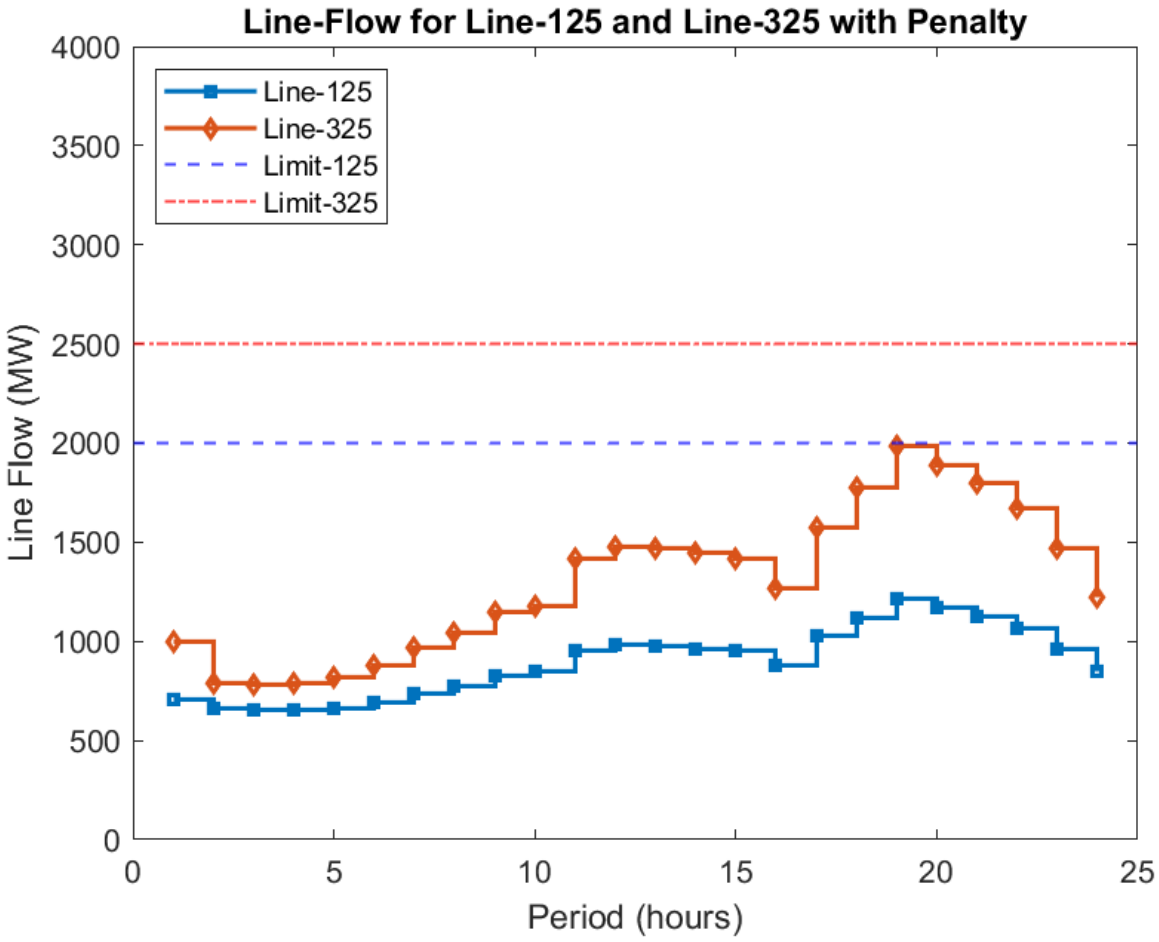


Figure 5.12: Heuristic case with targeted line penalties

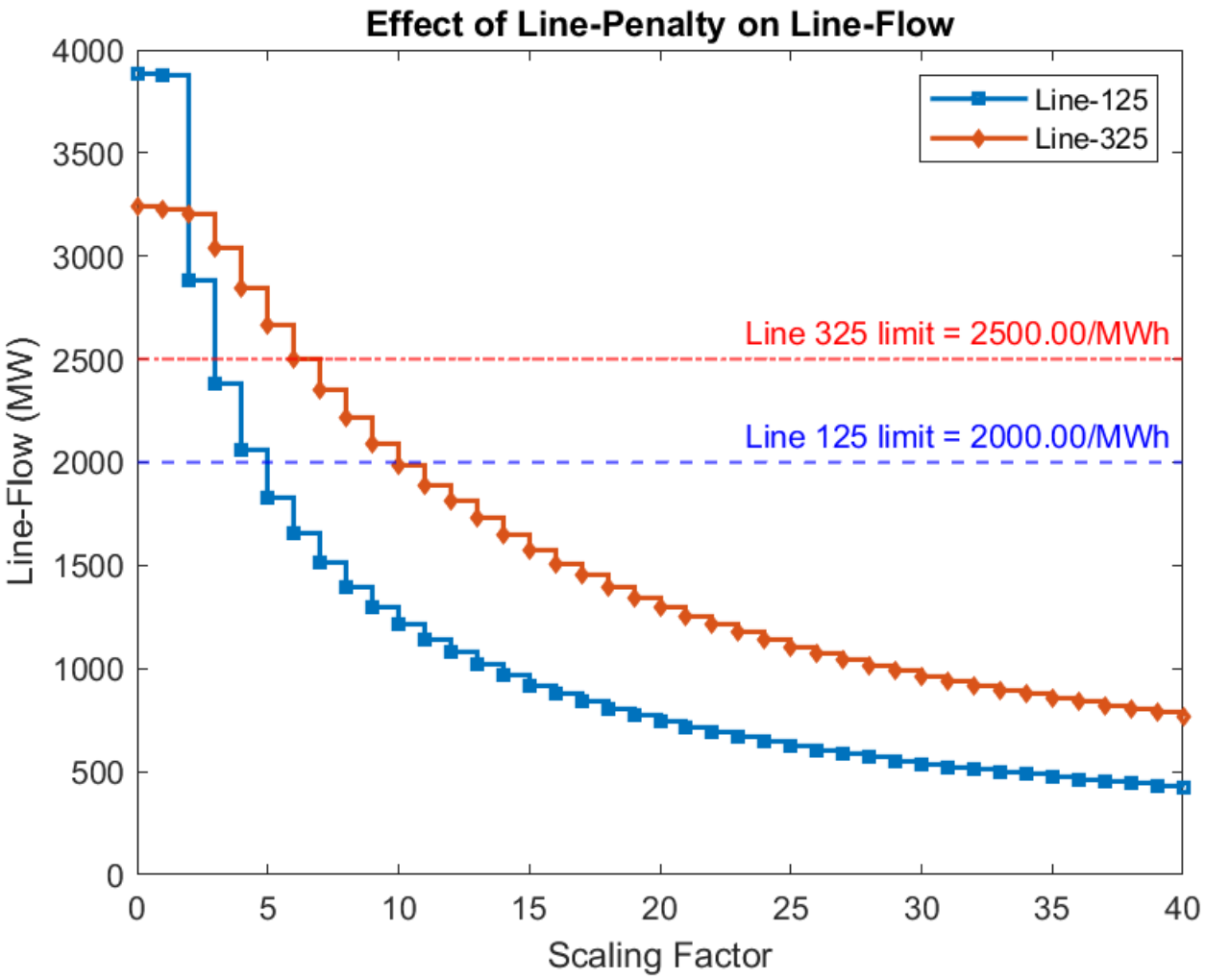


Figure 5.13: Line flow as a function of penalty

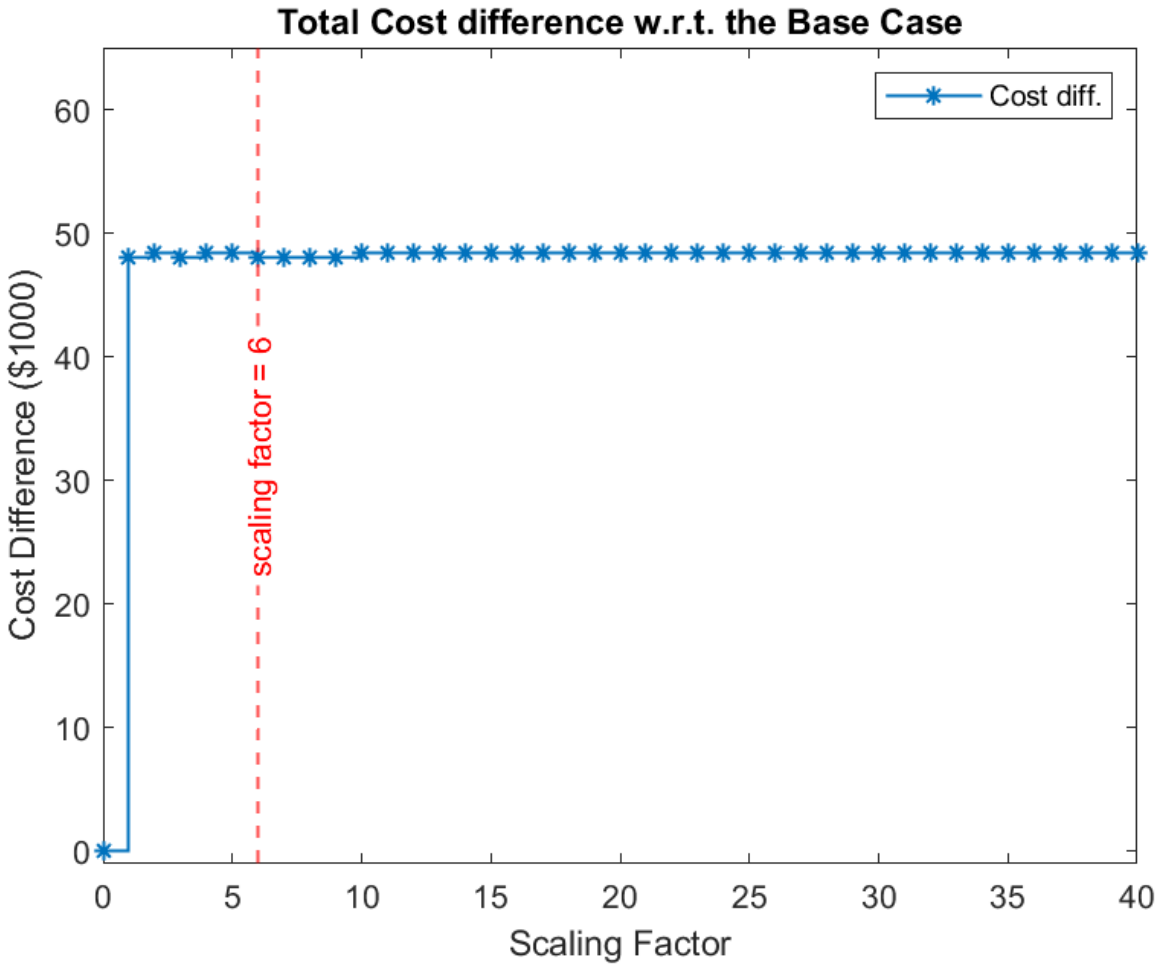


Figure 5.14: Total costs differences Using the base case as reference

run time required for solving SCUC problems with transmission constraints. As shown in Figures 5.13 and 5.14, choosing any scaling factor from 6 and above would eliminate all violations with no noticeable impact on the solution quality.

5.4.3 Discussion

The above investigation illustrates that the proposed heuristic can considerably reduce simulation run time by partly or fully eliminating repetitive solving of the SCUC problem. Instead of adding a list of predefined transmission constraints to the optimization problem in batches and solving repetitively, all the transmission lines with binding constraint limits can be penalized during a single round of simulation.

Another advantage of the proposed formulation is that the cost impact of the transmission line constraints settles down quickly and stays relatively the same for a wide range of scaling factors. This implies that there is no need for an added computational burden to get an optimum penalty or scaling factor value. Figure 5.14 shows that the generation cost stays considerably constant with increasing scaling factor.

As observed in Figures 5.11, 5.12, and 5.13, the power flow in lines 125 and 325 decreases as the penalty scaling factor increases. The heuristic takes advantage of the relationship between bus injection and line flow sensitivity by increasing the costs of injecting power through the buses to the transmission lines of interest. This increase in cost directly targets contributing generators, forcing them to either reduce their output or prevent them from being committed altogether.

The lines with transmission constraints could be pre-identified from historical data and previous studies or by pre-solving the SCUC problem. Figure 5.15 shows a proposed flowchart of a pre-solved SCUC algorithm. The solution of the pre-solved UC and ED is checked for transmission flow violations and all the branches with binding line flow limits are identified and penalized appropriately. The modified PTDF is then updated with the penalty value(s) and the optimization problem is resolved. The kind of modification applied to the PTDF and selected scaling factor are expected to be system dependent. Some systems might also require different values of scaling factors for different transmission lines with binding constraints.

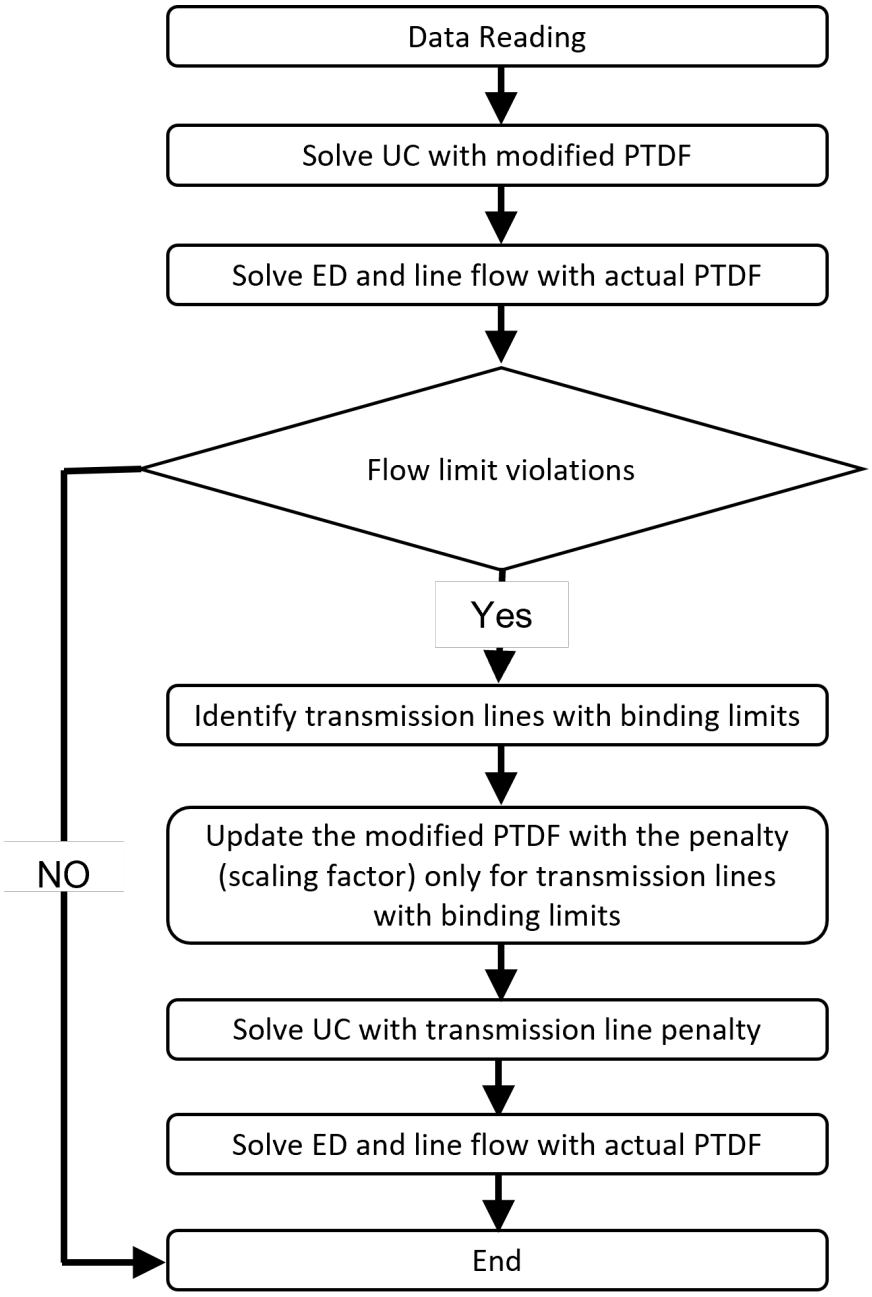


Figure 5.15: Flowchart for transmission penalty algorithm

In conclusion, the proposed LR with heuristic can act as a fast alternative tool for solving SCUC especially when the optimization problem has a high volume of transmission constraints and virtual transactions. It is important to note that the incremental nature of LR by default can help improve SCUC solutions with a high volume of virtual transactions since units are selected by iterating over λ, starting with cheaper units.

5.5 Large System Integration of Similar and Identical DER Units

The push for net-zero carbon emissions and expanding electrification will require some notable changes on the power grid [39]. While electricity demand continues to increase and a large capacity of high carbon emitting generators like coal are being decommissioned, other generation resources would be needed to fill this gap. Some of these required replacement generation capacities could come from DER which are usually small and non-traditional units. The integration of a large volume of DER on the power grid offers advantages such as resource diversification and grid flexibility, but not without some challenges. One of such challenges is the impact on solving SCUC as it relates to the increase in the number of binary variables [8, 49]. An added difficulty could arise from the fact that a notable number of similar and identical units could start showing up at different bus locations. For example, small modular reactors (SMR) from the same manufacturer could be owned by different utility companies.

5.5.1 Effect of a Large Volume of Similar and Identical Units on Simulation Run Time

In this section, the impact of a large volume of DER with similar or identical characteristics is investigated using a modified WECC 240 bus system model. Three system models with the number of units randomly scaled up to approximately 2X, 5X, and 10X respectively are considered. Starting with 143 units, the number of units is approximately doubled by adding 100 (DER) units for case 1. These units are made up of 10 different types of units

with identical capacities, ramp rates, and cost functions. The costs of the 10 types of units are also slightly different, making each unit type similar in cost to the next expensive unit type. The number of DER in case 2 and case 3 increased by a total of 500 and 1000 units respectively. To keep the system network constraints fairly constant, the new units are only added to the existing generation buses (generation centers). The UC was solved via the heuristic formulation from Section 3.3. Each of the 3 models is simulated 50 times to get a good average of the simulation time. The simulations were performed using a 2-Core 2.20GHz Intel(R) Core(TM) i5-5200U processor and 16 GB RAM. Figure 5.16 shows that the simulation run time for the proposed formulation is linear with increases in the number of DER. It is worth noting that this setup is only able to compare the simulation run time since the total generation mix (types and costs) changes a lot for each case.

5.5.2 Discussion

This investigation focuses on the impact of distributing small non-traditional similar and identical units on simulation run time. The setup is such that similar units are co-located and are also distributed across the system, while identical units only exist on different buses. A strong point of the formulation is that it can differentiate between both similar and identical units especially when they are marginal (near marginal) units. This formulation is unable to differentiate between identical units if they are co-located. It is worth noting that as the system gets larger if the number of iteration processes over the ED is not capped, the simulation time would increase considerably. Overall, the heuristic formulation scales well with the increasing number of distributed units.

5.6 Conclusions

In this chapter, several computational efficiency techniques were considered, using LR. Some challenges that are associated with SCUC and SCED as it relates to scalability were investigated.

The WECC 240 bus system data is first formatted for solving the UC and ED problems while highlighting the data modifications and challenges. For simplicity and consistency, the

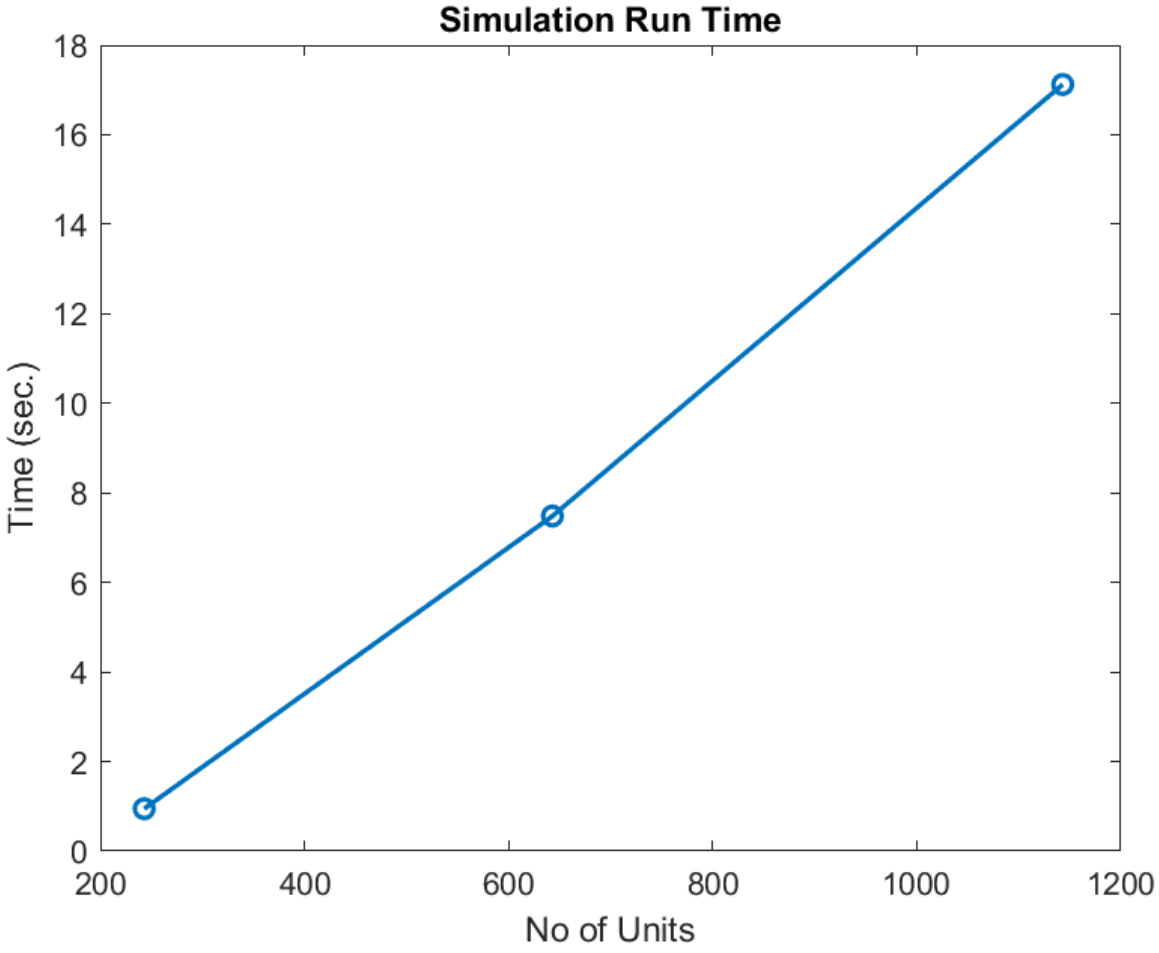


Figure 5.16: Simulation run time for increasing volume of DER

piecewise cost function data is converted to a quadratic cost function type. Next, the system flexibility requirement for load patterns with a high daily ramping requirement and a high daily peak were investigated. It was shown that if 3% of the daily peak load is available for DR, large spikes in LMP can be eliminated. DR is most effective if the shift in energy usage time can shave off the daily peak which can prevent expensive units from being committed. This work can help determine a good market price for DR since the reduction in energy cost can be calculated.

Methods of UC and ED solution improvements are studied using three algorithms. The classic ALR scales well and can provide a fairly good solution. A second algorithm (Heuristic-1) attempts to avoid over-commitment by committing the least possible number of units. The heuristic iterates over λ and solves the ED only once, thereby, only minimally impacting the simulation run time. A third algorithm (Heuristic-2), solves for the optimum number of units by iterating over λ and the price obtained from solving the ED. The solution improvement is tracked by comparing the total generation cost of the previous iteration (k-1) to the current iteration (k). Heuristic-2 is preferred to Heuristic-1 because it comes out with the best objective even though it has an impact on simulation run time.

Considering the effect of a high volume of transmission constraints and virtual transactions on UC solution and simulation run time, a transmission line penalty is proposed. This approach targets units that contribute significantly to the power flow on the transmission lines of interest and either reduce the output of the generators or prevent such generators from being committed. This algorithm can be used as a fast alternative for MIP since it can greatly reduce the number of iterations for solving SCUC and SCED. A notable advantage of this algorithm is that it is somewhat easy to choose a penalty value.

Finally, a scalability optimization study is performed for systems with similar and identical DER. The system volume of the DER is roughly increased by factors of 2, 5, and 10. The simulation run time scales linearly with the increase in the volume of DER in the system.

In general, the proposed LR formulations present alternative new and fast ways of solving optimization problems. These formulations can be combined with other techniques (MIP) to form hybrid optimization tools in the future.

Chapter 6

Conclusion and Future Work

6.1 Conclusion

The recent and continuous advancement in grid technologies is creating new challenges and difficulties for the existing methods of solving UC and ED. Power system operators are now faced with a future where a large volume of small MW units will dominate the grid. The possible increase in the volume of similar and identical units on different bus locations is also a real possibility. MIP technique is a state-of-the-art optimization tool but does not scale well with increasing binary variables. LR technique on the other hand scales well with increasing binary variables but performs poorly when similar and identical units are present in the generation mix. This work proposes LR algorithms and formulations that can improve the solution quality of SCUC and SCED with acceptable trade-offs in the simulation run time.

In Chapter 3, a modified UC formulation with system network losses is first derived using a heuristic. The heuristic uses the network PTDF and incorporates the loss effect using the line resistances as scaling factors. The immediate challenge is the values of the resistance are too small for penalizing the transmission lines appropriately. Hence, the need to include a weighting factor, which is system dependent. The calculated loss penalties are distributed appropriately using the network sensitivity. The proposed loss formulation is able to reduce the cost of generation and differentiate between similar and identical units that are not co-located.

To confirm the validity of the proposed formulation in Chapter 3, several benchmarks were performed using MIP in Chapter 4. Compared to MIP, the proposed LR formulation does not just distinguish between similar units but prioritizes units that are closer to the load center as well. For a small system with similar and identical units, the solution quality is in an acceptable range. The scalability test using a much larger RTS-GMLC 73 bus system shows that the proposed method scales linearly well with minimal trade-offs in solution quality. The proposed formulation can work as a good alternative for solving SCUC problems depending on the situation.

In Chapter 5, the computational efficiency of LR is investigated, considering the impact of integrating DER and concepts like DR and virtual transactions. First, the system flexibility requirement based on the available DR capacity and customers' response in time of need is considered. The study shows the sensitivity of marginal energy cost and LMP to actual committed DR as a percentage of the daily peak load. Simulation results on the WECC 240 bus system show that DR can improve the system flexibility especially when customers respond in such a way that shaves the peak load. Second, price iteration techniques for improving solution quality are considered. The best-performing algorithm iterates over λ and price (from ED) using the improvements in the total generation cost as a guide. The solution quality is improved with minimal impact on simulation run time. Third, the impact of transmission line limits on simulation run time is investigated. Taking advantage of the incremental nature of LR, a line flow penalty is proposed. The penalty targets the transmission lines of interest and distributes the added cost on generators that contribute to the line flow. Simulation results show a reduction in power flow on the transmission line of interest with a great potential for reductions in simulation run time. The cost of transmission limit constraint quickly settles down and stays relatively constant for a wide range of penalty values. This makes selecting a penalty value an easy task. Fourth, the integration of a large volume of similar and identical DER is considered. The number of units in the system is roughly scaled by factors of 2,5, and 10 using DER with similar and identical cost functions. The proposed formulation scales linearly well with the increasing number of distributed non-traditional similar and identical units.

6.2 Future Work

Considering the work to date, further research is needed for a real-world implementation of the proposed formulations and algorithms.

- **On unit commitment formulations**

    1. The proposed methods in this work are focused on a centralized algorithm. It would be of interest to investigate the benefit of the proposed methods on distributed UC algorithms. An area of interest would be the effect of the proposed line penalty on the way information can be exchanged between subproblems.
    2. While ALR is applied to some extent in this work, it was not integrated into the proposed formulation. This would be a good future area of research since the ALR can improve the convergence problems associated with LR in general.

- **On large scale integration of DER**

    1. The study involving large-scale integration of DER is only focused on scalability and simulation run time. It would be interesting to use Egret as a benchmark for solution quality and scalability. The challenge here is to model a corresponding large system in Egret.

- **On virtual transaction**

    1. This work assumed that the incremental nature of LR will automatically take care of the difficulty imposed by virtual transactions since it selects units starting with the cheaper ones. An investigation focusing on the impact of a high volume of virtual transactions combined with a high volume of transmission constraints on solution quality and simulation run time would be of interest.

Bibliography

[1] A. Rahman, H., Majid, M. S., Rezaee Jordehi, A., Chin Kim, G., Hassan, M. Y., and O. Fadhl, S. (2015). Operation and control strategies of integrated distributed energy resources: A review. *Renewable and Sustainable Energy Reviews*, 51:1412–1420. 2

[2] Albadi, M. and El-Saadany, E. (2008). A summary of demand response in electricity markets. *Electric Power Systems Research*, 78(11):1989–1996. 4

[3] Araj, J., Head, K., Hou, D., Hundiwale, A., Johnstone, T., Lehman, S., Liang, Z., Liu, H., Motley, A., Royal, M., Rudolph, J., Steckel, T., Stewart, J., Stewart, M., Webb, R., Wikler, K., Zhao, K., and Alderete, G. B. A. (2022). Summer Market Performance Report for September 2022. Technical report, California Independent System Operator (CAISO). xv, 101, 149, 150

[4] Asadinejad, A. (2017). Electricity Market Designs for Demand Response from Residential Customers. *PhD diss., University of Tennessee, 2017.*, page 194. 102

[5] Badakhshan, S., Kazemi, M., and Ehsan, M. (2015). Security constrained unit commitment with flexibility in natural gas transmission delivery. *Journal of Natural Gas Science and Engineering*, 27:632–640. 28

[6] Baldick, R. (1995). The generalized unit commitment problem. *IEEE Transactions on Power Systems*, 10(1):465–475. 15, 17

[7] Barrows, C., Preston, E., Staid, A., Stephen, G., Watson, J.-P., Bloom, A., Ehlen, A., Ikaheimo, J., Jorgenson, J., Krishnamurthy, D., Lau, J., McBennett, B., and O'Connell,

M. (2020). The IEEE Reliability Test System: A Proposed 2019 Update. *IEEE Transactions on Power Systems*, 35(1):119–127. 75

[8] Basaran Filik, U. and Kurban, M. (2010). Solving Unit Commitment Problem Using Modified Subgradient Method Combined with Simulated Annealing Algorithm. *Mathematical Problems in Engineering*, 2010:1–15. 126

[9] Beltran, C. and Heredia, F. J. (2002). Unit Commitment by Augmented Lagrangian Relaxation: Testing Two Decomposition Approaches. *Journal of Optimization Theory and Applications*, 112(2):295–314. 107

[10] Blaabjerg, F., Teodorescu, R., Liserre, M., and Timbus, A. (2006). Overview of Control and Grid Synchronization for Distributed Power Generation Systems. *IEEE Transactions on Industrial Electronics*, 53(5):1398–1409. 1, 2

[11] Bragin, M. A. and Luh, P. B. (2017). Distributed and asynchronous unit commitment and economic dispatch. In *2017 IEEE Power & Energy Society General Meeting*, pages 1–5, Chicago, IL. IEEE. 25

[12] Calvillo, C., Sánchez-Miralles, A., and Villar, J. (2015). Assessing low voltage network constraints in distributed energy resources planning. *Energy*, 84:783–793. 2

[13] Catalao, J. P. S., Mariano, S. J. P. S., Mendes, V. M. F., and Ferreira, L. A. F. M. (2007). Profit-Based Unit Commitment with Emission Limitations: A Multiobjective Approach. In *2007 IEEE Lausanne Power Tech*, pages 1417–1422, Lausanne, Switzerland. IEEE. 18

[14] Chandrasekaran, K., Hemamalini, S., Simon, S. P., and Padhy, N. P. (2012). Thermal unit commitment using binary/real coded artificial bee colony algorithm. *Electric Power Systems Research*, 84(1):109–119. 38

[15] Chen, Y., Casto, A., Wang, F., Wang, Q., Wang, X., and Wan, J. (2016). Improving Large Scale Day-Ahead Security Constrained Unit Commitment Performance. *IEEE Transactions on Power Systems*, 31(6):4732–4743. 12, 22, 31, 32, 96, 116, 117

[16] Chen, Y., Pan, F., Holzer, J., Veeramany, A., and Wu, Z. (2021). On Improving Efficiency of Electricity Market Clearing Software with A Concurrent High Performance Computer Based Security Constrained Unit Commitment Solver. In *2021 IEEE Power & Energy Society General Meeting (PESGM)*, pages 1–5, Washington, DC, USA. IEEE. 96, 117

[17] Chen, Y., Pan, F., Qiu, F., Xavier, A. S., Zheng, T., Marwali, M., Knueven, B., Guan, Y., Luh, P. B., Wu, L., Yan, B., Bragin, M. A., Zhong, H., Giacomoni, A., Baldick, R., Gisin, B., Gu, Q., Philbrick, R., and Li, F. (2022). Security-Constrained Unit Commitment for Electricity Market: Modeling, Solution Methods, and Future Challenges. *IEEE Transactions on Power Systems*, pages 1–14. 19

[18] Chen, Y., Wang, F., Wan, J., and Pan, F. (2018). Developing Next Generation Electricity Market Clearing Optimization Software. In *2018 IEEE Power & Energy Society General Meeting (PESGM)*, pages 1–5, Portland, OR. IEEE. 96

[19] Cheng, L., Zhou, X., Yun, Q., Tian, L., Wang, X., and Liu, Z. (2019a). A Review on Virtual Power Plants Interactive Resource Characteristics and Scheduling Optimization. In *2019 IEEE 3rd Conference on Energy Internet and Energy System Integration (EI2)*, pages 514–519, Changsha, China. IEEE. 4

[20] Cheng, L., Zhou, X., Yun, Q., Tian, L., Wang, X., and Liu, Z. (2019b). A Review on Virtual Power Plants Interactive Resource Characteristics and Scheduling Optimization. In *2019 IEEE 3rd Conference on Energy Internet and Energy System Integration (EI2)*, pages 514–519, Changsha, China. IEEE. 4

[21] Chuan-Ping Cheng, Chih-Wen Liu, and Chun-Chang Liu (2000). Unit commitment by Lagrangian relaxation and genetic algorithms. *IEEE Transactions on Power Systems*, 15(2):707–714. 35

[22] Cong Liu, Shahidehpour, M., Yong Fu, and Zuyi Li (2009). Security-Constrained Unit Commitment With Natural Gas Transmission Constraints. *IEEE Transactions on Power Systems*, 24(3):1523–1536. 21

[23] Dai, W., Yang, Z., Yu, J., Cui, W., Li, W., Li, J., and Liu, H. (2021). Economic dispatch of interconnected networks considering hidden flexibility. *Energy*, 223:120054. 17

[24] Deane, J., Ó Gallachóir, B., and McKeogh, E. (2010). Techno-economic review of existing and new pumped hydro energy storage plant. *Renewable and Sustainable Energy Reviews*, 14(4):1293–1302. xiii, 6, 8

[25] Denholm, P., O'Connell, M., Brinkman, G., and Jorgenson, J. (2015). Overgeneration from Solar Energy in California. A Field Guide to the Duck Chart. Technical Report NREL/TP–6A20-65023, 1226167, California Independent System Operator (CAISO). 2, 3

[26] Dvorkin, Y., Pandzic, H., Ortega-Vazquez, M. A., and Kirschen, D. S. (2015). A Hybrid Stochastic/Interval Approach to Transmission-Constrained Unit Commitment. *IEEE Transactions on Power Systems*, 30(2):621–631. 22

[27] EIA, C. (2020). Wind-has surpassed hydro as most-used renewable electricity generation source in U.S. *EIA Article*. 2, 3, 10

[28] EIA, C. (2021). U.S. energy facts explained. *EIA Article*. xiii, 23, 24

[29] EIA, C. (2022). Wholesale Electricity and Natural Gas Market Data. *EIA Article*. 149

[30] El Bakari, K., Myrzik, J. M. A., and Kling, W. L. (2009). Prospects of a virtual power plant to control a cluster of distributed generation and renewable energy sources. *44th International Universities Power Engineering Conference (UPEC);2009*, page 5. 2

[31] Fangxing Li and Rui Bo (2010). Small test systems for power system economic studies. In *IEEE PES General Meeting*, pages 1–4, Minneapolis, MN. IEEE. 41

[32] Feizollahi, M. J., Costley, M., Ahmed, S., and Grijalva, S. (2015). Large-scale decentralized unit commitment. *International Journal of Electrical Power & Energy Systems*, 73:97–106. 23, 28

[33] Gambella, C., Marecek, J., Mevissen, M., Ortega, J. M. F., Djukic, S. P., and Pezic, M. (2018). Transmission-Constrained Unit Commitment. arXiv:1806.09408 [cs, math]. 22

[34] Gonzalez-Castellanos, A., Thakurta, P. G., and Bischi, A. (2018). Flexible unit commitment of a network-constrained combined heat and power system. *arXiv:1809.09508 [math]*. arXiv: 1809.09508. 28

[35] Hsieh, E. and Anderson, R. (2017). Grid flexibility: The quiet revolution. *The Electricity Journal*, 30(2):1–8. 10

[36] ISO, N. (2020). NYISO 2020 Annual Report on Demand Response Programs. *NYISO*. xiii, 6, 7

[37] Jain, A., Yamujala, S., Das, P., Gaur, A. S., Bhakar, R., Mathur, J., and Kushwaha, P. (2020). Unit Commitment Framework to Assess Flexibility Resource Capability for High RE Penetration. In *2020 IEEE PES Innovative Smart Grid Technologies Europe (ISGT-Europe)*, pages 779–783, The Hague, Netherlands. IEEE. 29

[38] Jasmin, E., Imthias Ahamed, T., and Jagathy Raj, V. (2011). Reinforcement Learning approaches to Economic Dispatch problem. *International Journal of Electrical Power & Energy Systems*, 33(4):836–845. 38

[39] Jenkins, J. D., Luke, M., and Thernstrom, S. (2018). Getting to Zero Carbon Emissions in the Electric Power Sector. *Joule*, 2(12):2498–2510. 126

[40] Kargarian, A. and Fu, Y. (2014). System of Systems Based Security-Constrained Unit Commitment Incorporating Active Distribution Grids. *IEEE Transactions on Power Systems*, 29(5):2489–2498. 23

[41] Kargarian, A., Fu, Y., and Li, Z. (2015a). Distributed Security-Constrained Unit Commitment for Large-Scale Power Systems. *IEEE Transactions on Power Systems*, 30(4):1925–1936. 11

[42] Kargarian, A., Fu, Y., and Li, Z. (2015b). Distributed Security-Constrained Unit Commitment for Large-Scale Power Systems. *IEEE Transactions on Power Systems*, 30(4):1925–1936. 23

[43] Khodaei, A. and Shahidehpour, M. (2010). Transmission Switching in Security-Constrained Unit Commitment. *IEEE Transactions on Power Systems*, 25(4):1937–1945. 21

[44] Kim, J.-H. and Shcherbakova, A. (2011). Common failures of demand response. *Energy*, 36(2):873–880. 6

[45] Knueven, B., Ostrowski, J., and Watson, J.-P. (2018). Exploiting Identical Generators in Unit Commitment. *IEEE Transactions on Power Systems*, 33(4):4496–4507. 19

[46] Knueven, B., Ostrowski, J., and Watson, J.-P. (2020). On Mixed-Integer Programming Formulations for the Unit Commitment Problem. *INFORMS Journal on Computing*, page ijoc.2019.0944. 60

[47] Knueven, B. A. (2017). Almost Symmetries and the Unit Commitment Problem. *PhD diss., University of Tennessee, 2017.*, page 225. 19

[48] Kumar, S. S. and Palanisamy, V. (2007). A dynamic programming based fast computation Hopfield neural network for unit commitment and economic dispatch. *Electric Power Systems Research*, 77(8):917–925. 38

[49] Kurban, M. and Basaran Filik, U. (2009). A Comparative Study of Three Different Mathematical Methods for Solving the Unit Commitment Problem. *Mathematical Problems in Engineering*, 2009:1–13. 126

[50] Land, A. H. and Doig, A. G. (1960). An Automatic Method of Solving Discrete Programming Problems. *Econometrica*, 28(3):497. 18

[51] Lee, C., Liu, C., Mehrotra, S., and Shahidehpour, M. (2014). Modeling Transmission Line Constraints in Two-Stage Robust Unit Commitment Problem. *IEEE Transactions on Power Systems*. 21

[52] Li, F. and Bo, R. (2007). DCOPF-Based LMP Simulation: Algorithm, Comparison With ACOPF, and Sensitivity. *IEEE Transactions on Power Systems*, 22(4):1475–1485. 38, 41

[53] Li, Z., Wu, W., Wang, J., Zhang, B., and Zheng, T. (2016). Transmission-Constrained Unit Commitment Considering Combined Electricity and District Heating Networks. *IEEE Transactions on Sustainable Energy*, 7(2):480–492. 22

[54] Lima, R. M. and Novais, A. Q. (2016). Symmetry breaking in MILP formulations for Unit Commitment problems. *Computers & Chemical Engineering*, 85:162–176. 19

[55] Liu, G. (2014). Generation Scheduling for Power Systems with Demand Response and a High Penetration of Wind Energy. *PhD diss., University of Tennessee, 2014.*, page 177. 10, 15, 17

[56] Liu, J., Laird, C. D., Scott, J. K., Watson, J.-P., and Castillo, A. (2019). Global Solution Strategies for the Network-Constrained Unit Commitment Problem With AC Transmission Constraints. *IEEE Transactions on Power Systems*, 34(2):1139–1150. 22

[57] Lotfjou, A., Shahidehpour, M., Yong Fu, and Zuyi Li (2010). Security-Constrained Unit Commitment With AC/DC Transmission Systems. *IEEE Transactions on Power Systems*, 25(1):531–542. 21

[58] Ma, H. and Shahidehpour, S. (1999). Unit commitment with transmission security and voltage constraints. *IEEE Transactions on Power Systems*, 14(2):757–764. 21

[59] Ma, H. and Shahidehpour, M, S. (1998). Transmission-constrained unit commitment based on Benders decomposition. *International Journal of Electrical Power and Energy Systems*, 20(4):287–294. 18, 21

[60] Margot, F. (2002). Pruning by isomorphism in branch-and-cut. *Mathematical Programming*, 94(1):71–90. 19

[61] McAnany, J. (2021). 2021 Demand Response Operations Markets Activity Report: April 202. *PJM Demand Side Response Operations*. xiii, 7

[62] Meus, J., Poncelet, K., and Delarue, E. (2018). Applicability of a Clustered Unit Commitment Model in Power System Modeling. *IEEE Transactions on Power Systems*, 33(2):2195–2204. 20

[63] Murdock, E., H., Gibb, D., Andre, T., Sawin, L., J., and Brown, A. (2022). Renewables 2022 Global Status Report. *Renewable*. xiii, 2, 3

[64] Nikolaidis, P. and Poullikkas, A. (2020). Enhanced Lagrange relaxation for the optimal unit commitment of identical generating units. *IET Generation, Transmission & Distribution*, 14(18):3920–3928. 19

[65] Nogales, A., Wogrin, S., and Centeno, E. (2016). Impact of technical operational details on generation expansion in oligopolistic power markets. *IET Generation, Transmission & Distribution*, 10(9):2118–2126. 29

[66] Olival, P., Madureira, A., and Matos, M. (2017). Advanced voltage control for smart microgrids using distributed energy resources. *Electric Power Systems Research*, 146:132–140. 2

[67] Ostrowski, J., Anjos, M. F., and Vannelli, A. (2012). Tight Mixed Integer Linear Programming Formulations for the Unit Commitment Problem. *IEEE Transactions on Power Systems*, 27(1):39–46. 20

[68] Ostrowski, J., Linderoth, J., Rossi, F., and Smriglio, S. (2011). Orbital branching. *Mathematical Programming*, 126(1):147–178. 19

[69] Palmintier, B. S. and Webster, M. D. (2014). Heterogeneous Unit Clustering for Efficient Operational Flexibility Modeling. *IEEE Transactions on Power Systems*, 29(3):1089–1098. 20

[70] Pandzic, H., Ting Qiu, and Kirschen, D. S. (2013). Comparison of state-of-the-art transmission constrained unit commitment formulations. In *2013 IEEE Power & Energy Society General Meeting*, pages 1–5, Vancouver, BC. IEEE. 21

[71] Papavasiliou, A., Oren, S. S., and Rountree, B. (2015). Applying High Performance Computing to Transmission-Constrained Stochastic Unit Commitment for Renewable Energy Integration. *IEEE Transactions on Power Systems*, 30(3):1109–1120. 22

[72] Patton, J. (2019). 2018 STATE OF THE MARKET REPORT FOR THE MISO ELECTRICITY MARKETS. *MISO Market*, page 143. 11

[73] Pineda, S., Morales, J. M., and Jimenez-Cordero, A. (2020). Data-Driven Screening of Network Constraints for Unit Commitment. *IEEE Transactions on Power Systems*, 35(5):3695–3705. 22

[74] Poncelet, K., van Stiphout, A., Delarue, E., D'haeseleer, W., and Deconinck, G. (2014). A Clustered Unit Commitment Problem Formulation for Integration in Investment Planning Models. *TME Branch Working Paper*, 2014–19. 20

[75] Price, J. E. and Goodin, J. (2011). Reduced network modeling of WECC as a market design prototype. In *2011 IEEE Power and Energy Society General Meeting*, pages 1–6, San Diego, CA. IEEE. 97, 152

[76] Qiaozhu Zhai, Xiaohong Guan, and Jian Cui (2002). Unit commitment with identical units successive subproblem solving method based on Lagrangian relaxation. *IEEE Transactions on Power Systems*, 17(4):1250–1257. 19

[77] Rabbuni, G. and Guru Kumar, G. (2015). Unit commitment with transmission constraints in deregulated power market. In *2015 International Conference on Electrical, Electronics, Signals, Communication and Optimization (EESCO)*, pages 1–6, Visakhapatnam. IEEE. 22

[78] Ramanan, P., Yildirim, M., Chow, E., and Gebraeel, N. (2017). Asynchronous Decentralized Framework for Unit Commitment in Power Systems. *Procedia Computer Science*, 108:665–674. xiii, 25, 26, 27

[79] Saadat, H. (2010). *Power system analysis*. McGraw-Hill series in electrical and computer engineering. PSA Publishing, 3rd edition. 40

[80] Saboori, H., Mohammadi, M., and Taghe, R. (2011). Virtual Power Plant (VPP), Definition, Concept, Components and Types. In *2011 Asia-Pacific Power and Energy Engineering Conference*, pages 1–4, Wuhan, China. IEEE. xiii, 4, 5

[81] Salam, S. (2007). Unit Commitment Solution Methods. *World Academy of Science, Engineering and Technology*, page 6. 18

[82] Saravanan, B., Das, S., Sikri, S., and Kothari, D. P. (2013). A solution to the unit commitment problem—a review. *Frontiers in Energy*, 7(2):223–236. 17, 18

[83] Schrock, J. D. (2022). Optimization Methods for Day Ahead Unit Commitment. *PhD diss., University of Tennessee, 2022.*, page 73. 19

[84] Shuai Lu, Makarov, Y. V., Yunhua Zhu, Ning Lu, Kumar, N. P., and Chakrabarti, B. B. (2010). Unit commitment considering generation flexibility and environmental constraints. In *IEEE PES General Meeting*, pages 1–11, Minneapolis, MN. IEEE. 28

[85] Singhal, P. K. and Sharma, R. N. (2011). Dynamic Programming Approach for Large Scale Unit Commitment Problem. In *2011 International Conference on Communication Systems and Network Technologies*, pages 714–717, Katra, Jammu, India. IEEE. 18

[86] Streiffert, D., Philbrick, R., and Ott, A. (2005). A mixed integer programming solution for market clearing and reliability analysis. In *IEEE Power Engineering Society General Meeting, 2005*, pages 195–202, San Francisco, CA, USA. IEEE. xiii, 29, 30

[87] Subcommittee, P. (1979). IEEE Reliability Test System. *IEEE Transactions on Power Apparatus and Systems*, PAS-98(6):2047–2054. 75

[88] Sudhakar, A., Karri, C., and Jaya Laxmi, A. (2017). Profit based unit commitment for GENCOs using Lagrange Relaxation–Differential Evolution. *Engineering Science and Technology, an International Journal*, 20(2):738–747. 35

[89] Tejada-Arango, D. A., Lumbreras, S., Sanchez-Martin, P., and Ramos, A. (2020). Which Unit-Commitment Formulation is Best? A Comparison Framework. *IEEE Transactions on Power Systems*, 35(4):2926–2936. 15

[90] The-MathWorks-Inc. (2021). MATLAB Version: 9.10.0 (R2021a). 41, 61, 154

[91] Tongxin Zheng, Jinye Zhao, Feng Zhao, and Litvinov, E. (2012). Operational flexibility and system dispatch. In *2012 IEEE Power and Energy Society General Meeting*, pages 1–3, San Diego, CA. IEEE. 28

[92] Tosserams, S., Etman, L. F. P., Papalambros, P. Y., and Rooda, J. E. (2006). An augmented Lagrangian relaxation for analytical target cascading using the alternating direction method of multipliers. *Structural and Multidisciplinary Optimization*, 31(3):176–189. 107

[93] Uría-Martínez, R., Johnson, M. M., Shan, R., Samu, N. M., Oladosu, G., Werble, J. M., and Battey, H. (2021). U.S. Hydropower Market Report. *U.S. Department of Energy*, page 158. xiii, 6, 9

[94] Ventosa, M., Baillo, A., Ramos, A., and Rivier, M. (2005). Electricity market modeling trends. *Energy Policy*, 33(7):897–913. 10

[95] Wang, B., Liu, X., Zhu, F., Hu, X., Ji, W., Yang, S., Wang, K., and Feng, S. (2015). Unit Commitment Model Considering Flexible Scheduling of Demand Response for High Wind Integration. *Energies*, 8(12):13688–13709. 28

[96] Wang, S., Shahidehpour, S., Kirschen, D., Mokhtari, S., and Irisarri, G. (1995). Short-term generation scheduling with transmission and environmental constraints using an augmented Lagrangian relaxation. *IEEE Transactions on Power Systems*, 10(3):1294–1301. 107

[97] Wang, Y., Wu, L., and Li, J. (2018). A fully distributed asynchronous approach for multi-area coordinated network-constrained unit commitment. *Optimization and Engineering*, 19(2):419–452. 25

[98] Woeginger, G. J. (2003). Exact Algorithms for NP-Hard Problems: A Survey. *Springer*, 2570:185–207. 11, 12

[99] Wood, A. J., Wollenberg, B. F., and Sheble, G. B. (2014). *POWER GENERATION, OPERATION, AND CONTROL*. John Wiley & Sons, Inc., hoboken, New Jersey, third edition edition. 35, 36

[100] Yadav, D., Mekhilef, S., Singh, B., and Rawa, M. (2020). Analysis of Market to Market Interconnection Points during Overgeneration Scenario in a Market. In *2020 IEEE 5th International Conference on Computing Communication and Automation (ICCCA)*, pages 774–779, Greater Noida, India. IEEE. 33

[101] Zhang, L., Capuder, T., and Mancarella, P. (2016). Unified Unit Commitment Formulation and Fast Multi-Service LP Model for Flexibility Evaluation in Sustainable Power Systems. *IEEE Transactions on Sustainable Energy*, 7(2):658–671. 28

[102] Zhao, G. and Yamashiro, S. (2003). A method for unit commitment with transmission losses and flow constraint. *Electrical Engineering in Japan*, 142(4):9–19. 21

[103] Zimmerman, R. D., Murillo-Sanchez, C. E., and Thomas, R. J. (2011). MATPOWER: Steady-State Operations, Planning, and Analysis Tools for Power Systems Research and Education. *IEEE Transactions on Power Systems*, 26(1):12–19. 41, 48, 152

Appendices

A Data Information for WECC

The WECC hourly load data from August 10, 2004, was selected because it has the daily annual peak for the year. The renewable resources in the CAISO and WECC regional markets have increased drastically and will continue to increase into the future. Figure A.1 shows the current trend and the future projection of WECC peak demand (Source: https://www.wecc.org). Following this information, the WECC load pattern from Figure A.2 was modified to a projected load pattern with high renewable resources as seen in Figure A.3.

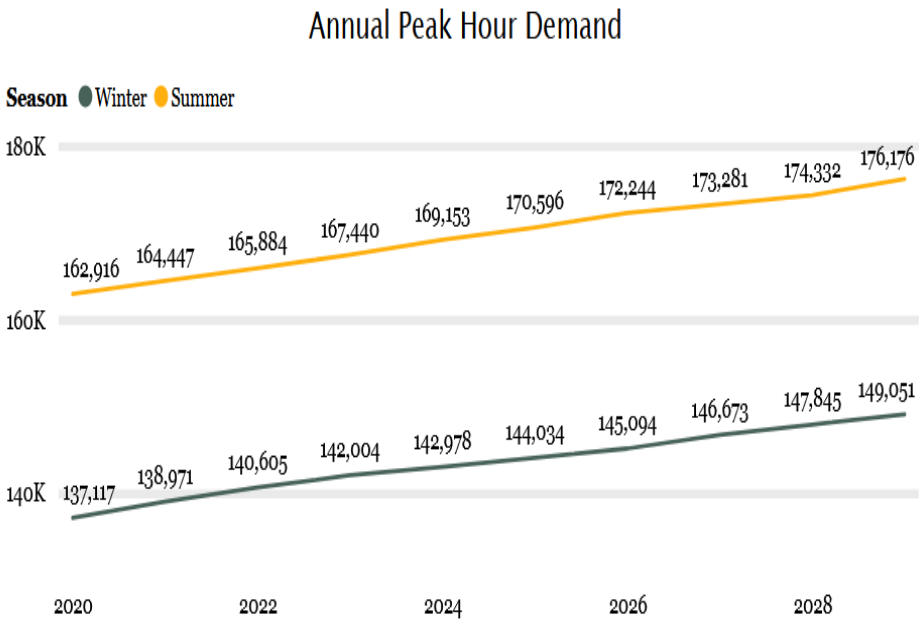


Figure A.1: WECC annual peak hourly demand

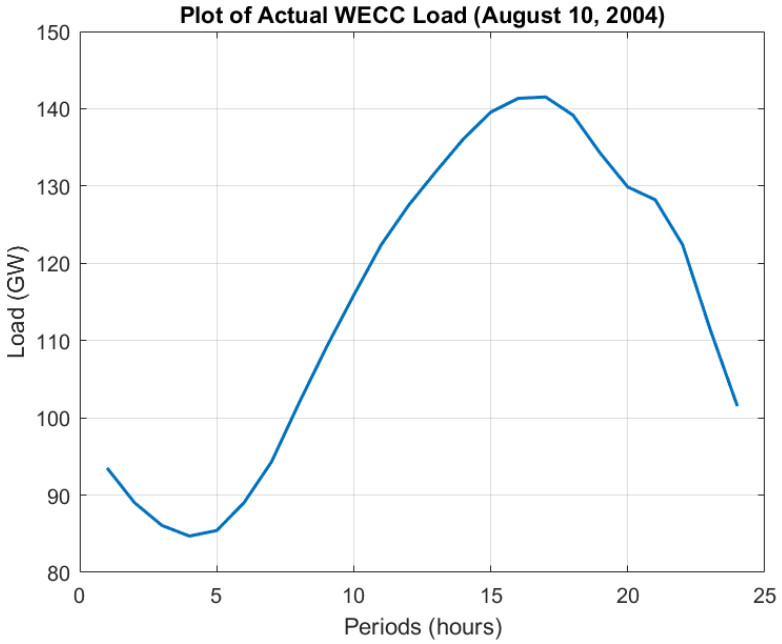


Figure A.2: WECC hourly load for August 10, 2004

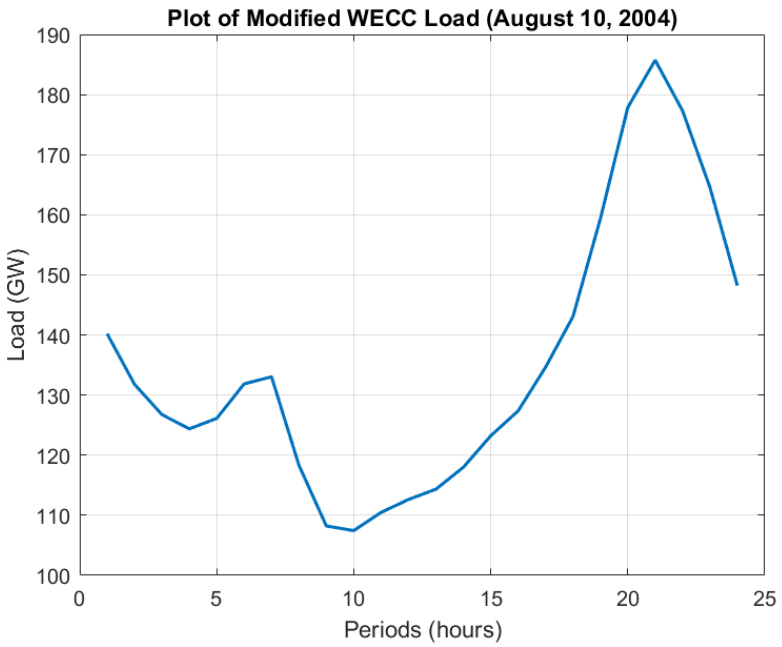


Figure A.3: Modified WECC load using CAISO RES data from July 2, 2022

B Load Peak and Spike in LMPs

The California ISO Summer Market Performance Report [3] is prepared annually. The 2022 edition shows that the load exceeded the 50,000 MW mark for the 3rd time in history. It can be observed that as the load approaches the resource adequacy (RA) line in Figure B.1, the daily average LPMs show spikes in price as seen in Figure B.2.

LMP spikes can also be observed at individual bus locations or hubs. The Intercontinental Exchange (ICE) data focuses on energy prices at specific trading hubs [29]. Figure B.3 shows the price of energy at the southern California hub (SP15) and northern California hub (NP15) over a range of trading days. The price spikes in SP15 and NP15 overlap well. This implies that the event is not isolated to a hub but results from a heavily loaded system. The observed high price is a function of a high daily peak.

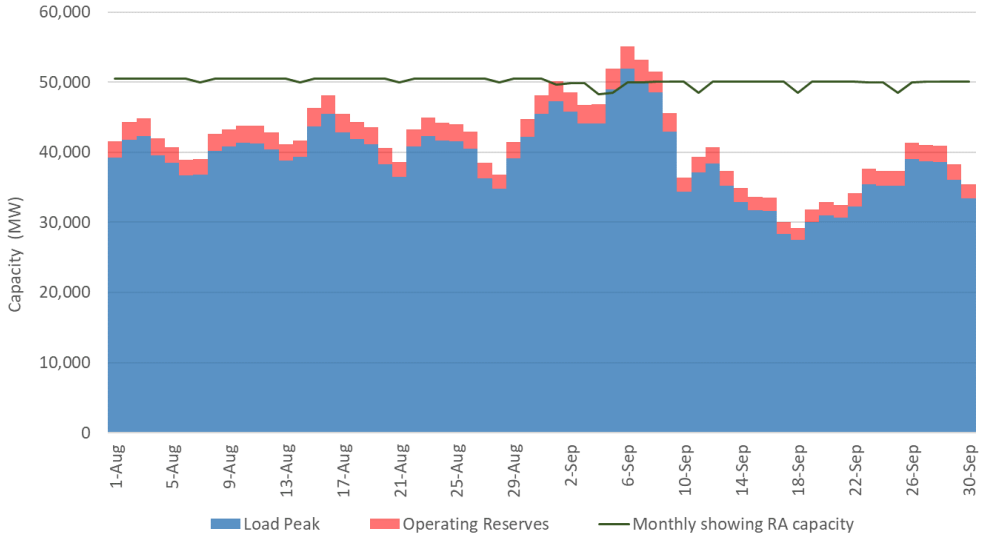


Figure B.1: Daily peaks and RA capacity for August and September 2022 [3]

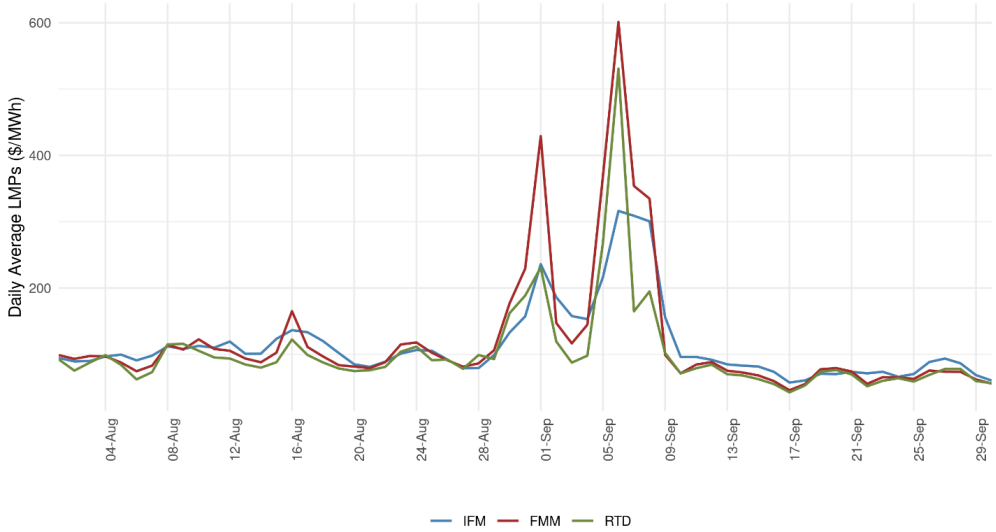


Figure B.2: Average daily prices across markets Aug-Sep 2022 [3]

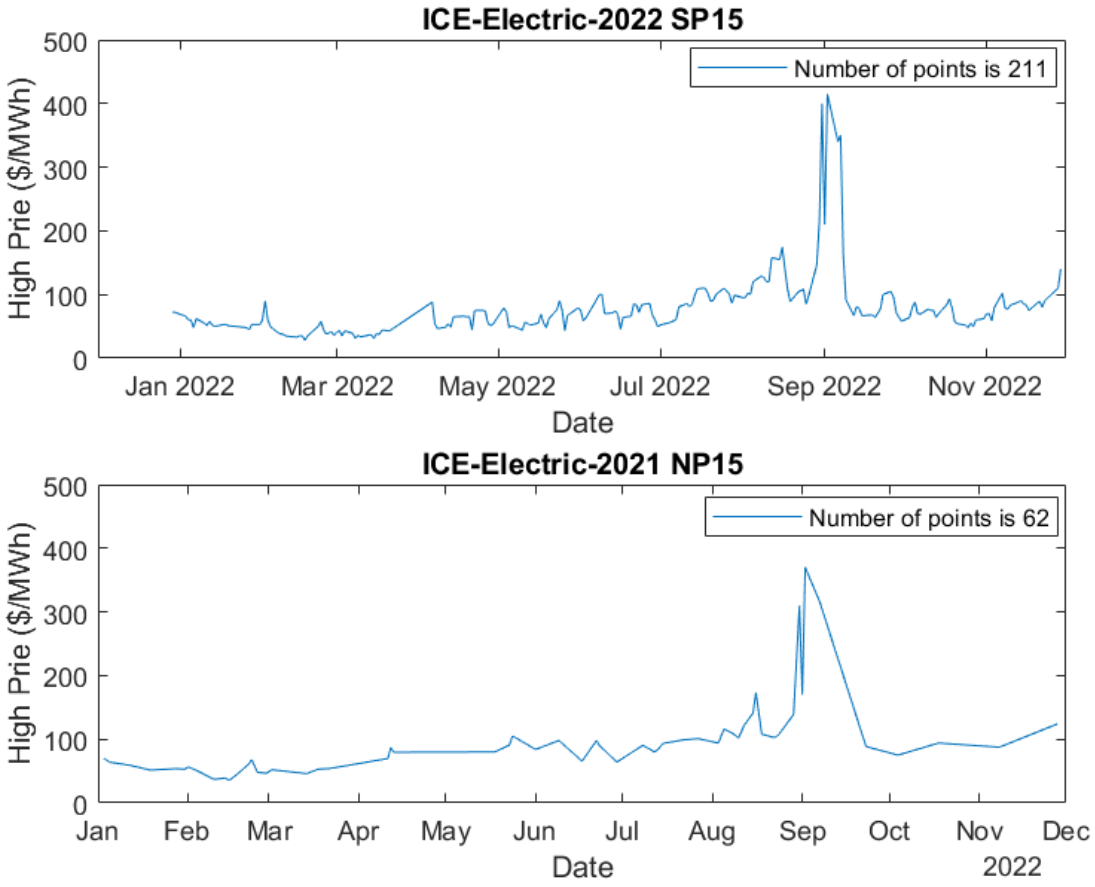


Figure B.3: Electricity prices variation at the SP15 and NP15 hubs.

C LR Formulations and Matlab Code

C.1 Data Process

The raw WECC 240 bus data is given in an Excel file and a PSSE case format is also available for dynamic studies [75]. First, the PSSE data is converted to a MATPOWER format using the psse2mpc command [103], with bus, branch, generator, and instantaneous load data but no generator cost data. The full load data and generator parameters are given in the Excel data. The generation costs are derived from the given generator parameters in both piecewise and quadratic cost function formats. The unit minimum and maximum capacities from the Excel data are compared with the MATPOWER data for consistency.

C.2 Code Implementation

For each simulation scenario, the load, network, and generator data are pre-processed in a separate MATLAB script. The output is saved in MATLAB format for easy access and loading. Before the iteration process starts, the unit minimum up and down times are fixed via a function that tracks and updates the up and down times of each unit. Binary codes (1/0) are generated for each generator. A unit that is allowed to come on if off or stay on if already on has a code of 1 while a unit that cannot come on during that period is assigned a code of 0. During the iteration process, the unit maximum and minimum capacity for the time period is fixed by calling a function. The function sets the ramp limits using the previous values of the units. For example, in period one, the previous output values of the units are given as part of the initial data while for subsequent periods, the result of the ED from the previous period is used. Next a function that commits units using the dual variable is called. The total capacity of the committed units is compared with the periodic load. If the sum of the maximum capacity exceeds the load and the sum of the minimum capacity is less than the load then the ED is solved as seen in Figure C.1 For scenarios with additional iteration requirements, the price from the ED is compared with the λ value (dual variable), and the improvement in the objective is used as the stopping criteria.

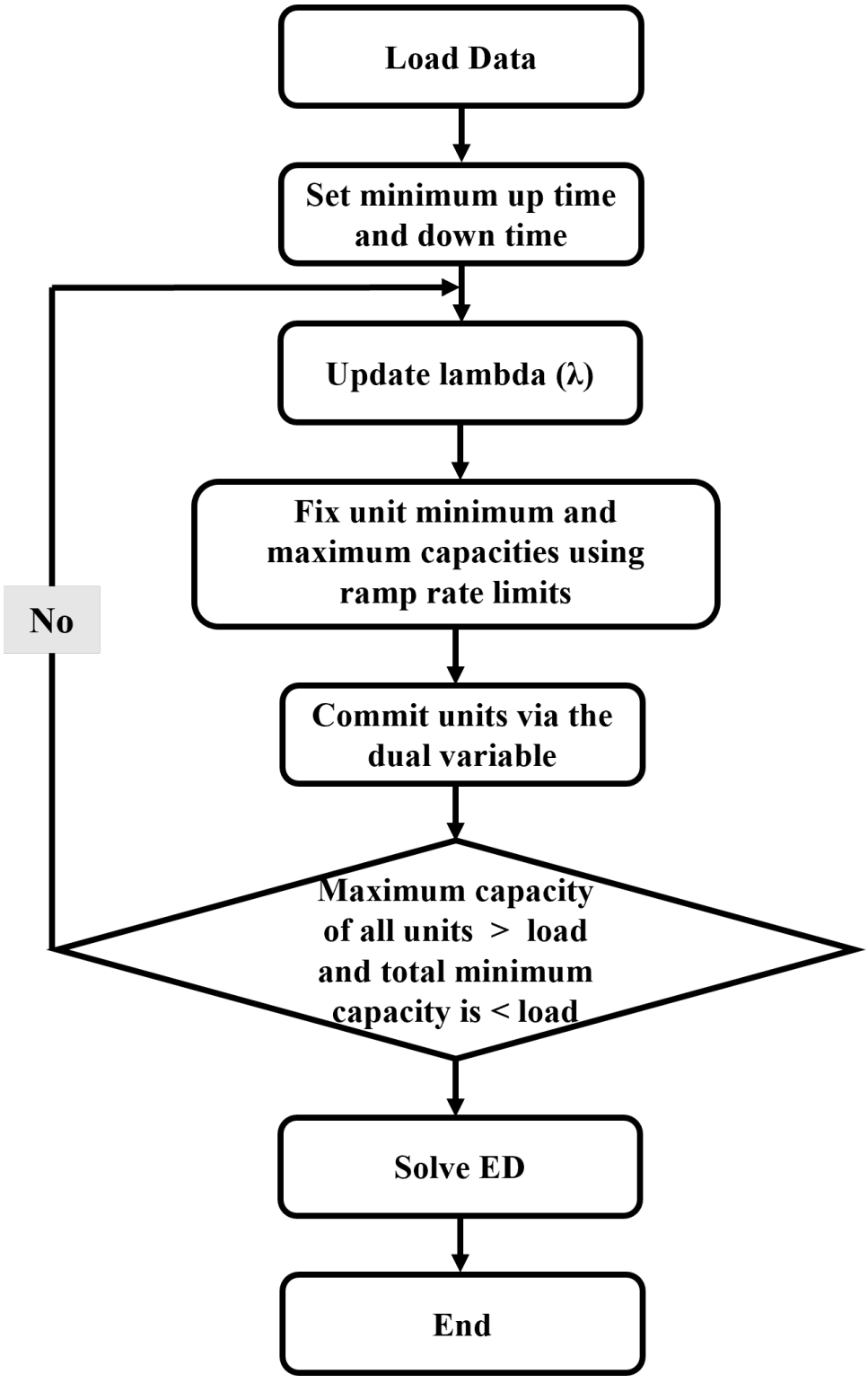


Figure C.1: Code flowchart

C.3 ED Implementation

Once the committed capacity equals or exceeds the demand and there are no violations found, the ED will be solved using a linear programming function or the quadratic programming function from MATLAB [90]. The UC values and the total period load demand form the equality constraint equation. Note that the minimum up time and down time have been implemented during the UC process because the ED is unable to commit or de-commit units. The unit periodic maximum and minimum capacities are the upper and lower bounds. In the case of a quadratic cost function, the objective function is made up of the quadratic part ($2c$) and the linear part (b). Where b and c are the linear and quadratic parts of the cost function.

Vita

Stephen Fatokun received his B.S. degree in engineering physics from Obafemi Awolowo University (Nigeria) in 2008 and an M.S. degree in physics from Western Illinois University in 2014. At the University of Tennessee, Knoxville, he received a second M.S. degree in electrical engineering and a Graduate Certificate degree in power and energy systems in 2019. He started his Ph.D. studies in energy science and engineering at the University of Tennessee, Knoxville, in January 2017. His research interest is in power system economics, market simulation, and power system operation and planning.